

Thermoresponsive Poly(glycidyl ether)s for Cell Sheet Fabrication

Dissertation zur Erlangung des akademischen Grades des
Doktors der Naturwissenschaften (Dr. rer. nat.)

eingereicht im Fachbereich Biologie, Chemie, Pharmazie
der Freien Universität Berlin

vorgelegt von

M.Sc. Silke Heinen

aus Köln

November 2017

Diese Arbeit würde unter Anleitung von Dr. Marie Weinhart und Prof. Dr. Rainer Haag im Zeitraum vom Januar 2014 bis November 2017 am Institut für Chemie und Biochemie der Freien Universität Berlin angefertigt.

1. Gutachter Prof. Dr. Rainer Haag
2. Gutachter Prof. Dr. Thomas Risse

Disputation am 26. Januar 2018

ACKNOWLEDGMENT

First of all I want to thank Dr. Marie Weinhart for her constant scientific support during the last years. I hold in high esteem the goal-oriented discussions and creative brainstorming we had as well as her critical mind challenging and thereby improving my research. I want to thank Prof. Dr. Rainer Haag for his scientific and financial support as well as for the opportunities he offered me to learn about the transfer of research results to market ideas and thereby develop useful skills besides the important scientific education. Further, I want to thank Prof. Dr. Thomas Risse for being the co-referee of this thesis. Moreover, my thanks go to all former and present members of the Weinhart and Haag group for their support and kind collaboration. In particular, I want to thank Dr. Anke Hoppensack for her advice in cell culture related questions but also for sharing her sense for comprehensible data representation, which improved many of my oral presentations, conference contributions and manuscripts. Furthermore, I want to thank M.Sc. Daniel Stöbener and M.Sc. Dennis Müller for their unlimited cooperativeness in our lab work routine as well as B.Sc. Melanie Uckert and Johanna Scholz for their support with cell culture experiments. Dr. José Luis Cuéllar-Camacho is kindly acknowledged for his collaboration, performing and analyzing numerous AFM measurements important for my projects. Special thanks go to M.Sc. Simon Rackow who helped me with my projects in the framework of his master thesis as well as to Dr. Tobias Becherer for guiding me during my master thesis, giving me my first research project in the Haag group and bringing me in contact with the interesting research topic: Thermoresponsive polymers for cell sheet fabrication. Further, I want to thank M.Sc. Karolina Walker and Dipl.-NanoSc. Michael Unbehauen for interesting discussions and their cordial friendship. Concerning all administrative issues Jutta Hass and Eike Ziegler are kindly acknowledged for their reliable support. My special thanks go to all members of the service and analytics department of the FU Berlin for their kind support and for the numerous measurements they performed. Furthermore, I want to thank the statistical consulting unit of the FU Berlin "fu:stat" for their advice on the statistical evaluation of my data. I am also grateful to the FCI "Fonds der Chemischen Industrie" for their generous financial support over two years through the Chemiefonds scholarship, which gave me the freedom to intensively investigate the really interesting topic of my doctoral thesis and to visit national and international conferences. Finally, my kind acknowledgements go to Dr. Pam Winchester, Dr. Anke Hoppensack and Dr. Marie Weinhart for proofreading my manuscripts.

Contents

| | |
|---|-----------|
| 1 INTRODUCTION | 1 |
| 1.1 General Aspects of Cell Sheet Engineering | 1 |
| 1.2 Thermoresponsive Polymers | 3 |
| 1.2.1 Phase Transition | 3 |
| 1.2.2 Determination of Phase Transition Temperatures in Solution | 5 |
| 1.2.3 Thermoresponsive Polymers for Cell Sheet Engineering | 7 |
| 1.2.4 Parameter to Adjust Phase Transition Temperatures | 15 |
| 1.2.5 Determination of Phase Transition Temperatures on Surfaces | 16 |
| 1.3 Thermoresponsive Surfaces for Cell Sheet Engineering | 18 |
| 1.3.1 Defined Coatings Prepared by Self-Assembly | 22 |
| 1.3.2 Correlation of Surface Parameters with Cell Response | 25 |
| 2 OBJECTIVES | 40 |
| 3 PUBLICATIONS AND MANUSCRIPTS | 42 |
| 3.1 A Perfect Match: Fast and Truly Random Copolymerization of Glycidyl Ether Monomers to Thermoresponsive Copolymers | 46 |
| 3.2 In-depth Analysis of Switchable Glycerol Based Polymeric Coatings for Cell Sheet Engineering | 77 |
| 3.3 Poly(glycidyl ether)-Based Monolayers on Gold Surfaces: Control of Grafting Density and Chain Conformation by Grafting Procedure, | |

| | |
|--|------------|
| Surface Anchor, and Molecular Weight | 105 |
| 3.4 Thermoresponsive Poly(glycidyl ether) Brushes on Gold: Surface Engineering Parameters and Their Implication for Cell Sheet Fabrication | 144 |
| 3.5 Transfer of Functional Thermoresponsive Poly(glycidyl ether) Coatings for Cell Sheet Fabrication from Gold to Glass Surfaces | 161 |
| 4 SUMMARY AND CONCLUSIONS | 208 |
| 5 OUTLOOK | 212 |
| 6 KURZZUSAMMENFASSUNG/ SHORT SUMMARY | 214 |
| 6.1 Kurzzusammenfassung | 214 |
| 6.2 Short Summary | 216 |
| 7 REFERENCES | 218 |
| LIST OF PUBLICATIONS AND CONFERENCE CONTRIBUTIONS | 233 |

1 INTRODUCTION

1.1 General Aspects of Cell Sheet Engineering

Within living tissue, adhesion of single cells to each other or to the surrounding protein environment, the extracellular matrix (ECM), plays a fundamental role in cell communication and regulation as well as in tissue development and maintenance. Most mammalian cells cultured *in vitro* are adherent cells, which require to attach firmly to a substrate in order to homeostatically reside, proliferate, differentiate, and migrate.¹ In static *in vitro* cell culture, cell adhesion onto solid substrates, such as tissue culture polystyrene petri dishes, is mediated by surface-adsorbed proteins and can be divided into three different phases. In phase I cells sediment onto the substrate and undergo an initial attachment through weak chemical bonding, such as hydrogen bonding, electrostatic, polar or ionic interactions, between the cell surface and the protein layer on the substrate or the substrate material itself. In phase II transmembrane proteins, so called integrins, anchor the cells to proteins or adhesion molecules on the substrate, cells flatten and attach more strongly to the surface. Integrin receptors are of integral importance for the cells sensing their environment, as they pass on mechanical and chemical information from the outside to the inside of the cells. The substrate materials' surface chemistry and thus hydrophilicity, topography with roughness and elasticity impact cell adhesion and thus proliferation and differentiation. In phase III of cell adhesion *in vitro*, cells fully spread on the substrate by reorganization of their cytoskeleton.¹⁻² The integrins thereby function as linkage between the intracellular actin filament of the cytoskeleton, to which they are attached through the focal adhesion domain, and the extracellular environment.^{1, 3} Formation of focal adhesion points allows for stable adhesion, but also directs cell migration, proliferation, and differentiation.¹⁻² In order to enhance the receptor-mediated adhesion important for signal-transmittance, cells secrete their own cell type-specific ECM consisting of adhesion proteins, such as fibronectin, vitronectin, collagen or laminin within 24 to 48 h after cell seeding.⁴ Proliferation of cells on the surface results in increasing cell density and allows for the development cell-cell contacts. The formation of a confluent cell monolayer results in a stationary phase without further cell proliferation. In order to further expand the cells they should be passaged slightly before reaching the stationary phase, which means that they are detached

from the current substrate and are reseeded in a lower cell density and in fresh medium onto another substrate. Adherent mammalian cells cultured on a solid substrate, such as tissue culture polystyrene, are conventionally detached by enzymatic treatment or mechanical scraping. Both methods are, however, detrimental to the cells and their ECM.⁵⁻⁶ Such treatments destroy or harm the protein-based environment of the cells and consequently leave singularized cells without ECM and altered cell surface proteins or small cell aggregates with a partially intact protein environment.⁷⁻⁸

Methods to detach cells while maintaining the ECM and intact cell-to-cell conjunction often rely on polymeric coatings, with switchable surface properties. An external trigger, of chemical or physical nature, induces a change in surface properties. In one state these surfaces allow for cell adhesion and proliferation, in the other state for the harvest of confluent cell sheets. Physical or energy-based stimuli employed for cell harvest are temperature, light, electric and magnetic field. Chemical-based stimuli that trigger cell adhesion and detachment are changes in pH, ionic strength and the presence of chemical substances or biomolecules, such as enzymes.⁹⁻¹¹ The by far most commonly applied trigger in cell sheet fabrication is temperature.¹² Adherent mammalian cells *in vitro* are generally cultures at 37 °C, thus at body temperature. However, some cell types, such as primary cells or cells of cell lines, can cope with a temporal decrease in temperature without their differentiation status being affected or undergoing apoptosis. Room temperature or even 4 °C are commonly applied to trigger cell sheet detachment from thermoresponsive surfaces.¹²

Confluent cell sheets, with an integral ECM, play an important role in tissue engineering and regenerative medicine.¹³⁻¹⁴ Stacking of cell sheets with maintained ECM and subsequent maturation allows for the assembling of functional, three-dimensional tissue constructs and is referred to as cell sheet engineering (Figure 1).¹⁵⁻¹⁶

In the following, basic aspects of thermoresponsive polymers in solution and on surfaces with relevance for cell sheet fabrication are discussed. Physical properties and phase transition behavior of thermoresponsive polymers in solution, surface parameters of the temperature-switchable coatings on different substrate materials as well as cell-substrate interactions of thermoresponsive polymers applied in cell sheet fabrication are reviewed.

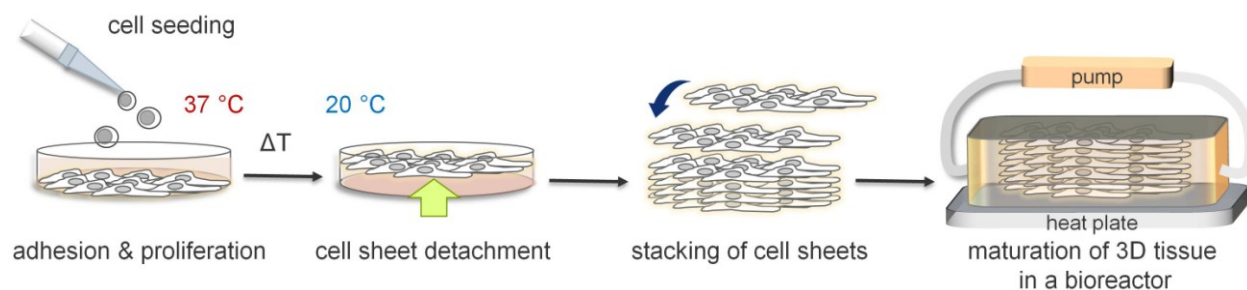


Figure 1 Scheme of a typical cell sheet engineering sequence including cell seeding, adhesion, and proliferation on as well as cell sheet detachment from thermoresponsive cell culture dishes to generate three-dimensional tissue by cell sheet stacking and subsequent maturation in a bioreactor.

1.2 Thermoresponsive Polymers

1.2.1 Phase Transition

Thermoresponsive polymers exhibit a phase transition in solution and when tethered to surfaces upon a temperature-trigger.¹⁴ These thermoresponsive polymers can either exhibit phase separation into a polymer-rich and a polymer-poor phase upon temperature increase or decrease. Polymers which display a miscibility gap upon heating possess a lower critical solution temperature (LCST), whereas polymers which undergo phase transition upon cooling exhibit an upper critical solution temperature (UCST).¹⁷ In the following, we will focus on LCST-type polymers, thus polymer chains turning from a fully dissolved state at temperatures below their transition temperature to a less soluble state above their transition temperature.¹⁸⁻¹⁹

Like any other spontaneously occurring physico-chemical process, the dissolution of a polymer in a solvent requires a negative free energy ΔG . According to the equation $\Delta G_{\text{mix}} = \Delta H_{\text{mix}} - T\Delta S_{\text{mix}}$, mixing of polymer and solvent is favored either for a sufficiently negative enthalpy term (ΔH_{mix}) or a sufficiently positive entropy contribution (ΔS_{mix}).²⁰ Additionally, the temperature impacts the free energy of mixing (ΔG_{mix}) and thus the dissolution of the polymer. The cause of the phase transition differs for non-polar polymer solutions and polar polymers dissolved in aqueous solutions.²⁰ LCST-type phase transitions in non-polar polymer solutions, e.g., in a solution of poly(propylene) in diethyl ether, are explained by the free volume theory of liquids. In polymer solutions, the free volume depends on temperature, pressure, and the polymer concentration. When a dense polymer is dissolved in a comparably highly expandable solvent,

the solvent loses an important part of its free volume. The mixing process of polymer and solvent is considered exothermic, but the loss in free volume adds an unfavorable entropy contribution. With rising temperature the difference in density, between the dense polymer solute and the strongly expandable solvent, increases and thereby entropy decreases. Above a certain temperature, the unfavorable entropy effect predominates thermodynamics of the mixture and phase separation occurs.²⁰⁻²¹ LCSTs for non-polar polymer-solvent systems are, however, rather rarely observed by coincidence, as the cloud point temperatures are often located above the boiling point of the respective solvent. Thus, high pressure is required to investigate the phase transition of such systems.²⁰⁻²³ Poly(propylene)s with different molecular weights, for example, exhibit LCSTs between 141 and 164 °C in diethyl ether.²¹ Identification of non-polar polymers that reveal a phase transition in organic solvent under mild conditions is quite rare.²⁴⁻²⁶

In contrast, many LCST-type polymers, which show a phase transition in aqueous solution under mild conditions, are known.²⁷ These polymers usually contain both hydrophilic and hydrophobic moieties.²⁸ The hydrophilic moieties contribute to the dissolution of the polymer in aqueous solution at low temperatures by the formation of hydrogen bonds, which results in a gain in enthalpy. The non-polar parts of the polymer solute induce an extra ordering of the surrounding water molecules known as "hydrophobic hydration", which, in turn, is entropically unfavorable. Above a certain temperature, this unfavorable entropy term outweighs the exothermic enthalpy of mixing and a phase separation of polymer and water arises.^{10, 20, 29}

For poly(*N*-isopropylacrylamide) (PNIPAM), the most prominent thermoresponsive polymer to date, a sharp coil-to-globule transition of single polymer chains is observed at around 32 °C. This sharp LCST-type transition is attributed to cooperative interactions between the nearest-neighbor water molecules bound via hydrogen bridging along the polymer chain. These cooperative interactions on the one hand support the hydration of the thermoresponsive polymer at low temperatures, but on the other hand promote a joint dehydration of the polar groups when temperature rises above the transition temperature. This collective dehydration results in a sharp phase transition.²⁹⁻³² For biological applications polymers with a phase transition in aqueous solution and a transition temperature within the physiologically relevant regime are important.²⁷

Several thermoresponsive polymers have been intensively investigated for their phase transition temperatures in solution and on surfaces.^{19, 29, 33} To obtain detailed information on the thermal behavior of such polymers their phase diagrams have been determined. For polymers that exhibit a phase transition from a homogeneous phase to a two-phase system with increasing temperature (Figure 2a), a LCST can be pinpointed from the absolute minimum of the demixing curve (Figure 2b).¹⁹ All other points on the demixing curve solely represent temperatures, at which a clouding of the solution occurs due to demixing of the aqueous phase, and are thus called cloud point temperatures (CPT). However, in literature the term LCST is sometimes mistakenly also use for CPTs which are not located at the minimum of the demixing curve.

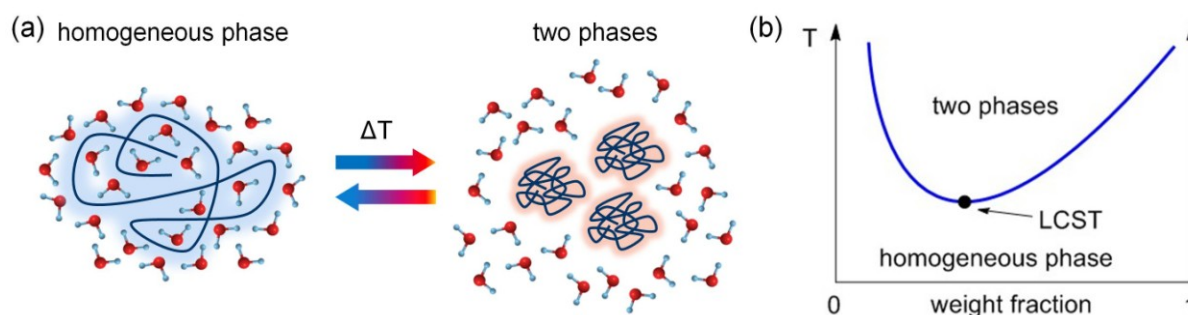


Figure 2 (a) Sketch of the temperature-induced conformational changes of LCST-type polymer chains. (b) A schematically depicted phase diagram of a polymer with a LCST-type phase transition behavior. The LCST corresponds to the absolute minimum of the curve.

Below the LCST, polymer and solvent are miscible in all weight fractions. In order to draw up a demixing curve and characterize the onset of demixing, so the LCST, phase transition temperatures of various polymer-solvent compositions need to be examined. A variety of methods can be utilized to determine phase transition temperatures.

1.2.2 Determination of Phase Transition Temperatures in Solution

Phase transitions of thermoresponsive polymers in solution are commonly investigated by UV-Vis transmittance measurements at a wavelength between 500 and 650 nm, differential scanning calorimetry (DSC), visual determination of turbidity, light scattering at a wavelength between 448 and 654 nm, nuclear magnetic resonance (NMR), and refractometry measurements at a wavelength of 589 nm. Solutions of different polymer-solvent compositions are heated and cooled gradually, while identifying the phase transition.¹⁹

Optical measurement techniques, such as UV-Vis and light scattering measurements as well as visual inspection observe changes in turbidity. In UV-Vis measurements the decrease in transmittance while heating the polymer solution is determined at constant wavelength. The temperature-induced formation of polymer aggregates in solution leads to an increase in light scattering and thus to a decrease in the transmitted light intensity. Important for UV-Vis measurements in order to determine correct CPTs is the absence of any absorption of light by the polymer at the applied wavelength, an adequate temperature increment for the stepwise increase of temperature and a sufficient equilibration time at the respective temperature before the measurement.³⁴ Alternatively, the change in intensity of scattered light can be measured at different angles and at a distinct wavelength by dynamic and static light scattering.¹⁹ In dynamic light scattering the fluctuation in scattering intensity of single polymer coils or polymer aggregates is studied, whereas in static light scattering the time-averaged scattering intensity is determined. For both methods the temperature-dependent polymer coil or aggregate sizes influence the scattering intensity. However, a certain minimum scattering intensity and thus a certain minimum molecular weight is required in order to determine reliable phase transitions by scattering techniques. The refractive index of a polymer solution can be determined by refractometry measurements. The refractive index is related to the specific volume of a probe, which is temperature dependent and to the molecular bond polarisability, namely the specific refractivity. For most materials, the latter is almost independent of temperature and pressure. For thermoresponsive polymer solutions, however, considerable changes in specific refractivity upon phase separation can be detected by refractometry.³⁵

The DSC is a thermoanalytical technique, which measures the difference in heat flow required to maintain the same temperature in sample and reference, while the sample is undergoing a phase transition. For polymers exhibiting a LCST, demixing is associated with an endothermic process observed by DSC. The onset of the endotherm is assumed to be related to the beginning coil-to-globule transition, whereas the peak of the endotherm might indicate the formation of aggregates from the globular polymer chains.^{19, 36} The preaggregation event during the coil-to-globule transition can also be observed by NMR spectroscopy in D₂O, revealing peak shifts and peak broadening, induced by changes in the hydration environment of certain chemical groups of the polymer.³⁷⁻³⁸

The particular measurement technique influences the precise outcome of the phase transition temperature. Therefore, when comparing phase transition temperatures the method with which it was determined should always be stated. Besides the specific measurement technique, the criterion defined to identify the demixing temperature, the temperature scan rate and range as well as the respective wavelength in optical measurements, impact the resulting demixing curve and thus the derived LCST.¹⁹ Criteria for the identification of the phase transition temperature differ for the particular measurement techniques. Phase transition temperatures deduced from transmittance measurements, for example, were identified either at the point of first deviation from the base line of the transmittance curve, at 2, 10, or 50% reduction in transmittance or from the inflection point of the transmittance curve.^{19, 34} Demixing temperatures determined from DSC measurements, were deduced from the onset of the endotherm, the maximum of the DSC endotherm, the maximum of the derivative of the DSC heating endotherm, or more complex approaches.¹⁹

Measurements at different temperatures and thus heating and cooling are indispensable to determine phase transition temperatures. Heating and cooling rates are commonly chosen between 0.025 and 1 K min⁻¹, with and without equilibration at each temperature step. High heating and cooling rates might provoke a hysteresis, with remixing temperatures being lower than demixing temperatures (see Figure 4b). More details on the hysteresis in phase transition are given in Chapter 1.2.3. Optical methods to determine the phase transition which rely on transmittance and scattering intensity are impacted by the applied wavelength and wavelength-dependent refractive index, thus different light sources might alter the results.¹⁹

1.2.3 Thermoresponsive Polymers for Cell Sheet Engineering

PNIPAM is the most popular thermoresponsive polymer in general and for application in cell sheet engineering in particular. LCSTs between 24 and 34 °C, were reported for PNIPAM, which is within the relevant temperature range for cell sheet fabrication.¹⁸⁻¹⁹ Besides the PNIPAM homopolymer several PNIPAM copolymers have been investigated for their thermal behavior in aqueous solution and for their performance in cell sheet fabrication. Incorporation of a more hydrophobic comonomer, such as *N-tert*-butylacrylamide (NtBAM),³⁹⁻⁴² *N-n*-butylacrylamide,⁴³ and *N*-(1-phenylethyl)acrylamide,⁴⁴ in a PNIPAM copolymer decreases the

phase transition temperature. Copolymerization of NIPAM with more hydrophilic monomers, such as diethylene glycol methacrylate,⁴⁵ hydroxypropyl methacrylate,⁴⁶ ethylpyrrolidone methacrylate,⁴⁷ *N,N*-dimethylaminopropyl acrylamide,⁴² 3-acrylamidopropyl trimethylammonium chloride,⁴² *N*-vinylacetamide,⁴⁸ and acrylic acid,⁴⁸ in turn, increases the phase transition temperature.

In search of novel, PNIPAM-free, thermoresponsive polymers, suitable for cell sheet engineering, poly(2-alkyl-2-oxazoline),⁴⁹⁻⁵⁰ oligoethylene glycol-based poly[2-(2-methoxyethoxy)ethyl methacrylate-*co*-oligo(ethylene glycol) methyl ether methacrylate] (poly(MEO₂MA-*co*-OEGMA))⁵¹⁻⁵⁴ and poly[tri(ethylene glycol) monoethyl ether methacrylate],⁵⁵ poly(*N*-vinylcaprolactam),⁵⁶ poly(glycidyl ether)s,⁵⁷⁻⁵⁸ and poly(vinyl methyl ether)s,⁵⁹ as well as elastin-like peptides/polymers,⁶⁰⁻⁶² and methylcellulose hydrogels⁶³⁻⁶⁵ have been developed. Their chemical structures are given in Figure 3.

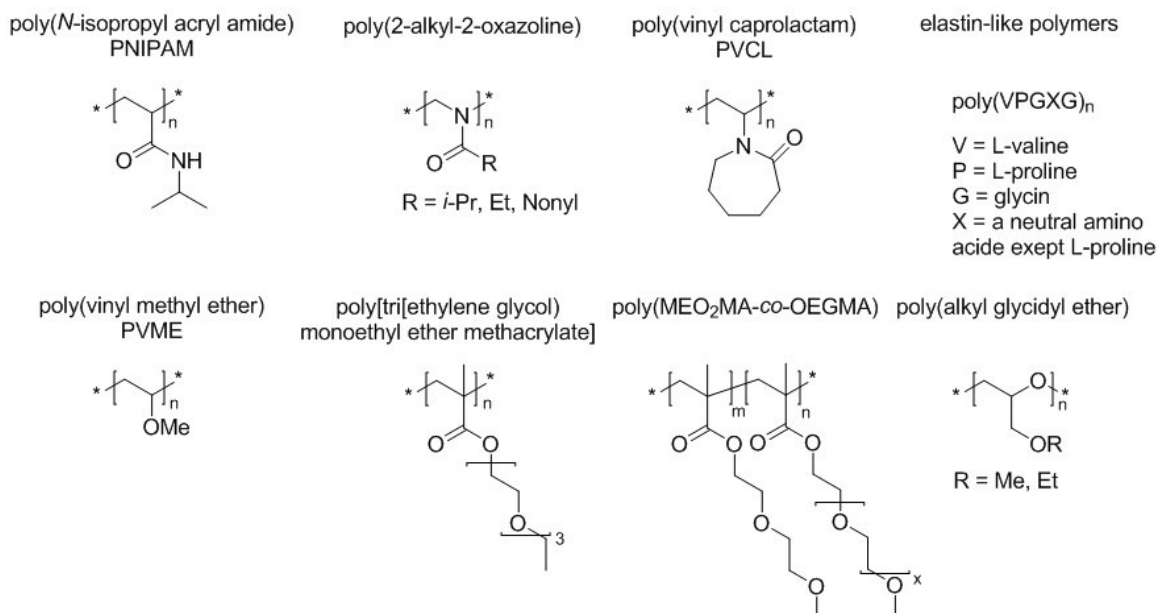


Figure 3 Compilation of selected thermoresponsive polymers applied on surfaces for cell sheet fabrication.

Some of these polymers exhibit phase transition temperatures within the physiologically relevant range only for an appropriate copolymer composition. Phase transition temperatures of low molecular weight (3 kDa) alkyl glycidyl ether-homopolymers, such as poly(ethyl glycidyl ether) (poly(EGE)) and poly(methyl glycidyl ether) (poly(GME)) in aqueous solution, for

example, are 15 and 60 °C, respectively, at a concentration of 1 wt%.⁶⁶⁻⁶⁷ The relation between the comonomer ratio of GME and EGE is strictly linear to the demixing temperature for low molecular weight polymers of 5 kDa.⁶⁸ Therefore, phase transition temperatures of the copolymers of GME and EGE can be tuned to cover the physiologically relevant temperature regime.^{57, 68}

2-alkyl-2-oxazoline-homopolymers such as poly(2-ethyl-2-oxazoline), poly(2-isopropyl-2-oxazoline), and poly(2-*n*-propyl-2-oxazoline) with degrees of polymerization of ~100 exhibit phase transition temperatures of 90, 36, and 25 °C, respectively, determined at a concentration of 5 mg mL⁻¹ in aqueous solution.⁶⁹ Copolymerization of these monomers allows for the adjustment of the demixing temperature between 25 and 90 °C. The type of comonomer distribution within the copolymer, random or gradient, additionally impacts the phase transition behavior of these polymers. For poly(2-alkyl-2-oxazoline) random copolymers no hysteresis between de- and remixing temperatures was observed. Gradient copolymers, however, showed a hysteresis in phase transition at concentrations as high as 5 mg mL⁻¹. This effect disappeared at concentrations as low as 0.5 mg mL⁻¹.⁶⁹ Furthermore, the formation of micelle-like structures was observed for gradient copolymers. The polymer chain end, with more hydrophobic comonomers incorporated, is buried inside the micelle core.⁶⁹⁻⁷⁰ In extreme cases of gradient structures, the polymer behaves more like a block copolymer than a random copolymer.

Thermoresponsive block copolymers can exhibit different types of phase transition behavior. The block besides the thermoresponsive part can either leave the phase transition temperature unchanged, increase or decrease the phase transition temperature or introduce a second responsiveness.²⁹ For block copolymers of PNIPAM and either polystyrene or poly(*tert*-butyl methacrylate) as a second more hydrophobic block, the phase transition temperature is unchanged compared to the one of a PNIPAM homopolymer.²⁹ The incorporation of hydrophobic moieties in a second block does not decrease the phase transition temperature as it does in random or gradient copolymers. The phase transition temperature of block copolymers of PNIPAM and PEO, with a minimum molecular weight of ~ 2 kDa, instead, increased compared to the transition temperature of the PNIPAM homopolymer.⁷¹ An example for a double thermoresponsive polymer is the poly(OEGMA)-*block*-poly(*N*-isopropyl methacrylamide) (PNIPMAM) with a first phase transition at 50 °C ascribed to the collapse of PNIPMAM and a

second transition at 65 °C associated with the dehydration of poly(OEGMA).⁷² The formation of micelle-like structures is commonly observed for block copolymers with parts that differ in hydrophilicity.²⁹

The thermal behavior of a thermoresponsive polymer is thoroughly described by the respective phase diagram (see Figure 2a). The phase diagram compiles phase transition temperatures of a specific polymer in a selected solvent over a wide range of polymer-solvent compositions, thereby revealing the miscibility gap of the polymer with the solvent. Miscibility gaps of thermoresponsive polymers can differ in their width, and in the temperature regime they cover. Phase transition behavior can be assigned to the phenomenological classification of type I, II, and III (cf. Figure 5-8). The LCST of type I thermoresponsive polymers shifts towards lower polymer concentrations with increasing molecular weight, thus the polymer follows the classical Flory-Huggins behavior (cf. Figure 6,7). For polymers of type II the position of the LCST is molecular weight independent (cf. Figure 5). Type III polymers exhibit two LCSTs, one in the low concentration regime, where they behave like a type I polymer and another one in the high concentration regime where they exhibit type II behavior. Accordingly, phase diagrams corresponding to type III polymers are bimodal (cf. Figure 8).^{29, 73}

For some polymer-solvent mixtures high concentration solutions are not accessible, which results in incomplete phase diagrams, possibly without a minimum in the demixing curve. In these cases the LCST cannot be determined.

Phase diagrams of thermoresponsive polymers do not provide information on sharpness and hysteresis of the actual phase transition at a given concentration. The shape of the respective measurement curve can reveal information on the sharpness of the transition. A high slope of a transmittance curve determined by UV-Vis measurements (Figure 4a,b compared to 4c) or a narrow width of an endotherm measured by DSC (Figure 4d) indicate a sharp phase transition. Hysteresis in phase transition can be observed comparing demixing and remixing curves (Figure 4c). The difference in phase transition temperatures determined from heating and cooling curves is attributed to the formation of intra- and intermolecular hydrogen bonds and aggregation during demixing. Consequently remixing is retarded as it requires breaking up of these previously formed hydrogen bonds and aggregates to allow dissolution.³⁴ Prolonged times above the phase

transition temperature might result in macroscopic phase separation with a polymer-enriched phase of high density and a dilute phase. In the polymer-enriched phase a kind of partial vitrification might take place, which further decelerates remixing of polymer and solvent.²⁹

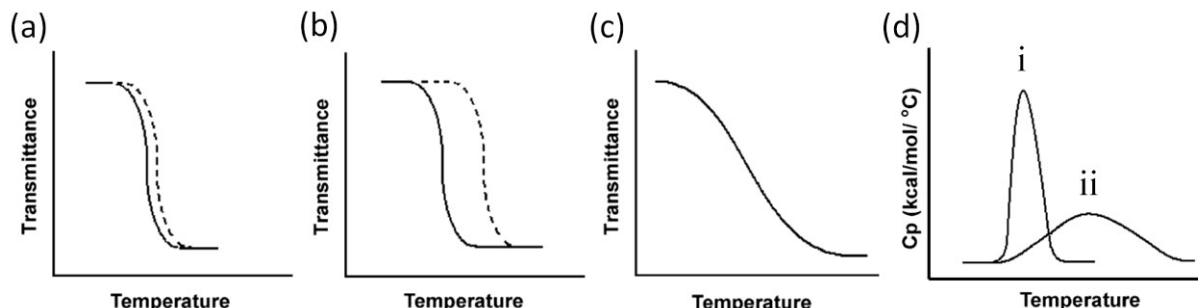


Figure 4 Turbidity curves (a-c) and thermogram shapes (d) for thermoresponsive polymers exhibiting a LCST. (a) Sharp, reversible phase transition with low hysteresis. (b) Sharp phase transition with pronounced hysteresis between heating (dashed line) and cooling (solid line) curves. (c) Gradual phase transition. (d) Thermogram with different shapes: A narrow (i) and a broader (ii) endotherm.¹⁰

For PNIPAM in water numerous phase diagrams were compiled covering various concentration regimes and different molecular weights (Figure 5).¹⁹

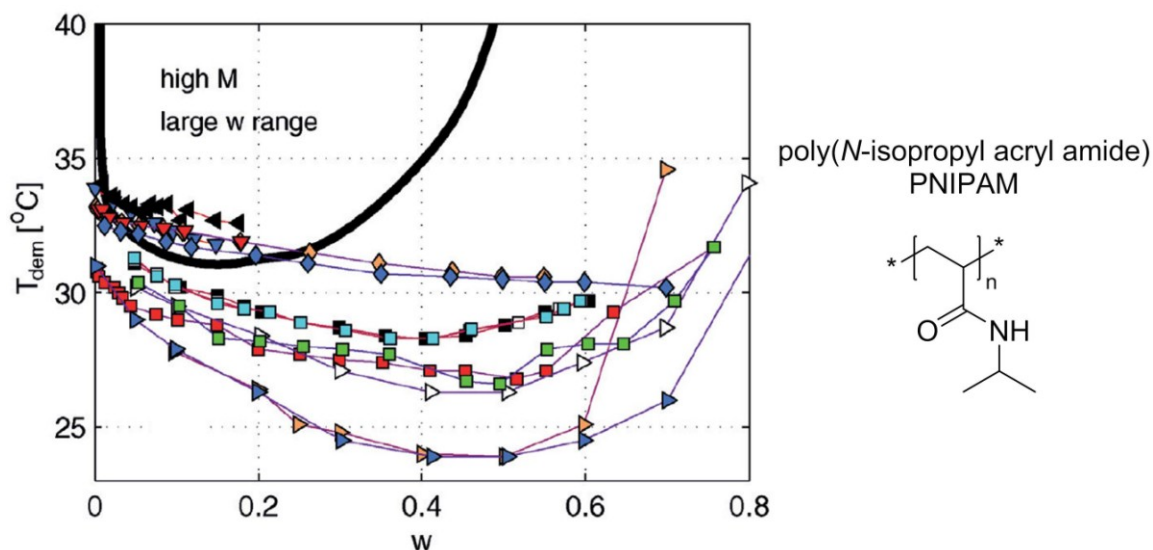


Figure 5 Compilation of phase diagrams of high molecular weight PNIPAM reported by different researches, indicated by the different symbols. Phase transition was investigated over large weight fraction (w) ranges, recorded at different heating rates via different measurement

techniques. The solid line represents the first phase diagram ever stated for PNIPAM by Heskins and Guillet.¹⁹

These phase diagrams differ depending on the covered concentration regime and on experimental factors, such as the measurement technique, temperature ramping and the criterion to define the point of read-out for the phase transition temperature.^{19, 34} The shape of the demixing curve as well as the weight fraction corresponding to the LCST vary, however, the origin of this divergence is not yet understood.¹⁹ The LCST was observed to be rather unaffected by the molecular weight, therefore PNIPAM was classified as a polymer with a type II phase transition behavior.^{29, 73} The reported LCSTs range from about 24 to 34 °C at weight fractions of polymer in solvent around 0.5.¹⁹ The sharpness of phase transition as well as the hysteresis in phase transition between heating and cooling of PNIPAM is concentration and heat rate dependent.^{19, 34} The highly systematic study of Osváth *et al.* revealed a sharp phase transition for concentrations ranging from about 20 to 0.1 wt%. Only for lower concentrations the slope of the transmittance curves decreased. Furthermore, Osváth *et al.* observed a minimal width of hysteresis (<1 °C) for a concentration of 5 wt%. For lower and higher concentrations the difference between the phase transition temperatures deduced from demixing and remixing curves increased up to 7 °C.³⁴

Phase diagrams of poly(*N*-vinyl caprolactam) (PVCL) dissolved in water were also determined for polymers of different molecular weights (Figure 6).⁷³ The LCST of PVCL shifts with increasing molecular weight, to both lower weight fractions and lower temperature, thus PVCL follows the Flory-Huggins miscibility behavior and is therefore classified as type I thermoresponsive polymer.^{29, 73} Meeussen *et al.* observed a LCST of 30 °C for a 275 kDa PVCL and a LCST of around 37 °C for a 9 kDa polymer.⁷³ The weight fractions corresponding to the LCSTs of PVCL were close to 0.1 and therefore low compared to the weight fractions of around 0.5 observed at the LCST of PNIPAM. For PVCL gels no hysteresis between temperature-dependent gel collapse and swelling curves was observed.⁷⁴

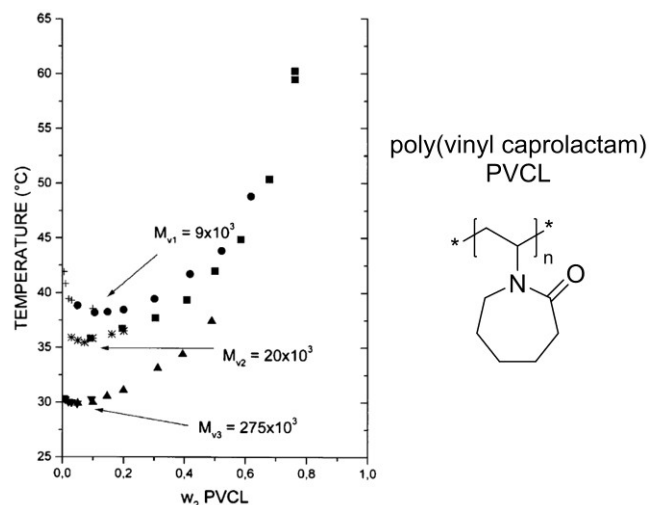


Figure 6 Phase diagrams of PVCL in water for three samples with molecular weights of 9, 20, and 275 kDa. Solid circle, square and upright triangle symbols represent demixing temperatures determined by DSC measurements at a heating rate of $3\text{ }^{\circ}\text{C min}^{-1}$, whereas crosses, stars and downward pointing triangles identify cloud point temperatures obtained from turbidity measurements at a heating rate of $2\text{ }^{\circ}\text{C min}^{-1}$.⁷³

For poly(2-ethyl-2-oxazoline) in water phase diagrams also suggest a type I phase transition behavior (Figure 7).⁷⁵

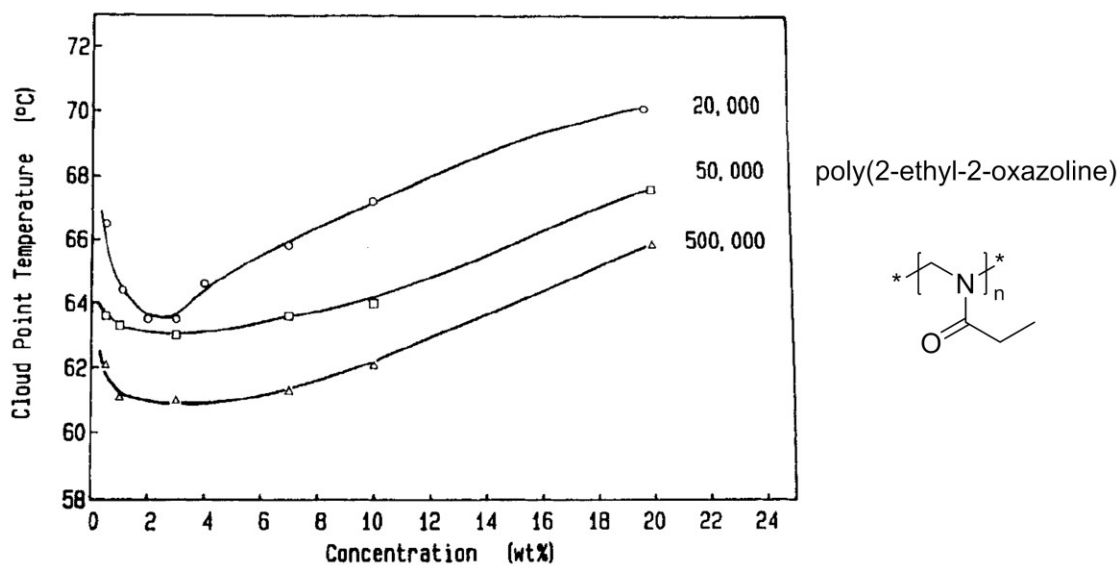


Figure 7 Phase diagrams of poly(2-ethyl-2-oxazoline)s in water were determined for three samples with molecular weights of 20, 50, and 500 kDa. Cloud point temperatures were determined by visual observation and averaged from the temperatures obtained at a heating rate of approximately $0.6\text{ }^{\circ}\text{C min}^{-1}$ and a cooling rate of $0.3\text{ }^{\circ}\text{C min}^{-1}$.⁷⁵

LCSTs of poly(2-ethyl-2-oxazoline) range from 61 to 64 °C depending on the molecular weight (20 to 500 kDa) at weight fractions below 3 wt%.⁷⁵⁻⁷⁶ For other poly(2-alkyl-2-oxazoline)s no phase diagrams were reported, but phase transition temperatures, adjustable from 25 to 100 °C, were investigated at selected concentrations by a variety of methods.³³ Poly(2-alkyl-2-oxazoline)s exhibit sharp phase transitions in 1 wt% aqueous solutions, even for gradient copolymers.⁷⁷ For sufficiently high concentrations of poly(2-alkyl-2-oxazoline)s in aqueous media only minor or no hysteresis of the phase transition was observed.^{70, 78} Oleszko-Torbus *et al.*, however, reported on hysteresis of up to 9 °C for gradient copolymers of poly(2-alkyl-2-oxazoline)s with molecular weights of around 10 kDa at a concentration of 5 mg mL⁻¹ in water determined by turbidity measurements.⁶⁹

Phase transition temperatures of poly(vinyl methyl ether) (PVME) dissolved in water are strongly influenced by concentration and molecular weight. PVME is an example for a type III thermoresponsive polymer with a bimodal phase diagram (Figure 8).⁷⁹

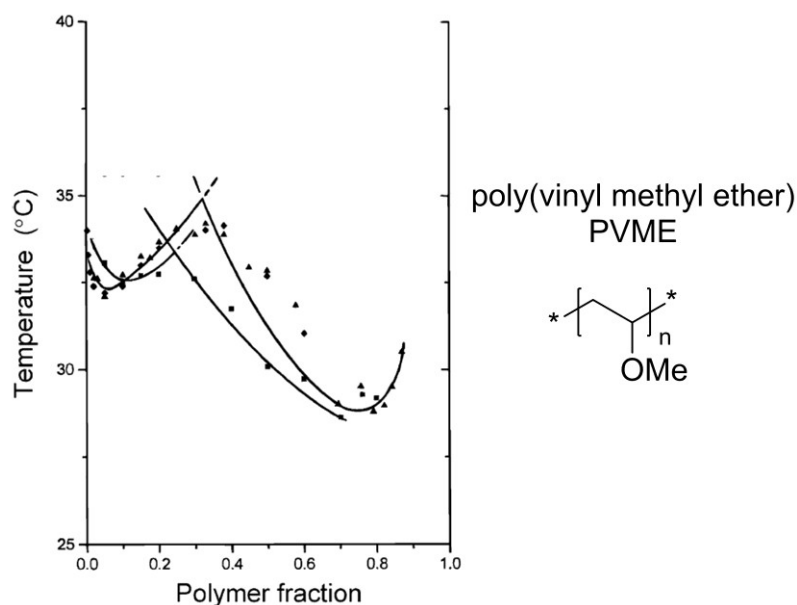


Figure 8 Bimodal phase diagram of PVME in water for two samples with molecular weights of 11 and 19 kDa. Demixing temperatures were obtained from the onset of the endotherm determined by DSC measurements at heating rates of 0.1 °C min⁻¹.

At low concentrations the critical point is molecular weight dependent and ranges from 32-33 °C at a molar fraction below 30 wt%. At high concentrations (molar fraction > 30 wt%) the critical solution temperature is molecular weight independent and at approximately 28 °C.^{29, 33, 73}

All other thermoresponsive homo- and copolymers applied in cell sheet engineering have only been investigated for some phase transition temperatures at selected concentrations, but no phase diagrams have been compiled. Therefore their LCSTs are unknown.

Poly(MEO₂MA-*co*-OEGMA) exhibits phase transitions in water without considerable hysteresis between heating and cooling cycles. UV-Vis transmittance curves reveal a rather steep slope, indicating a sharp phase transition (cf. Figure 4a). The phase transition temperature of a poly(MEO₂MA-*co*-OEGMA) with 5% OEGMA units was molecular weight independent at a constant concentration. With increasing concentration from 1 to 10 mg mL⁻¹ demixing temperatures shifted from 35 to around 32 °C.⁸⁰⁻⁸¹

Phase transition temperatures of poly(glycidyl ether)s are strongly affected by the alkyl side chain, the molecular weight and the concentration of the solution.⁶⁶⁻⁶⁸ Poly(GME-*ran*-EGE) in aqueous solutions only reveal small hysteresis between heating and cooling curves. Furthermore, phase transition regimes sharpen with increasing molecular weight and concentration.⁸²

1.2.4 Parameter to Adjust Phase Transition Temperatures

A variety of parameters, such as polymer composition, molecular weight of the polymer, polymer concentration in solution or grafting densities on surfaces, as well as additives in the solvent, like salts, impact the phase transition temperature.

For biological applications of LCST-type thermoresponsive polymers, the phase transition temperatures in buffered solutions, such as cell culture medium or phosphate buffered saline (PBS), are more relevant than transition temperatures in water.⁸³ For a variety of thermoresponsive polymers a decrease in phase transition temperature is observed in the presence of kosmotropic ions, such as NH₄⁺, K⁺, Na⁺, CO₂²⁻, H₂PO₄⁻, F⁻, Cl⁻.⁸⁴⁻⁸⁸ The so called "salting-out" effect is induced by these small ions with a high charge density as they strongly interact with water thereby altering the hydrogen bond interactions of the thermoresponsive polymer with the surrounding water molecules.⁸⁴⁻⁸⁵

The specific phase transition temperature of a thermoresponsive polymer solution is obviously concentration dependent as illustrated by the phase diagram. For experiments, aside the determination of phase diagrams, a decrease in phase transition temperature with increasing polymer concentration is commonly described, indicating that experiments are often conducted at concentrations lower than the weight fraction corresponding to the LCST. Within this low concentration regime (weight fraction < weight fraction at LCST), intermolecular interactions are more pronounced for higher concentrations as decreasing distances between polymer chains enhance collision frequency and sticking probability of the more hydrophobic parts of the polymer chains.^{29, 82}

The molecular weight of the polymer impacts the phase transition temperature not only for type I and III thermoresponsive polymers but also for type II polymers in dilute solutions. Under high dilution conditions the local concentration of polymer segments is higher for larger polymers. Similar to high concentrations in general, intramolecular interaction of the polymer segments is more likely at high local concentration. Thus the phase transition temperature in dilute solutions is decreased with increasing molecular weight.⁸² Such molecular weight and concentration dependence of the phase transition temperature was observed for PNIPAM⁸⁹⁻⁹⁰, poly(2-ethyl-2-oxazoline)⁹¹ and p(GME-*co*-EO)⁹². A rather low concentration and molecular weight dependence of the phase transition temperature, instead, was reported for poly(MEO₂MA-*co*-OEGMA)⁸⁰ at low molecular weights (2 kDa to 11 kDa) as well as for high molecular weight PNIPAM (molecular weights > 30 kDa)^{90, 93}.

The strongest impact on the phase transition temperature of thermoresponsive polymers, however, has the incorporation of either hydrophilic or hydrophobic moieties either via copolymerization as discussed in 1.2.3 or via postmodification.

The phase transition temperature of polymer chains tethered to a surface might additionally be influenced by the underlying substrate material and its hydrophilicity,⁹⁴⁻⁹⁵ or by functional end-groups.⁹⁶ The grafting density of polymer chains on surfaces might influence the phase transition temperature of the polymer similarly as the polymer concentration does in solution.

1.2.5 Determination of Phase Transition Temperatures on Surfaces

Methods to determine the phase transition temperature of thermoresponsive polymers on surfaces differ from those suitable for studies in solution. Measurement techniques, such as quartz crystal microbalance with dissipation (QCM-D) (Figure 9a), ellipsometry (Figure 9b), contact angle (Figure 9c), and atomic force microscopy (AFM) (Figure 9d) measurements are applied in order to determine phase transitions on surfaces.

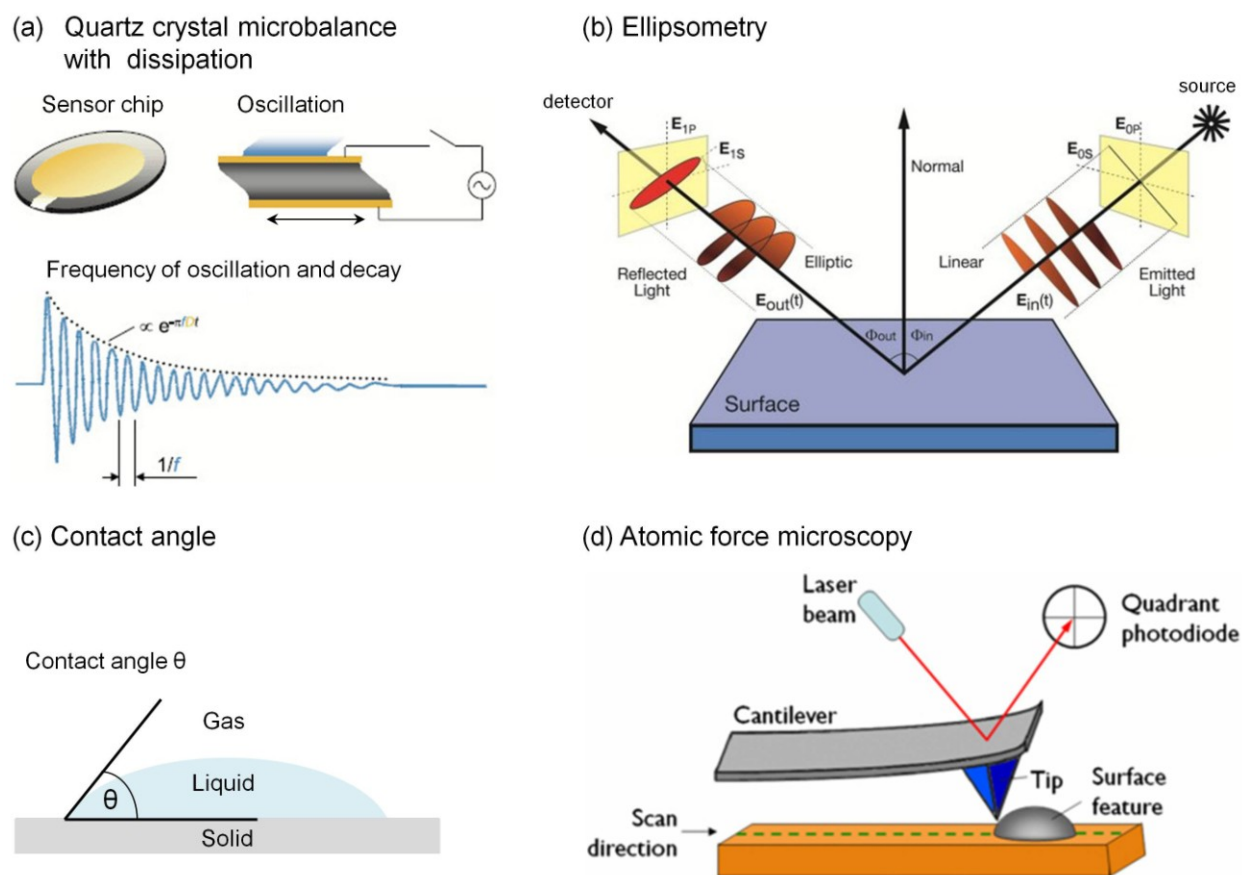


Figure 9 Schematic representations of methods to determine surface characteristics and phase transition on surfaces. (a) QCM-D measurements reveal solvated layer thicknesses and the amount of mass closely associated with the surface.⁹⁷ (b) The dry layer thickness of thin polymer films can be determined by ellipsometry measurements.⁹⁸ (c) Contact angle measurements reveal the surface hydrophilicity. (d) By AFM surface morphology and layer thickness can be visualized.⁹⁹

QCM-D measurements detect shifts in the frequency of oscillation of the quartz crystal, which are induced by changes in the mass closely associated with the surface. The phase

transition can be monitored by this technique, as a swollen coating contains more water and therefore couples more mass to the sensor surface compared to a collapsed coating. During the thermally-induced collapse of a coating, a decrease in mass and thus an increase in frequency is observed. Additionally, changes in dissipation (the decay of the frequency of oscillation) can point out conformational alteration of the surface coating, as a swollen, viscoelastic coating dampens the oscillation more severely compared to a collapsed, and thus stiffer coating.¹⁰⁰⁻¹⁰² Ellipsometry measurements of thermoresponsive coatings in aqueous solution reveal changes in layer thickness upon swelling and collapse, induced by an alteration of the hydration of the bulk polymer.^{101, 103} Contact angle measurements, instead, demonstrate changes in surface hydrophilicity. AFM measurements can evidence differences in the coatings morphology and in layer thickness below and above the phase transition temperature.¹⁰²⁻¹⁰³

1.3 Thermoresponsive Surfaces for Cell Sheet Engineering

Under standard cell culture conditions at 37 °C surface-confined, thermoresponsive polymer chains are collapsed, poorly hydrated and coatings are, in some cases, hydrophobic. Coatings allow for protein adsorption from cell culture medium and for subsequent, protein-mediated attachment and proliferation of adherent cells. A decrease in temperature below the phase transition temperature, however, results in improved hydration and thus swelling of the polymer chains and in a possibly increased surface hydrophilicity of the coating. This transition deteriorates protein adhesion and triggers detachment of cells together with their ECM. In Figure 10 cell adhesion and thermally-induced cell sheet detachment are depicted schematically.

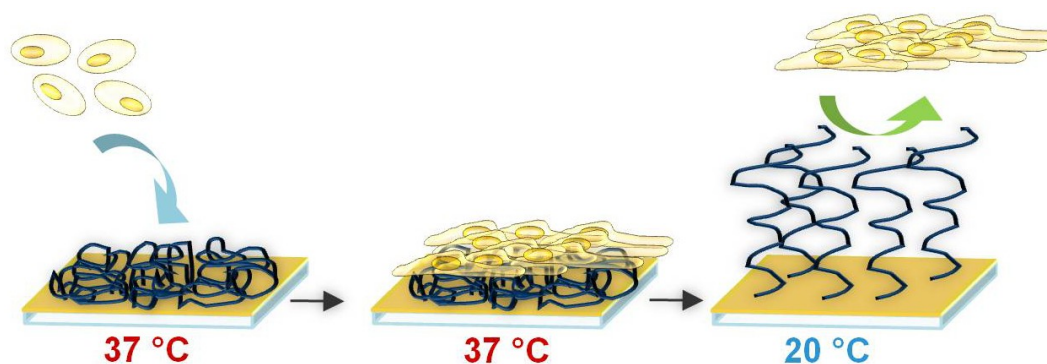


Figure 10 Scheme of cell adhesion, proliferation, and temperature-triggered cell sheet release from thermoresponsive polymer coatings.

Thermoresponsive surface coatings suitable for cell harvesting have been prepared by a variety of methods on several substrate materials, such as polystyrene^{7, 104-107}, glass^{50-51, 55, 108-109}, and gold¹¹⁰⁻¹¹¹. The structural precision of the resultant coating, surface-tethered polymer brush or hydrogel, depends on the applied coating technique. Schematic representations of some coating techniques and polymeric coatings are shown in Figure 11.

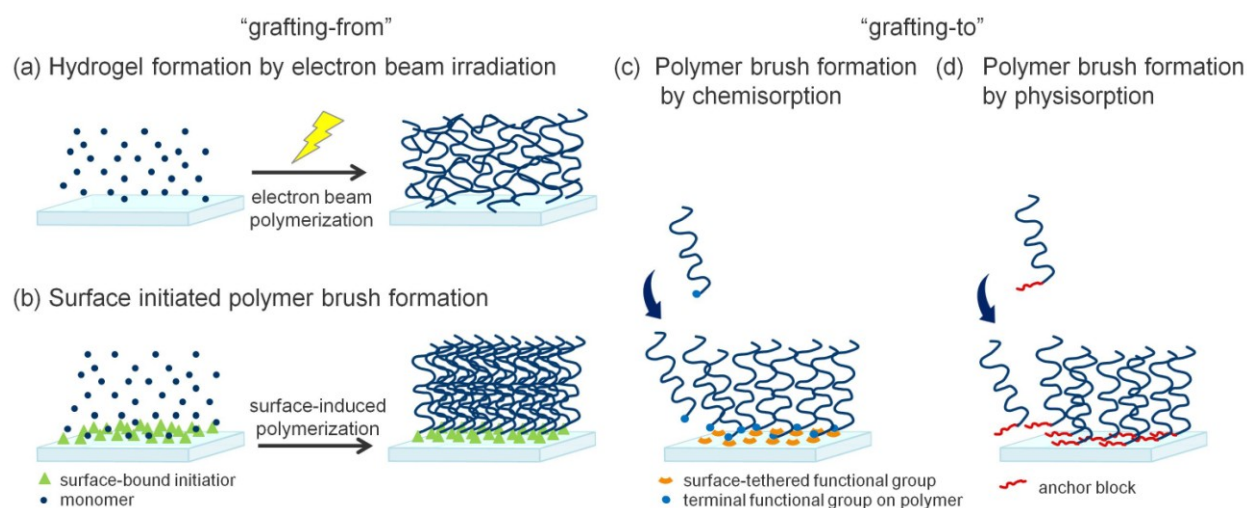


Figure 11 Selected surface coating techniques, "grafting-to" and "grafting-from", respectively, to form polymer brush and hydrogel coatings.

Hydrogels usually possess a lower structural precision than surface-tethered polymer brushes, due to an often uncontrolled and poorly defined crosslinking (Figure 11). Nevertheless, thermoresponsive hydrogels were prepared by a variety of methods, comprising irradiation-induced polymerization, chemical vapor deposition, and sol-gel formation.

In 1990 Okano and coworkers prepared the first thermoresponsive coatings for cell sheet fabrication by electron beam irradiation of NIPAM on tissue culture polystyrene (TCPS) dishes (cf. Figure 11a).¹⁰⁴ This coating technique is nowadays applied to produce the commercially available PNIPAM-coated polystyrene-based cell culture ware, traded under the name UpCell™.¹⁵ Polymerization by electron beam irradiation is prone to batch-to-batch variability and generates, as already mentioned, hydrogel layers with a poorly defined structure.¹¹²⁻¹¹⁴ Nevertheless, this method was applied on several substrate materials comprising polystyrene^{15, 115-117}, glass^{108, 114} and poly(ethylene terephthalate) (PET) porous membranes¹¹⁸. To date,

electron beam irradiation is one of the most successful approaches to prepare thermoresponsive coatings for cell sheet fabrication, however, requires expensive technology and expertise.¹²

Not only PNIPAM but also thermoresponsive poly(vinyl ether) hydrogels were prepared by irradiation polymerization. These coatings, however, require a modification with cell adhesive moieties, such as RGD peptides, laminin or chondroitin-6-sulfate, to allow for cell adhesion and proliferation.^{59, 119}

Another method to prepare thermoresponsive hydrogels is the plasma polymerization of NIPAM vapor which was applied for PNIPAM deposition on glass substrates, silicon wafers and TCPS.^{5, 7, 120} This method is an one-step, solvent-free, vapor-phase approach, but similar to electron beam irradiation, expensive and often not commonly available. Plasma polymerization is furthermore susceptible to monomer fragmentation associated with a possible loss of functionality.

An irradiation-free approach to generate thermoresponsive hydrogels is the initiated chemical vapor deposition, which was applied to generate poly(*N*-vinyl caprolactam) hydrogels on glass substrates.⁵⁶

All these precedingly described methods are highly equipment-demanding and thus unavailable to most laboratories.

A more accessible and less equipment-demanding method to prepare functional cell culture supports, relies on copolymerization of NIPAM and acrylamide benzophenone (AcBzPh). Such copolymers allow for the generation of UV-crosslinked hydrogels on polystyrene and PET substrates.¹²¹ Other simple approaches, to prepare thermoresponsive hydrogels on TCPS dishes, are solvent-casting or spin-coating of methylcellulose with subsequent gelation at 37 °C.⁶³⁻⁶⁵ Although methylcellulose hydrogels benefit from a straightforward preparation technique, these surfaces suffer from poor cell adhesiveness and thus require a collagen treatment in order to be applicable in cell sheet fabrication.

The low structural precision of thermoresponsive hydrogels, with the need for cell adhesive modifications, in some cases, renders meaningful correlations of detailed surface parameters with biological response difficult or even unfeasible.

Somewhat more defined polymer brushes can be prepared by surface-induced controlled living polymerizations (Figure 11b).^{53-55, 109, 113, 122-123} Surface parameters, such as layer thickness, grafting density, and molecular weight of the polymer chains, are generally adjustable by "grafting-from" methods, but are often poorly characterized.¹²⁴⁻¹²⁵ In many studies, surface characterization is limited to layer thickness and morphology determination, neglecting a thorough analysis of grafting density, molecular weight and polydispersity of the polymer chains within the coating.^{51, 113, 123} Molecular weight and polydispersity of the surface-tethered polymers can be precisely characterized when applying cleavable surface-bound initiators, which allow for the release of the polymer (e.g. via hydrolysis), and a subsequent characterization via GPC or Maldi-TOF measurements.¹²⁵ Nonetheless, molecular weights and polydispersities are oftentimes only approximated, assuming comparable polymerization kinetics of monomers on the surface and in solution.^{55, 122} Furthermore, grafting densities of polymer chains within brush coatings are commonly approximated by the average density of the preassembled initiator on the surface, thereby disregarding the actual surface-induced grafting efficiency.^{109, 122} The consequentially vague chain density approximations hinder valid comparisons between coatings originating from different studies or prepared by different coating approaches.¹²⁵

Surface-induced polymerization, however, yields exceptionally high grafting densities, especially for sterically-demanding high molecular weight polymers.¹²⁴ Moreover, surface-induced polymerization enables the preparation of gradient structures. Such gradient polymer brushes allow for the correlation of layer thickness with cell response within a fully identical setting.¹²³

Thermoresponsive polymer brushes of PNIPAM and oligoethylene glycol methacrylate-based polymers prepared by "grafting-from" are successfully applied in cell sheet fabrication.^{51, 55, 113, 122}

Coatings with a high structural precision can be prepared by "grafting-to" approaches (Figure 11c,d). Extensively characterized polymers with well-known molecular weights, polydispersities, chemical compositions and anchor moieties can be applied for a straightforward generation of surface coatings. These detailed information on the polymers combined with a defined amount of deposited polymer mass and a known coating morphology, allow for the

precise determination of the polymers' grafting density. Hence, an in-depth understanding of the thermoresponsive coating can be achieved.¹²⁵⁻¹²⁸ Simple "grafting-to" approaches comprise methods like solvent casting,^{41, 129} spin coating,^{46, 130-132} dip coating,^{39, 58, 110-111} and the preparation of Langmuir films.¹³³⁻¹³⁴ Coatings applied for cell sheet fabrication were prepared by the aforementioned methods with PNIPAM, OEGMA-based polymers and poly(glycidyl ether)s. A more preparatively challenging "grafting-to" approach is the surface-induced termination reaction applied for the generation of poly(oxazoline) coatings.⁵⁰

"Grafting-to" strategies can result in both covalently and non-covalently immobilized polymer coatings.¹³⁵ Covalent attachment commonly involves reactive groups on the surface which allow coupling with an appropriately-functionalized, reactive polymer chain (cf. Figure 11c).^{46, 50, 136-139} Polymer brushes can be obtained either from polymers with one functional, terminal group or from block copolymers with a suitable anchor block (cf. Figure 11d).¹²⁴ The self-assembly of polymers, in order to generate polymer brushes, relies on substrate specific driving forces which are described for gold, glass and synthetic polymer substrates in detail in the following chapter 1.3.1.

1.3.1 Defined Coatings Prepared by Self-Assembly

The formation of self-assembled monolayers (SAMs) of alkylthiols on gold was intensively investigated over the last decades.¹⁴⁰⁻¹⁴¹ The main driving force for such self-assembly processes is the formation of the chemisorptive bond between thiol and gold, which gains a binding energy of 40-50 kcal mol⁻¹.^{140, 142} In the case of alkylthiols an additional contribution is made by van der Waals' interactions between the methylene groups of the staggered alkyl chains with 1.0 to 1.9 kcal mol⁻¹ for each methylene group.¹⁴³ Furthermore, the entropy of the system is increased due to the release of solvent molecules which surrounded the thiol group.¹⁴²

The spatial arrangement of thiolate groups on gold surfaces is dictated by the nearest-neighbor distance between the gold atoms (Figure 12). The geometric structure of alkylthiols assembled on gold, however, is influenced by additional parameters, such as the alkyl chain length and functional end-groups. These structures are therefore complex and still under debate.¹⁴⁰ The self-assembling process can be divided in two steps, the initial fast adsorption within the first minute which accounts for 90% of the final film thickness and contact angle and

the slow rearrangement step which takes several hours.¹⁴¹ Rearrangement can take place as the reaction between thiolates and gold is fully reversible.¹⁴⁰ Adsorption and rearrangement rates of alkylthiols within SAMs are dependent on the alkyl chain length.¹⁴¹

For thiol-terminated polymer chains, grafting densities are much lower compared to those observed for alkylthiols, due to the high sterical demand of the polymer. A commonly observed nearest-neighbor distance of alkylthiolates on a Au(111) lattice, with a $(\sqrt{3} \times \sqrt{3})R30^\circ$ arrangement (Figure 12), is 0.5 nm which translates into a density of 4.6 molecules nm⁻².¹⁴⁴

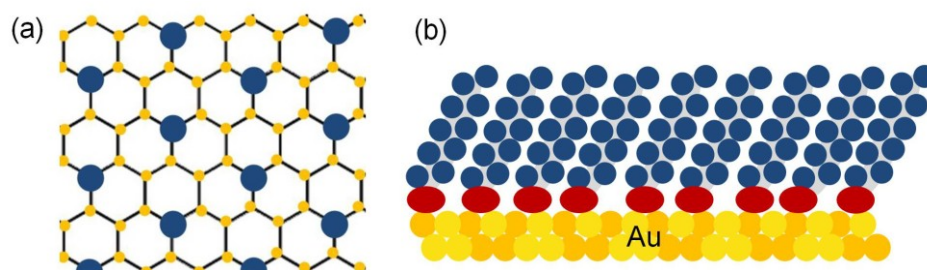


Figure 12 Schematic representation of the $(\sqrt{3} \times \sqrt{3})R30^\circ$ arrangement of alkylthiolates (large blue circles/chains) on a Au(111) lattice, with the gold atoms being represented as small yellow circles in (a) topview and (b) sideview. Alkyl chains are tilted in an angle of 30° to the substrate normal.

Instead, grafting densities of thiolated PEG, with different molecular weights, assembled on amorphous gold surfaces were reported to be 0.33 - 0.92 chain nm⁻² for 2 kDa,^{145,146} 0.12 - 0.54 chain nm⁻² for 5 kDa,¹⁴⁵⁻¹⁴⁶ 0.38 chain nm⁻² for 10 kDa,¹⁴⁶ and 0.19 chain nm⁻² for 20 kDa¹⁴⁶ with mercaptoacetic acid or ethylene thiol anchor groups, respectively. Thiolated PNIPAM with a molecular weight of 3 kDa, chemisorbed on gold surfaces by self-assembly in methanol solution at room temperature, reached a density of 0.22 chain nm⁻².¹²⁷

Substrate specific modification of glass surfaces is commonly based on the self-assembly of silane moieties, as well as on multivalent ionic interactions between the negatively charged glass surface and a positively charged polymer.

Trichloro- or trialkoxysilane groups can covalently and irreversibly attach to hydroxylated surfaces, such as glass or silicon wafers with a silicon dioxide top layer, and thereby form chemically and mechanically robust layers.^{141, 147} The in-situ crosslinking of silane groups to

polysiloxane provides the driving force of the assembly process.¹⁴⁸ Such covalent siloxane networks do not exhibit long-range molecular orders such as thiol-based SAMs, but still ultimately determine the molecular packing.¹⁴¹ Trichloro- or trialkoxysilane groups are sensitive towards hydrolytic cleavage.¹⁴⁷ Reaction with water on the one hand promotes the formation of well-packed monolayers, when traces of water are adsorbed on the surface. On the other hand water hydrolyzes the silane groups and thereby renders them surface-unreactive. The emerging hydroxyl groups, react with remaining, non-hydrolyzed silyl groups and can thus form multilayer networks.^{141, 147}

Polymer brushes on glass surfaces can be formed by covalent attachment of polymers equipped with an organosilane moiety in terminal position.¹⁴⁹⁻¹⁵² Alternatively, the substrate can be modified by silanization in order to generate reactive groups on the surface which allow coupling with appropriately end-functionalized polymers.¹³⁶⁻¹³⁸

Self-assembly of polymers on glass surfaces can furthermore, rely on physisorption of organic cations, such as quaternary ammonium salts.¹⁴¹ Ionic adsorbate-surface interactions between the negatively charged glass surface and the positively charged anchor group allow for the growth of monolayers.^{141, 153-154} These ionic interactions are essentially entropy-driven, gaining degrees of freedom for water molecules and small counterions, when released from the charged surface or from charged polymer anchor groups. The net energy of ion pair formation, however, is low, contributing only a few kilojoules per mol.¹⁵⁵

Multivalent interactions of positively charged polymers, such as poly(amine)s, with glass surfaces allow for the formation of stable coating.¹⁵⁶⁻¹⁶¹ Block copolymers with a cationic anchor block, physisorbed on glass substrates, are able to build up polymer brushes under the prerequisite of weak interaction between the surface and the brush forming block.^{124, 160-161} These block copolymers possess an enhanced shelf-life compared to silane-terminated polymers and furthermore, prevent the formation of multilayers when adsorbed to glass surfaces.¹⁴¹ The grafting process, however is strongly pH and concentration dependent.^{153-154, 156-157, 162}

A straightforward coating approach of synthetic polymer substrates, like polystyrene or PET, is based on hydrophobic interactions. Hydrophobic interactions are entropically favored, as they reduce the surface area covered by a hydration shell, in which water molecules are translationally

and rotationally restricted.¹⁶³ A variety of block copolymers consisting of a hydrophobic anchor block and a thermoresponsive part were applied to built up polymer brushes suitable for cell sheet fabrication.^{39, 107, 121, 132-134, 164-166}

Substrate-independent surface modification can be achieved by precoating with a polydopamine (PDA) adhesion layer (Figure 13). PDA precoatings form on a variety of substrate materials, such as noble metals, oxide layers, ceramics and synthetic polymers.¹³⁹ The stabilizing interaction between the PDA precoating and the substrate varies for the different materials.¹⁶⁷ For metal oxide surfaces, such as titanium dioxide, the formation of a charge-transfer complexes as well as the development of coordinative bonds with the catechol moiety were suggested.¹⁶⁸⁻¹⁶⁹ Binding via hydrogen bonds was proposed for the interaction between the catechol group and mica surface,¹⁶⁸ the assembly of PDA precoatings on inert polymer surfaces, such as polystyrene, was attributed to van der Waals' interactions,¹⁶⁷ and nucleophile presenting surfaces were expected to form covalent bonds with PDA.¹⁷⁰

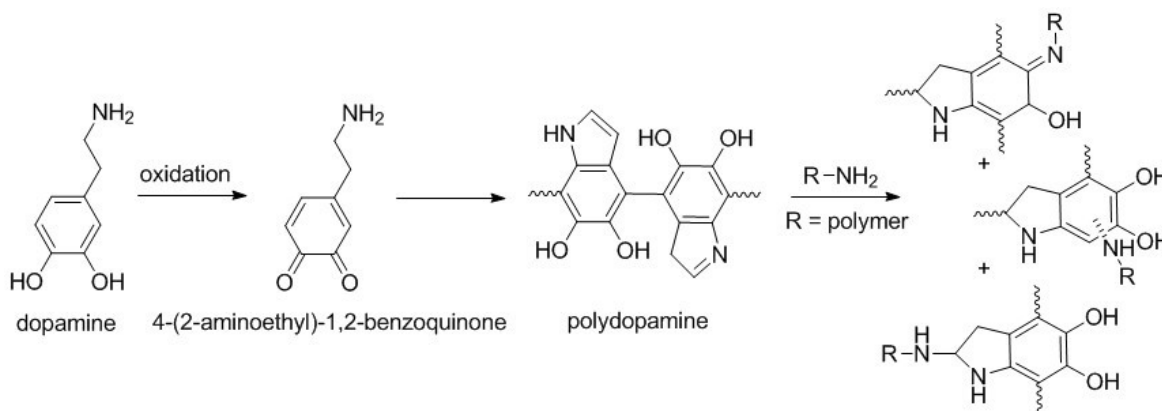


Figure 13 Discussed pathway for the formation of polydopamine and covalent coupling of nucleophilies, such as amines.^{139, 171-172}

Subsequently, polymers with a nucleophilic terminus, such as an amine or thiol group, can be covalently grafted to the PDA precoating via Michael or Schiff base reaction and thereby form polymer brushes that are stably anchored on the surface (Figure 13).^{139, 173}

Taken together, there is a full range of coating techniques reported to prepare thermoresponsive coatings. The coatings vary in their chemical composition and structural

precision. In the following chapter 1.3.2 correlations of surface coating parameters with cell response are discussed.

1.3.2 Correlation of Surface Parameters with Cell Response

Thermoresponsive polymer coatings were intensively investigated for their surface characterizing parameters^{100, 102, 174-175} as well as for their temperature-dependent cell interactions.^{109, 122, 176} However, correlations of both are rarely described in literature. Interesting parameters to be considered for correlations of thermoresponsive brush structures with cell response are chemical composition, molecular weight, and polydispersity of the polymer, layer thickness and chain grafting density (or the reciprocal surface area per polymer chain), as well as degrees of chain overlap, surface morphology, and hydrophilicity above and below the surface's transition temperature. All of these structural surface parameters are directly accessible, without relying on too many theoretical assumptions, for surfaces prepared by a "grafting-to" approach through measurements, such as NMR, GPC, ellipsometry, QCM-D, AFM, XPS and contact angle measurements. Cell adhesion and proliferation can be monitored by microscopic examination, cell viability and metabolic activity accessed by cell assays, and cell sheet detachment can be observed macroscopically.

Particularly well-suited for structure-property correlations are thoroughly characterized polymer brush coatings, prepared by a "grafting-to" approach, which adhere cells without the need of additional cell adhesion promoting biomolecules.^{50, 128, 177} Dworak,⁵⁰ Okano,^{132, 134} Duschl,¹¹¹ Weinhart^{128, 177} and their respective coworkers performed such studies on polymer brush coatings prepared by "grafting-to" approaches, which combine structural parameters with cell response.

Dworak and coworkers reported on poly(2-alkyl-2-oxazoline) brushes, which they prepared by a combined living polymerization/termination reaction on an amino functionalized glass surface (Figure 14).⁵⁰ Polymer brushes of poly(2-isopropyl-2-oxazolines) (PIPOx, 22.5 and 42.0 kDa) and of poly[(2-nonyl-2-oxazoline)-*co*-(2-ethyl-2-oxazoline)] (PENOX, 14.0 to 21.8 kDa) were investigated for their layer thickness and morphology by ellipsometry and AFM measurements, respectively. AFM measurements revealed, that smooth poly(oxazoline) coatings could be obtained only after annealing of the substrates at above 206 °C. Without annealing,

coatings exhibited a crystalline structure. For laterally homogeneous coatings, grafting densities of 0.16 and 0.26 chains nm^{-2} (PIPOx) as well as 0.19 to 0.22 chains nm^{-2} (PENOX) were calculated from layer thickness and molecular weight of the polymer chains. After performing an in-depth characterization of brush coatings of the two thermoresponsive poly(oxazoline)s, PIPOx and PENOX, with varied layer thicknesses (5 to 11 nm) and molecular weights (14 to 42 kDa), Dworak *et al.* only investigated cell adhesion and cell sheet detachment of human dermal fibroblasts on two selected surfaces.

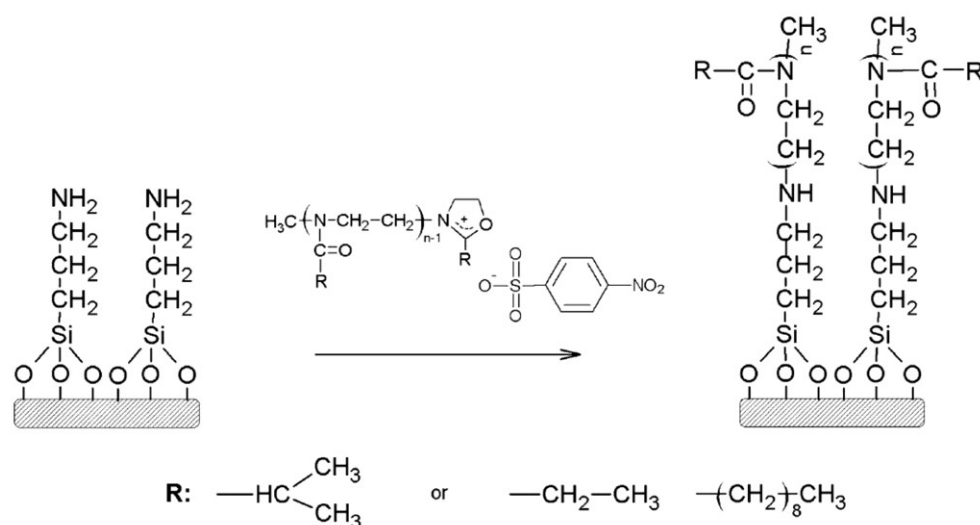


Figure 14 Scheme of the modification of an amino-prefunctionalized glass surface with poly(2-alkyl-2-oxazoline) homo- and copolymers prepared from the monomers isopropylloxazoline, ethylloxazoline and nonylloxazoline, respectively, via living polymerization/termination reaction.⁵⁰

On these two surfaces cells grew similarly to the tissue culture polystyrene (TCPS) control and detached as confluent cell sheets at 20 °C within 30 min. Although, structural parameters and cell behavior were investigated thoroughly, an effect of surface properties on biological response was not extracted.⁵⁰ A follow-up study, however, revealed an enhanced cell adhesion of human dermal fibroblasts on PIPOx (20 kDa) coatings with high crystallinity but an accelerated cell sheet detachment on coatings without crystallites.⁴⁹

Okano and coworkers investigated PNIPAM brush coatings applying different "grafting-to" approaches, the Langmuir-Schaefer method and the self-assembly of block copolymers, respectively.^{132, 134} Sakuma *et al.* prepared brush coatings of PNIPAM (4.7, 13.9, 40.4 kDa),

equipped with a terminal dodecyl group, on hexyltrimethoxysilane-modified hydrophobic glass coverslips by the Langmuir-Schaefer method. The amount of deposited polymer on the glass surface was adjusted by the surface pressure and determined by attenuated total reflectance Fourier-transformed infrared (ATR/FTIR) spectroscopy. For the polymers with different molecular weights, assembled in varied amounts of PNIPAM molecules at the air-water interface (0.5 , 1 and $2 \mu\text{g cm}^{-2}$), amounts of polymer within the coating were determined to be 0.45 to $1.18 \mu\text{g cm}^{-2}$. Meaningful average grafting densities of the polymer chains, however, could not be deduced from these results due to some surface inhomogeneities indicated by AFM measurements. Within this study, adhesion of bovine carotid artery endothelial cells (BAECs) was observed to be similar for all investigated PNIPAM coatings. Coatings with increasing amounts of deposited polymer and decreasing molecular weight of the PNIPAM, however, accelerated cell detachment. Within this interesting structure-property correlation only single cell detachment, but no cell sheet release was investigated.¹³⁴

Nakayama *et al.* could release intact cell sheets, assembling block copolymers with a hydrophobic anchor block and a PNIPAM block on TCPS.¹³² The two blocks had similar length and the whole polymer a molecular weight of 25.1 kDa . Polymer deposition was adjusted by the polymers concentration (0.1 , 0.3 , and $0.5 \text{ wt}\%$) of the spin coating solution and was determined to range from 0.87 to $1.81 \mu\text{g cm}^{-2}$ by ATR/FTIR spectroscopy. Ellipsometry measurements revealed layer thicknesses of 2 to 23.3 nm . AFM measurements showed a smooth morphology of the coatings with a low roughness of less than 2 nm . Calculations of grafting densities of the thermoresponsive chains and thus an assignment to brush or mushroom regime were not conducted. However, Nakayama *et al.* correlated cell adhesion and cell sheet detachment of BAECs to the amount of grafted PNIPAM. With decreasing layer thickness, the amount of adherent cells increased and thus the culture time for reaching confluence decreased. Detachment of single cells and harvest of cell sheets was faster for thicker coatings. The coating with a medium layer thickness of 15.5 nm was found to be the most appropriate for the application in cell sheet fabrication.¹³²

Uhlig *et al.* studied self-assembled monolayers of poly(MEO₂MA-*co*-OEGMA), with an incorporated disulfide group, on gold surfaces (Figure 15).¹¹¹ The molecular weight (20 - 25 kDa), the comonomer ratio of MEO₂MA and OEGMA as well as the number of repeating units in the

oligo ethylene glycol side chain were varied. A layer thickness of 4.5 nm and a molecular density of $0.23 \text{ molecules nm}^{-2}$ was determined for one of the investigated polymer monolayers. The surface coverage, however, is not easy to determine, as the OEGMA side chains differ in their length, which impacts the polymer coils radius. Additionally the morphology was not investigated. Nevertheless, the coating was considered to be densely coated.

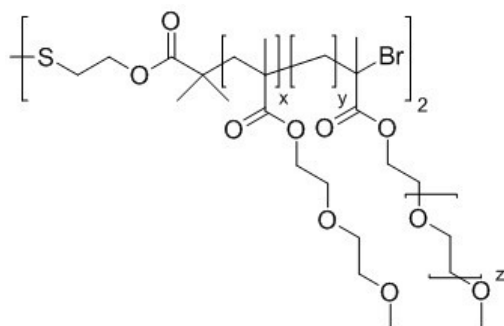


Figure 15 Chemical structure of the poly(MEO₂MA-*co*-OEGMA) with a disulfide terminus for immobilization on a gold surface.¹¹¹

The chemical composition of the polymers strongly influenced adhesion of L929 mouse fibroblast cells. The polymer with the short OEG side chains (4 instead of 9 repeating units) allowed for the shortest time for attachment and spreading of the cells (2 days). The impact of polymer composition on the single cell detachment was less pronounced. Poor cell adhesion prohibited confluent cell growth and thus cell sheet harvest.¹¹¹

Detailed information on the correlation of poly(glycidyl ether) brushes assembled on gold and glass surfaces can be found in chapter 3. Polymers with a sulfur-containing anchor group were assembled on gold, where as an amide-containing anchor block within a thermoresponsive block copolymer allowed for assembly on glass substrates. For polymers with molecular weights ranging from 2 to 25 kDa dry layer thicknesses from 1.0 to 6.2 nm and grafting densities in both the mushroom- and the brush-like regime were obtained. The prerequisites for successful cell sheet detachment of NIH3T3 mouse fibroblasts and human dermal fibroblasts are a laterally homogeneous morphology of the coatings as well as a full surface shielding with polymer under cell detaching conditions.^{110, 128, 177}

For polymer brushes prepared by "grafting-from" approaches the correlation of structural parameters with cell adhesion and detachment was performed by Okano,^{109, 113, 122} Gao,¹²³ Dworak,⁵⁵ Laschewsky,⁵¹ and their respective coworkers. For these coatings more assumptions were made in order to determine surface parameters, however, some interesting correlations with cell response were performed.

Takahashi *et al.* reported on surface-induced RAFT polymerization of PNIPAM brushes with varying grafting densities of 0.02-0.04 chains nm⁻² and different molecular weights of 23, 49, and 58 kDa and correlated these surface parameters with the cell response.¹²² For PNIPAM brushes on silane-modified glass surfaces, in the investigated grafting density range, they stated, that only coatings at the highest grafting density reproducibly detached cell sheets of BAECs at 20 °C. Additionally, increasing detachment times were observed (<0.5, <1, <24h) with decreasing polymer chain length. Furthermore, PNIPAM brushes of the longest, investigated polymer chains at the medium grafting density also effectively detached confluent cell sheets.¹²² The grafting densities of the polymer chains, in this study, however, were only approximated by the density of the surface-tethered initiator, disregarding the actual surface-induced grafting efficiency. Further, the molecular weights of the polymers within the coatings were estimated by the molecular weights determined for polymers evolved in solution during the polymerization reaction. Moreover, morphology and thickness of the surface coatings were not investigated. Hence, within this study an elucidative matrix of cell sheet detachment in dependence on grafting density and chain length is presented. However, the results from these investigations are poorly comparable to other studies, due to many approximations in the characterization of structural parameters.

Nagase *et al.* studied PNIPAM brushes prepared by surface-induced ATRP from glass surfaces modified with silane-terminated initiators and inert silane-modified coadsorbers in different concentrations (100%, 50%, 25%).¹⁰⁹ The amount of grafted polymers (0.35-1.39 µg cm⁻²) was influenced by both initiator and monomer concentration and was investigated by ATR/FTIR. AFM measurements revealed an increase in the root mean square (rms) surface roughness (1.17, 3.29 and 6.28°nm) with decreasing initiator concentration. Only coatings with an initiator concentration of 100% were considered as laterally homogeneous. Grafting densities, however, could not be determined from the amount of grafted polymer, as the molecular weights

of the polymer chains were not investigated. Nagase *et al.* classified grafting densities as high, medium and low according to the adjusted initiator concentration, and assumed chain lengths to be low for high initiator concentration and high for low initiator concentration at constant monomer concentration. BAEC adsorption and single cell detachment was correlated to the initiator concentration and the amount of grafted polymer. Nagase *et al.* concluded from their study, that brush density and length as well as the coadsorbers' properties are important factors for the biological response.¹⁰⁹ Hence, they did not recommend specific surface parameters suitable for cell adhesion and detachment.

Another study of Okano and coworkers comprised the preparation of PNIPAM brushes by surface-induced ATRP from polystyrene substrates modified with a poly(4-vinylbenzyl chloride) coating as macroinitiator.¹¹³ The amount of grafted polymer ($0.4\text{--}8.2\text{ }\mu\text{g cm}^{-2}$), determined by ATR/FTIR spectroscopy, and the resulting dry layer thickness ($1.8\text{--}64.7\text{ nm}$), measured by ellipsometry, was adjusted by the monomer concentration and reaction time. Molecular weight of the PNIPAM chains, morphology of the coating and grafting densities were not investigated. BAEC adhesion and detachment was correlated to the amount of grafted polymer/layer thicknesses and revealed a decrease in cell adhesion with increasing amounts of PNIPAM on the surface. Intact cell sheets detached from coatings with a layer thickness of 10.9 nm within one hour. Surfaces with higher layer thicknesses (30.4 nm and above) did not allow cells to grow confluent.¹¹³ Mizutani *et al.* suggested an optimal layer thickness, for cell adhesion and cell sheet detachment, of 10.9 nm , which is comparable to the optimal layer thickness of 15.5 nm Nakayama *et al.* proposed for PNIPAM coatings on TCPS.

Gao and coworkers prepared PNIPAM brushes on glass substrates with a gradient layer thickness up to 200 nm by surface-induced ATRP and correlated the film thickness to adhesion and detachment of cells of the human liver cell line HepG2.¹²³ Ellipsometry and AFM measurements revealed the layer thickness and morphology of the PNIPAM brushes. The layer thickness increased linearly with polymerization time and the surface roughness increased slightly with increasing layer thickness. Thermoresponsive coatings up to 45 nm layer thickness supported cell adhesion, whereas the lower limit in film thickness, to allow for effective single cell detachment, was observed to be 20 nm for HepG2 cells. Molecular weights of the polymers at different positions on the gradient sample as well as grafting densities were not investigated.

However, Gao and coworkers presented a straightforward gradient approach to correlate the thickness of PNIPAM brushes with their performance in cell culture.¹²³ The observed layer thicknesses of PNIPAM coatings on glass surfaces of 20-45 nm, suitable for cell adhesion and detachment, were rather high compared to the 10.9 and 15.5 nm optimal layer thickness of PNIPAM brushes on TCPS presented by Okano and coworkers. Interestingly, for PNIPAM hydrogels prepared by electron beam irradiation lower optimal layer thicknesses were observed on glass compared to TCPS substrates.¹¹⁴⁻¹¹⁵

Besides PNIPAM, other thermoresponsive coatings were prepared by the "grafting-from" approach. Dworak *et al.* reported on poly[tri(ethylene glycol) monoethyl ether methacrylate]-coated glass surfaces prepared by surface-induced ATRP polymerization for controlled fibroblast culturing (Figure 16).⁵⁵

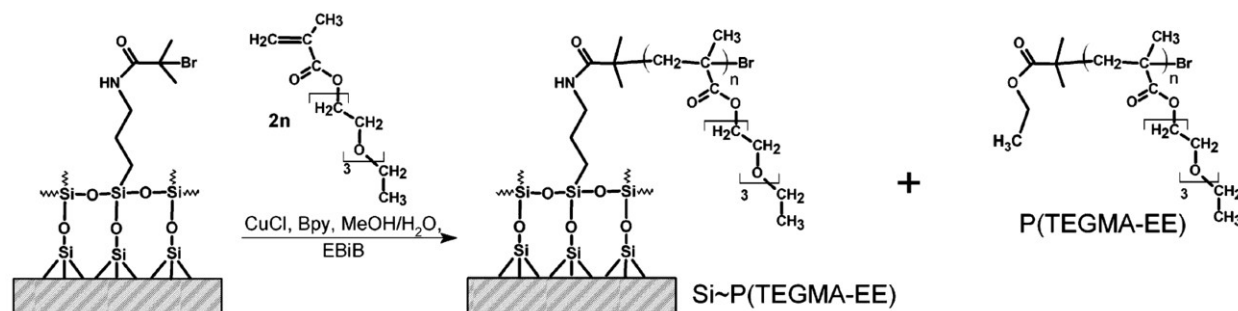


Figure 16 Surface-induced ATRP of poly[tri(ethylene glycol) monoethyl ether methacrylate] (P(TEGMA-EE)) on initiator-prefunctionalized glass and silicon substrates.⁵⁵

Dworak *et al.* assumed molecular weights (23-189 kDa) of the surface-tethered polymer chains to be similar to the molecular weights measured for the polymers evolved in solution. Layer thicknesses (3-18 nm) of the polymer brushes were adjusted by the polymerization time (1-21 h). AFM measurements revealed smooth morphologies of the coatings. All coatings with reaction times ≤ 6 h possessed grafting densities of $0.1 \text{ chain nm}^{-2}$. Dworak *et al.* only performed adhesion and cell sheet detachment studies with human fibroblasts on coatings prepared with polymerization times of 6 and 21 h. These two monolayer coatings with layer thicknesses of 9 and 18 nm, respectively, behaved similarly in cell adhesion and detached cell sheets within 40 to 60 min at 17.5 °C.⁵⁵

Other oligoethylene glycol-based polymer brushes were prepared by Wischerhoff *et al.*⁵¹ They grafted poly(MEO₂MA-*co*-OEGMA) brushes by surface-induced ATRP from a macroinitiator layer, which was adsorbed on an adhesive polyelectrolyte coating, which itself was assembled on a glass substrate. Layer thicknesses of 15 to 150 nm of the grafted thermoresponsive polymer and root mean square roughness of 20 nm were reported. Grafting densities could not be determined due a lateral inhomogeneity and unknown molecular weights. High layer thicknesses of poly(MEO₂MA-*co*-OEGMA) brushes of 70 nm supported cell adhesion and single cell detachment of L929 cells.⁵¹ This layer thickness is quite high compared to the layer thickness of the OEG-based coating suitable for cell adhesion and cell sheet detachment studied by Dworak *et al.*,⁵⁵ as well as compared to layer thicknesses of PNIPAM coatings appropriate for temperature-triggered cell harvest.

Gels or gel-like structures prepared via "grafting-to" procedures are less defined compared to polymer brushes, but resemble the group of thermoresponsive coatings which are prepared with the easiest and most straightforward coating methods, such as dip and spin coating. Coating characteristics were correlated to cell behavior for such surfaces by Rochev^{39, 121, 131, 178} as well as Lu⁴⁶ and their respective coworkers.

Nash *et al.* prepared thermoresponsive coatings for cell sheet fabrication on PET and glass substrates by spin coating of PNIPAM with molecular weights of 20-25 kDa, dissolved in ethanol at concentrations ranging from 2 to 20% w/v.¹⁷⁸ Profilometry analysis evidenced layer thicknesses of 26 to 2166 nm. AFM measurements revealed smooth surface morphologies with rms roughness of 4.9±4.4 nm at least for the 100 nm-thick coating. NIH3T3 mouse fibroblasts adhered and proliferated on the PNIPAM coatings, independent on the layer thickness. The cells' metabolic activity ranged from 84 to 104% compared to the PET controls for the coatings of different layer thickness. Intact NIH3T3 cell sheets as well as human mesenchymal stem cells (hMSC) single cells detached from 100 nm thick layers at 4 °C. Interestingly, in this study, PNIPAM coatings spin coated onto PET and glass substrates with thicknesses of 100 nm and more supported cell adhesion and proliferation.¹⁷⁸ The majority of reports, instead, defines upper limits of lower 50 nm for PNIPAM layer thicknesses to allow proper cell adhesion.

Dzhoyashvili *et al.* also prepared PNIPAM coatings simply by spin coating and correlated the thicknesses of the resulting non-crosslinked PNIPAM films with cell attachment, proliferation and cell sheet detachment.¹³¹ PNIPAM with a broad molecular weight range from 20 to 40 kDa was dissolved in ethanol at different concentrations (5-80 mg mL⁻¹) and spin coated on glass and PET discs. Optical profilometry analysis revealed layer thicknesses of 50-900 nm and AFM measurements proved smooth morphologies with rather low rms roughness of 3.9±2.6 nm to 7.3±4.1 nm compared to the high layer thickness. High metabolic activity (100% normalized to the PET control) was observed for cells of the mouse stromal cell line MS-5 cultured on PNIPAM films of 50 and 80 nm. For further increasing layer thicknesses the metabolic activity decreased to 30%. Cells grew confluent within 48 h when seeded at a density of 40.000 cells cm⁻² only on the control and the 50 nm thick PNIPAM film. After seven days of cell culture, intact cell sheets detached at 4 °C from PNIPAM coatings with 50 and 80 nm thickness, within 25-30 min.¹³¹ In contrast to Nash *et al.*, in this report an upper limit in layer thickness to support proper cell attachment of 80 nm was stated. Compared to other studies on PNIPAM brushes^{113, 132} or hydrogels prepared by electron beam irradiation,¹¹⁴⁻¹¹⁵ however, 50 and 80 nm layer thickness are still high to allow for cell sheet fabrication.

Healy *et al.* physisorbed PNIPAM and poly(NIPAM-*co*-NtBAM) from aqueous solutions above their LCST at 40 °C as well as below their LCSTs at 20 and 10 °C, respectively, on TCPS and PET substrates (Figure 17).³⁹

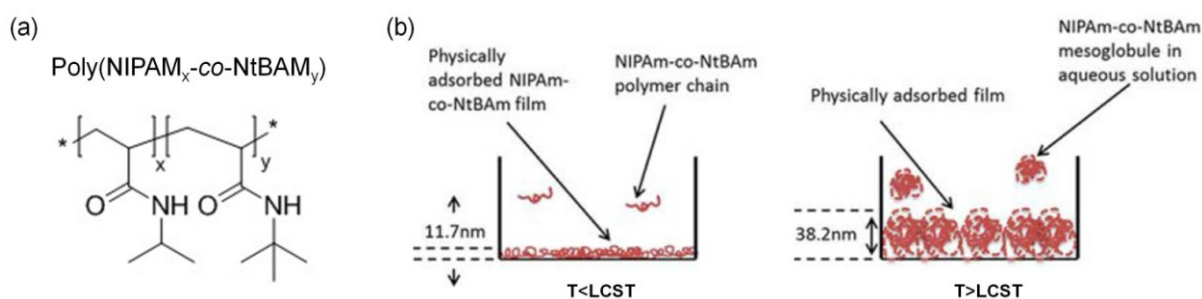


Figure 17 (a) Chemical structure of poly(NIPAM-*co*-NtBAM) and (b) physisorption of the copolymer to the hydrophobic substrate above and below the LCST.³⁹

Below the LCST the PNIPAM (co)polymer chains in aqueous solution are fully solubilized and swollen. Above the LCST, however, the polymer chains are in there collapsed, less hydrated

state with a smaller hydrodynamic radius, possibly forming aggregates. The solution is turbid, and thus this grafting procedure is known as cloud point grafting. Cloud point grafting is known to increase grafting densities of polymer chains within coatings compared to full solubility grafting.^{146, 179-180} PNIPAM and copolymer coatings with layer thicknesses ranging from 7.1 to 38.2 nm revealed strong lateral inhomogeneities, indicated by high rms surface roughness values of 7.7 to 26.9 nm. For the high molecular weight copolymer (325 kDa) layer thickness and surface roughness strongly increased when grafted at temperatures above the LCST compared to physisorption at low temperatures. For the shorter PNIPAM chains (20-25 kDa) the two different grafting conditions led to similar layer thicknesses and morphologies. An alamarBlue assay was performed to assess the human pulmonary microvascular endothelial cells' (HPMEC) metabolic activity on coated and control surfaces. When cultured on the copolymer coatings prepared below the LCST, the assay revealed 100% proliferation and viability of HPMECs, normalized to the TCPS and PET controls. The cells' metabolic activity on physisorbed PNIPAM was comparably low with about 40% normalized to the controls. Cell sheet detachment from the copolymer coatings prepared below the LCST, was the slowest (60 ± 9.2 min) of all investigated coatings within this study. In contrast, cell sheets detached in about 20 min from PNIPAM coatings, independent on the grafting conditions, and in 30 min from the copolymer coatings prepared above the LCST. Nevertheless, the more hydrophobic copolymer coating prepared below the LCST with a layer thickness of 11.7 ± 2.9 nm was considered to be the most appropriate for cell sheet fabrication.³⁹

Based on the promising results of the physisorbed poly(NIPAM-*co*-NtBAM) coatings Healy *et al.* published a follow-up study relying on copolymers containing acrylamide benzophenone (AcBzPh) as an additional UV-crosslinkable moiety.¹²¹ With this, the stability of the coating was intended to be increased compared to purely physisorbed polymer layers. Poly(NIPAM-*co*-NtBAM-*co*-AcBzPh) and poly(NIPAM-*co*-AcBzPh) with molecular weights of 320 and 310 kDa, respectively, formed physically adsorbed films on TCPS and PET with thicknesses of 13.2 ± 3.3 nm to 33.1 ± 4.6 nm with rms roughness of 11.8 ± 3.5 nm to 32.9 ± 7.2 nm. Cell metabolic activities of HPMECs were higher on coatings grafted below the LCST (90-100%) compared to those physisorbed above the LCST (~ 50%). In line with the previously performed study, high cell proliferation and viability came along with slower cell sheet detachment of 50 ± 3 min for

poly(NIPAM-*co*-AcBzPh) and 210 ± 10 min for poly(NIPAM-*co*-NtBAM-*co*-AcBzPh) coatings prepared below the LCST. Coatings prepared with the same copolymers above the LCST detached cells within 40 ± 2 min and 120 ± 8 min, respectively. Poly(NIPAM-*co*-AcBzPh) coatings grafted below the LCST with a layer thickness of 13.2 ± 3.3 nm was considered to be the most appropriate coating for cell sheet fabrication.¹²¹ The two studies of Healy *et al.* recommend operationally simple coating procedures which allow for the preparation of functional coatings for reasonably fast cell sheet harvest.^{39, 121}

Yang *et al.* also relied on a functional moiety to covalently adhere the PNIPAM coating on the substrate and to allow for crosslinking within the coating.⁴⁶ Poly(NIPAM-*co*-hydroxypropyl methacrylate-*co*-3-(trimethoxysilyl)propyl methacrylate) with a molecular weight of 119 kDa was deposited on glass substrates by spin coating. Dry layer thicknesses of approximately 4, 14 and 17 nm were adjusted by the PNIPAM copolymer concentration (1, 5 and 10 mg mL^{-1}) in ethanol and were determined by ellipsometry measurements. AFM measurements revealed an increase in surface roughness with increasing polymer concentration of the spin coating solution. HeLa (human cervix epithelial cell line) and HEK293 (human embryonic kidney cell line) cells adhered and grew confluent on coatings with layer thicknesses up to 14 nm. Single HeLa cells and confluent HEK293 cell sheets detached temperature-triggered from layers with thicknesses of 14 and 4 nm, respectively.⁴⁶ These layer thicknesses of PNIPAM copolymer coatings suitable for thermally-induced cell release are comparable to those found for the dip coating procedures described by Healy *et al.*^{39, 121} and by Okano and coworkers^{113, 132} for PNIPAM brushes.

For thermoresponsive hydrogels prepared by an irradiation-induced "grafting-from" process, the least surface parameters are known. However, Okano and coworkers proposed limits for layer thicknesses, suitable for cell sheet fabrication.¹¹⁴⁻¹¹⁵

Akiyama *et al.* reported on PNIPAM hydrogels prepared by electron beam irradiation on TCPS substrates.¹¹⁵ Coating thicknesses and the amounts of deposited mass were adjusted by the NIPAM concentration in a 2-propanol solution. The two layer thicknesses of 15.5 ± 7.2 nm and 29.5 ± 8.4 nm were determined by AFM measurements after UV-excimer laser ablation of the grafted coating. The amounts of deposited mass of $1.4 \pm 0.1 \text{ } \mu\text{g cm}^{-2}$ and $2.9 \pm 0.1 \text{ } \mu\text{g cm}^{-2}$, were

measured by ATR/FTIR. Both surface coatings were rather inhomogeneous with a rms roughness of 7.7 and 16.5 nm, respectively. Even though, layer thicknesses of the two investigated coatings were the same within the range of error, the two coatings exhibited different properties in cell adhesion of BAECs. On the coating with the lower amount of grafted polymer, cells attached and confluent cell sheet were harvested induced by a thermal trigger. In contrast, on the coating with the higher amount of grafted PNIPAM, cells could not adhere and thus culture to confluency was impossible. The conclusion Akiyama *et al.* drew from this study "In the present study, we demonstrate that thickness and the amount of grafted PIPAAm layers have significant influence on surface properties in terms of thermoresponsive cell adhesion and detachment and approximately 20-nm thickness is the key factor for the PIPAAm-grafted surface to achieve adhesive cell adhesion and detachment with temperature."¹¹⁵ is controversial, as the thicknesses determined for the two investigated coatings are not significantly different and no intermediate layer thickness around 20 nm was investigated.

Fukumori *et al.*¹¹⁴ prepared PNIPAM coatings similarly to Akiyama *et al.*¹¹⁵ but on glass substrates. The NIPAM concentrations in 2-propanol for polymerization by electron beam irradiation were 5 and 40 wt.% and resulted in coatings with thicknesses of 3.3 ± 0.3 nm and 8.8 ± 0.2 nm, respectively, determined after UV-excimer laser ablation of the polymer layer by AFM measurements. The amounts of grafted polymer of $0.80 \pm 0.07 \mu\text{g cm}^{-2}$ and $1.35 \pm 0.07 \mu\text{g cm}^{-1}$ were investigated by ATR/FTIR. AFM measurements proved a rather smooth surface morphology. BAECs adhered on the PNIPAM gel coatings with the lower layer thickness of 3.3 nm, but not on the thicker gel coating with 8.8 nm. In general the hydrophilicity of the substrate might influence the phase transition of the crosslinked surface-tethered gel. The more hydrophilic glass substrate was assumed to promote the dehydration process at elevated temperatures less pronouncedly compare to the more hydrophobic TCPS substrate. Therefore, cell adhesion on PNIPAM hydrogels coated on glass was only supported by thin coatings of around 3.3 nm.¹¹⁴ For polymer brush coatings, in turn, higher layer thicknesses suitable for cell adhesion were observed on glass¹²³ compared to TCPS^{113, 132} substrates. Fukumori *et al.* observed the release cell sheets at 20 °C within 30 min from the PNIPAM coating on glass with a layer thickness of 3.3 nm.¹¹⁴

A variety of coating methods were applied to generate surfaces suitable for cell sheet fabrication. Chain length, layer thickness, amount of grafted polymer, grafting density, and morphology of the coatings are important parameters to describe the surface structure and to tune cell adhesion and detachment. From the aforementioned studies, however, no common optima of these parameters could be concluded, due to the variety of polymers, substrate materials and cell types investigated. The correlation of surface parameters with cell response, however, is indispensable for an in-depth understanding of the mechanisms of cell adhesion and cell sheet detachment as well as for a sophisticated design of new coatings optimized for specific cell types. Cell types examined in the previously described studies on structure-property correlations were bovine carotid artery endothelial cells (BAEC), human pulmonary microvascular endothelial cells (HPMEC),^{39, 121} human dermal fibroblasts,^{50, 55} and cells from cell lines such as L929^{51, 111} and NIH3T3¹⁷⁸ mouse fibroblasts, MS-5 mouse stromal cells,¹³¹ HepG2 human liver cells,¹²³ HeLa human cervix epithelial cells⁴⁶ and HEK293 human embryonic kidney cells⁴⁶. Cell types applied for therapeutic application, successfully harvested from thermoresponsive coatings are summarized in Table 1.

Table 1 Overview of cell types harvested from PNIPAM coatings for therapeutic applications.

| Cell type | Therapeutic application | Lit |
|------------------------------------|---|-----------|
| oral mucosal epithelium cells | corneal reconstruction | [181] |
| | prevention of the formation of strictures after esophageal endoscopic submucosal dissection | [182] |
| | prevention of intrauterine adhesions | [183] |
| myoblasts from skeletal muscles | treatment of dilated cardiomyopathy | [184] |
| periodontal ligament-derived cells | periodontal regeneration | [185] |
| chondrocytes from the knee joints | cartilage repair | [186-187] |
| dermal fibroblasts | treatment of intraoperative air leaks of the lung | [188] |
| nasal mucosal epithelial cells | regeneration for the middle ear mucosa | [189] |
| hepatocytes | metabolically active hepatic tissues | [190-191] |
| islet cells | treatment of diabetes mellitus | [192] |
| different stem cells | variety of applications | [193-197] |

Cell adhesiveness varies for different cell types. Therefore, substrate properties of thermoresponsive coatings need to be adjusted in order to successfully culture and harvest a variety of different cells.¹⁹⁸ An example for poorly adhesive cells are smooth muscle cells (SMCs). In order to facilitate the adhesion of SMCs and their growth to confluency Takahashi *et al.* terminally modified PNIPAM brushes with functional groups, such as maleimide, 3-maleimidopropionic acid and *N*-propyl maleimide. The terminal carboxylation of the PNIPAM (COOH-PNIPAM) chains allowed for a strong adhesion of the SMCs as well as for a rapid detachment. On unmodified PNIPAM brushes with a high amount of grafted polymer ($0.41 \mu\text{g cm}^{-2}$) SMCs could not reach confluence due to insufficiently strong attachment. On terminally unmodified PNIPAM brushes with lower amounts of grafted polymer ($<0.17 \mu\text{g cm}^{-2}$) SMCs adhered and proliferated similar as on COOH-PNIPAM coatings, however, detachment of cells was slower and less effective compared to COOH-PNIPAM brushes.¹⁹⁸

The differences in adhesiveness between cell types, however, does not only require specific and individual surface modification to allow for proper cell adhesion and proliferation, but also enables a thermally-modulated cell separation. Nagase *et al.* seeded four cell types, human umbilical vein endothelial cells (HUVECs), normal human dermal fibroblasts (NHDFs), human aortic SMCs and human skeletal muscle myoblast cells (HSMs) on PNIPAM brushes, with a grafting density of $0.36 \text{ chains nm}^{-2}$ and molecular weight of 12.8 kDa, prepared by surface-induced ATRP. Cells of the four cell types adhered differently within 24 h at 37 °C and detached at 20 °C with distinct rates. They co-cultured HUVECs and HSMs and separated them by their different cell detachment properties.¹⁹⁹ Similar studies on cell separation of different cell types were performed with PNIPAM copolymers.⁴²⁻⁴³

2 OBJECTIVES

Thermoresponsive polymer coatings optimized for cell sheet fabrication are the basis of scaffold-free tissue engineering, a milestone in regenerative medicine.¹⁴ Weinhart *et al.* proved thermoresponsive poly(glycidyl ether)s, composed of GME and EGE comonomers, tethered to gold surfaces, to be suitable for temperature-triggered cell sheet harvest.⁵⁸ The objective of this work shall be to understand and engineer parameters which influence the functionality of the poly(glycidyl ether) coatings with respect to cell adhesion, proliferation and thermally-induced cell sheet detachment.

To gain fundamental insight into the system, the copolymerization of GME and EGE, regarding the comonomers reactivity ratios, in order to deduce the structural composition of the copolymer, shall be investigated. Furthermore, the influence of comonomer ratio, structural composition and molecular weight of the polymer as well as concentration and salt content in aqueous solution on the phase transition behavior of poly(GME-*ran*-EGE) in solution shall be examined.

In order to derive surface design guidelines for functional thermoresponsive poly(glycidyl ether) brushes, the temperature-dependent biological response of proteins and cells to detailed structural features of the respective thermoresponsive monolayer coatings shall be correlated. For such correlations, reproducible procedures for the formation of various monolayers of different thickness and grafting density are required. Polymer molecular weights, sulfur-containing anchor groups and the coating procedure need to be varied in order to adjust surface characteristics. Structural surface parameters like morphology, layer thickness, chain grafting density, polymer chain distance (l) on the surface and polymer radius (R_g , $R_{f,bad}$, $R_{f,\theta}$) of the individual polymers of various molecular weight have to be investigated and used to calculate the individual degree of chain overlap ($2 R l^{-1}$) in different polymer coatings. The degree of chain overlap, as a normalized surface index, allows for appraisal of surface coverage by the grafted polymer chains, and thus for the assignment of the polymer conformation within the monolayer to the mushroom- or brush-like regime. Thereby a fair and meaningful comparison with other

thermoresponsive polymer monolayer coatings and their performance in cell sheet fabrication will be possible.

For structure-property correlations of in detail characterized poly(glycidyl ether) brushes on gold, studies on cell response shall be performed. The thereby deduced design guidelines for functional thermoresponsive polymer coatings applicable in cell sheet harvest shall be employed to transfer the system from the model substrate gold to the more application-relevant substrate glass.

A block copolymer with a thermoresponsive part and an amine-containing anchor block shall be created to coat glass substrates. Surface parameters of the resultant coatings have to be investigated for their fit to the requirements laid down by the previously stated design guidelines for functional thermoresponsive coatings. In case the block copolymer coatings on glass meet the requirements they shall be applied in cell culture experiments. These experiments on cell adhesion and cell sheet detachment shall investigate the validity of the guidelines not only for poly(glycidyl ether) brushes on gold surfaces but also for poly(glycidyl ether) coatings on glass substrates.

3 PUBLICATIONS AND MANUSCRIPTS

This work comprises a thorough investigation of thermoresponsive poly(glycidyl ether) (PGE) copolymers composed of GME and EGE, coatings thereof on the model substrate gold and the application-relevant substrate glass, as well as the application of these coatings in temperature-triggered cell sheet fabrication with NIH3T3 mouse fibroblasts and human dermal fibroblasts. In 2011 Weinhart *et al.* demonstrated the suitability of poly(GME-*co*-EGE) brushes assembled on gold for temperature-controlled cell adhesion and cell sheet detachment. Within the presented studies this approach was systematically examined in order to profoundly understand the parameters which are important for the functionality of the coating. The reactivity ratios of GME and EGE were determined for the monomer-activated anionic ring-opening polymerization with NOct₄Br or NBu₄N₃ as initiator and *i*-Bu₃Al as activator. Phase transition temperatures were scrutinized by UV-Vis spectroscopy depending on salt content, polymer concentration, comonomer ratio, molecular weight, and polymerization technique. Linear thermoresponsive poly(glycidyl ether)s with defined molecular weights, polydispersity and functional end-groups were postmodified with sulfur-containing anchor moieties to allow for self-assembly on gold surfaces. Grafting densities and surface morphologies were investigated by QCM-D, ellipsometry and AFM measurements, respectively. For laterally homogeneous coatings degrees of chain overlap were calculated, as normalized parameters which identify the polymer chain conformation within monolayer coatings as mushroom-like and brush-like. Surface parameters of PGE coatings were correlated to the biological response of proteins and cells on such surfaces above and below the phase transition temperatures of the PGEs. Results of this correlation were considered in order to transfer the functional PGE coating from gold to glass substrates. A block copolymer composed of a thermoresponsive poly(GME-*ran*-EGE) block and an amine-containing anchor block assembled on glass allowed cell adhesion, proliferation and for thermally-triggered, highly reproducible cell sheet detachment in less than 30 min.

The author designed and synthesized polymers of different molecular weights, applied for the determination of phase transition temperatures and for gold surface modification, by monomer-activated anionic ring-opening polymerization, and characterized these polymers. The polymer

prepared by the non-activated anionic ring-opening polymerization was synthesized by S. Schmitt during his practical internship under the supervision of the author and was characterized by the author. Copolymerizations for the investigation of the reactivity ratios of GME and EGE as well as the corresponding data evaluation were performed by the author and M.Sc. S. Rackow in the course of this master thesis under supervision of the author. M. Selent conducted GPC measurements. Dr. A. Schäfer performed temperature-dependent NMR measurements and the author evaluated the results. The author performed and analyzed UV-Vis and DLS measurements. Dr. M. Weinhart and the author provided the concept of research. Research was planned and organized by the author. The author wrote the article "A Perfect Match: Fast and Truly Random Copolymerization of Glycidyl Ether Monomers to Thermoresponsive Copolymers" (Chapter 3.1).

Dr. T. Becherer and Dr. M. Weinhart wrote the article "In-depth Analysis of Switchable Glycerol Based Polymeric Coatings for Cell Sheet Engineering" (Chapter 3.2). Synthesis and characterization of phase transition temperatures in water and in PBS of methoxide initiated poly(GME-*co*-EGE)s with comonomer ratios of 2:3, 1:5 and 0:1 were performed by the author. Further, the author performed cell adhesion and detachment studies, cell viability assays and characterized of cell behavior on coatings of poly(glycidyl ether)s with different comonomer ratios, analyzed data and depicted the results. All other experiments were conducted and evaluated by Dr. T. Becherer. Prof. Dr. R. Haag, Dr. T. Becherer and Dr. M. Weinhart provided the concept of research. Research was planned and organized by Dr. T. Becherer and the author.

For a detailed surface structure investigation, the author postmodified poly(glycidyl ether)s with sulfur-containing anchor groups for self-assembly on gold surfaces, characterized the polymers, modified surfaces, characterized the monolayer coating by QCM-D and ellipsometry measurement and analyzed data. M.Sc. D. Stöbener performed MALDI-TOF-MS measurements and Dr. M. Weinhart analyzed the data. Dr. M. Weinhart and the author provided the concept of research. Research was planned and organized by the author. The author wrote the article "Poly(glycidyl ether)-Based Monolayers on Gold Surfaces: Control of Grafting Density and Chain Conformation by Grafting Procedure, Surface Anchor, and Molecular Weight" (Chapter 3.3).

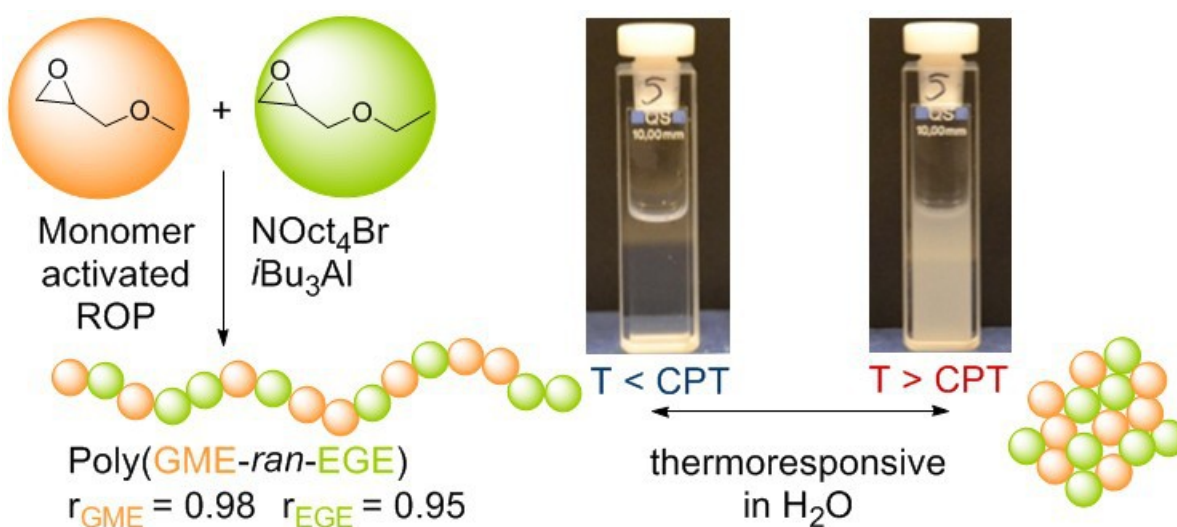
For the correlation of surface parameters with biological response, the author performed cell adhesion and cell sheet detachment studies, determined protein adsorption from cell culture medium by SPR experiment and analyzed the data thereof. Dr. José Luis Cuéllar-Camacho performed AFM measurements to investigate the coatings' morphology, and analyzed the data. Dr. M. Weinhart and the author provided the concept of research. Research was planned and organized by the author. Dr. M. Weinhart and the author wrote the article "Thermoresponsive Poly(glycidyl ether) Brushes on Gold: Surface Engineering Parameters and Their Implication for Cell Sheet Fabrication" (Chapter 3.4).

For the transfer of the thermoresponsive poly(glycidyl ether) coatings from gold to glass substrates, M.Sc. S. Rackow synthesized, postmodified and characterized a block copolymer, in the course of his master thesis under supervision of the author. The author performed DLS measurements, coated surfaces and characterized them by ellipsometry, contact angle and QCM-D measurements. Dr. José Luis Cuéllar-Camacho performed AFM measurements and analyzed the data. XPS spectroscopic measurements were performed by D. Treu and J. Radnik and data was analyzed by M.Sc. I. Donskyi. Cell adhesion, proliferation, viability studies and data analysis thereof were performed by the author. The author and Dr. M. Weinhart provided the concept of research. Research was planned and organized by the author. The author wrote the manuscript "Transfer of Functional Thermoresponsive Poly(glycidyl ether) Coatings for Cell Sheet Fabrication from Gold to Glass Surfaces" (Chapter 3.5).

3.1 A Perfect Match: Fast and Truly Random Copolymerization of Glycidyl Ether Monomers to Thermoresponsive Copolymers

Silke Heinen, Simon Rackow, Andreas Schäfer, and Marie Weinhart*

Copolymerization of GME and EGE by a monomer-activated anionic ring-opening polymerization with NOct₄Br as initiator and *i*-Bu₃Al as activator allowed for truly random incorporation of the monomers within the polymer chain. Phase transition temperatures of the thermoresponsive and highly biocompatible poly(GME-*ran*-EGE)s in aqueous solution varied with molecular weight of the polymer and concentration in solution.



This chapter was published in:

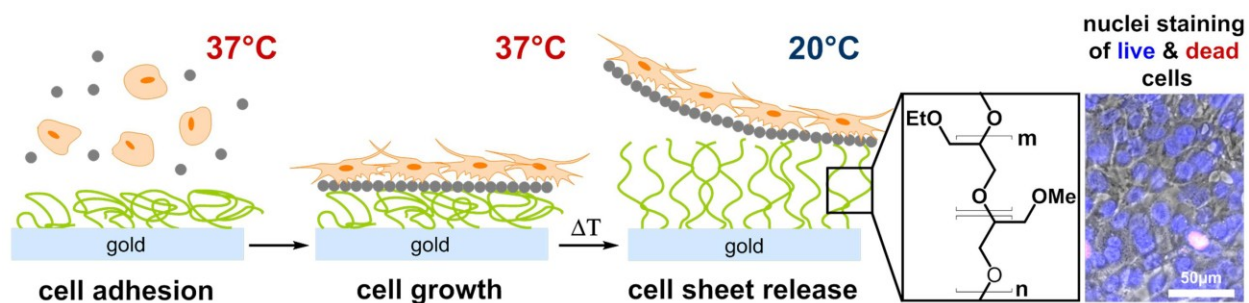
Heinen, S.; Rackow, S.; Schäfer, A.; Weinhart, M., A Perfect Match: Fast and Truly Random Copolymerization of Glycidyl Ether Monomers to Thermoresponsive Copolymers. *Macromolecules* **2017**, 50 (1), 44-53.

DOI: <https://doi.org/10.1021/acs.macromol.6b01904>

3.2 In-depth Analysis of Switchable Glycerol Based Polymeric Coatings for Cell Sheet Engineering

Tobias Becherer, Silke Heinen, Qiang Wei, Rainer Haag, Marie Weinhart*

A series of poly(GME-*co*-EGE) with different comonomer ratios was prepared and studied for their thermoresponsive properties in solution and on the surface. Switchable surface coatings were investigated for their temperature-dependent protein adsorption, cell adhesion and cell sheet detachment properties.



This chapter was published in:

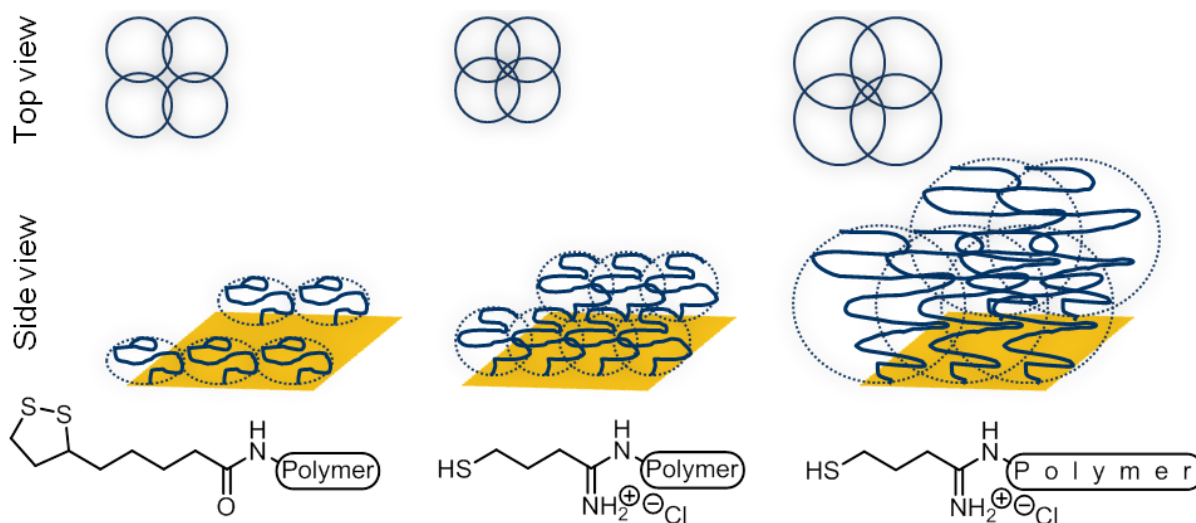
Becherer, T.; Heinen, S.; Wei, Q.; Haag, R.; Weinhart, M., In-depth analysis of switchable glycerol based polymeric coatings for cell sheet engineering. *Acta Biomaterialia* **2015**, 25, 43-55.

DOI: <https://doi.org/10.1016/j.actbio.2015.06.036>

3.3 Poly(glycidyl ether)-Based Monolayers on Gold Surfaces: Control of Grafting Density and Chain Conformation by Grafting Procedure, Surface Anchor, and Molecular Weight

Silke Heinen and Marie Weinhart*

Reproducible coating procedures for well-defined surface coatings of poly(GME-*ran*-EGE) assembled on gold were established, and polymer brushes were thoroughly characterized with respect to layer thickness, grafting density, anchor distance and degree of chain overlap. Control of chain overlap in brush and mushroom regimes on planar gold substrates was attained for monolayer coatings of poly(GME-*ran*-EGE) by adjusting the polymer's molecular weight and sulfur-containing anchor group as well as the conditions for the "grafting-to" procedure.



This chapter was published in:

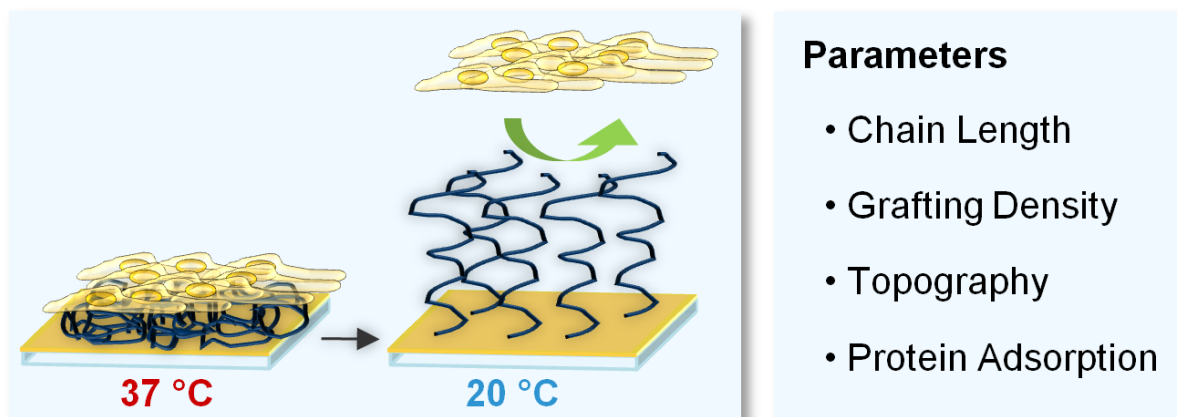
Heinen, S.; Weinhart, M., Poly(glycidyl ether)-Based Monolayers on Gold Surfaces: Control of Grafting Density and Chain Conformation by Grafting Procedure, Surface Anchor, and Molecular Weight. *Langmuir* **2017**, 33 (9), 2076-2086.

DOI: <https://doi.org/10.1021/acs.langmuir.6b03927>

3.4 Thermoresponsive Poly(glycidyl ether) Brushes on Gold: Surface Engineering Parameters and Their Implication for Cell Sheet Fabrication

Silke Heinen, José Luis Cuéllar-Camacho, Marie Weinhart*

Surface design parameters such as grafting density and molecular weight were directly correlated with temperature-dependent serum protein adsorption and cell response. Hence, surface engineering parameters of well-defined poly(glycidyl ether) monolayers for reproducible cell sheet fabrication have been identified.



This chapter was published in:

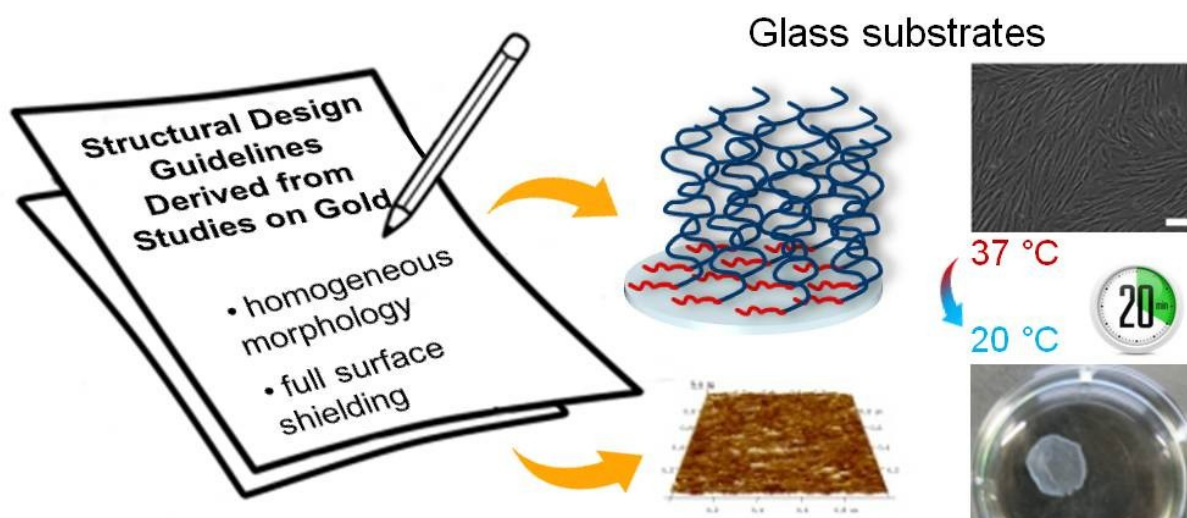
Heinen, S.; Cuéllar-Camacho, J. L.; Weinhart, M., Thermoresponsive poly(glycidyl ether) brushes on gold: Surface engineering parameters and their implication for cell sheet fabrication. *Acta Biomaterialia* **2017**.

DOI: <https://doi.org/10.1016/j.actbio.2017.06.029>

3.5 Transfer of Functional Thermoresponsive Poly(glycidyl ether) Coatings for Cell Sheet Fabrication from Gold to Glass Surfaces

Silke Heinen, Simon Rackow, José Luis Cuéllar-Camacho, Ievgen S. Donskyi, Marie Weinhart*

Functional thermoresponsive poly(glycidyl ether) coatings were transferred from the model substrate gold to application-relevant glass substrates, based on the previously derived structural design guidelines. Glass substrates coated with a block copolymer, composed of a poly(GME-*ran*-EGE) block and an amine-containing anchor block, allowed for cell adhesion and proliferation as well as for fast and highly reproducible detachment of cell sheets.



This chapter was submitted:

Heinen, S.; Rackow, S.; Cuéllar-Camacho, J. L.; Donskyi, I.; Weinhart, M., Transfer of Functional Thermoresponsive Poly(glycidyl ether) Coatings for Cell Sheet Fabrication from Gold to Glass Surfaces. *J. Mater. Chem. B* **2018**.

DOI:°<http://doi.org/10.1039/C7TB03263C>

4 SUMMARY AND CONCLUSIONS

Thermoresponsive poly(glycidyl ether) (PGE) coatings applied in mammalian cell culture enable the fabrication of confluent cell sheets. The studies in this work address fundamental questions of surface confined thermoresponsive polymers with respect to physicochemical properties and the respective biological response. Therefore, we investigated the polymerization of PGEs, modified the polymers with various surface-anchor groups and studied their application as a functional coating on gold and glass substrates. Further, we characterized the coatings with respect to grafting density, morphology, and degree of chain overlap. These structural parameters were correlated to their ability to adhere mammalian cells and detach confluent cell sheets without enzymatic treatment, but simply by the temperature-induced phase transition of the surface-tethered polymer. Moreover, the phase transition of PGEs in solution and on surfaces was analyzed and compared.

Thermoresponsive PGE copolymers of GME and EGE were synthesized by a monomer-activated, anionic ring-opening polymerization with NOct₄Br as initiator and *i*-Bu₃Al as activator, in order to obtain polymers with precisely adjustable molecular weights, narrow polydispersity, and defined end-groups. A truly random incorporation of the comonomers was accomplished, indicated by the monomer reactivity ratios of $r_{\text{GME}} = 0.98$ and $r_{\text{EGE}} = 0.95$, determined by the Kelen-Tüdös approach.⁸²

We investigated the phase transition of PGEs in aqueous solution for the impact of salt content,⁵⁷ polymer concentration,^{57, 82} comonomer ratio,^{57, 82} molecular weight,⁸² and polymerization technique⁸² by UV-Vis transmittance. The phase transition temperature of aqueous polymer solution was decreased by increasing one or more of the following parameters such as salt content, polymer concentration, amount of the comonomer EGE within the polymer, and molecular weight. The phase transition broadened with decreasing polymer concentration, molecular weight or an increasing gradient of the comonomers within the polymer.⁸² Conformational changes of the PGE copolymers during the phase transition were studied by ¹H and ¹³C NMR spectroscopy in D₂O and revealed only a partial dehydration of side chains and backbone during the collapse of the copolymer.⁸²

In order to reproducibly coat gold substrates with end-group-functionalized PGEs at adjustable grafting densities, we established two "grafting-to" approaches by grafting the preformed polymers from ethanol solution and under cloud point conditions (CPG) at 32 °C in PBS buffer. The copolymers with a GME:EGE composition of 1:3 feature different molecular weights (2, 9, 24 kDa) and were equipped with varying sulfur-containing anchor groups (2-iminothiolane; C₄SH, thiocetic acid; C₈SS-, 11-mercapto-1-undecanol; C₁₁SH). Besides the grafting procedure, anchor groups also influenced the grafting densities and hence controlled the tethered polymers' chain conformation.¹²⁸

We examined "wet" and "dry" layer thicknesses by QCM-D and ellipsometry measurements and deduced the respective degrees of solvation, grafting densities and degrees of chain overlap from these measurements. The latter is a normalized parameter, which was defined as the ratio of twice the radius of gyration to the anchor distance ($2 R_g l^{-1}$) and indicated whether the assembled polymer chains in the monolayers were in the mushroom-like ($2 R_g l^{-1} < 1$) or in the brush ($2 R_g l^{-1} > 1.4$) regime. Polymer chains within all coatings were found to be in the brush regime, independent of molecular weight, grafting procedure, and anchor group, except for the 2 kDa PGE equipped with the sterically demanding disulfide-containing anchor ($2 R_g l^{-1} = 1.0 \pm 0.1$). CPG allowed for higher degrees of chain overlap compared to grafting from ethanol, independent of the used sulfur-containing anchor group for polymers with 2 and 9 kDa molecular weight. Only for surface-tethered polymers with 24 kDa molecular weight the degrees of chain overlap were identical for both grafting methods. Coatings prepared with the 9 kDa molecular weight polymer resulted in the highest chain packing density, with $2 R_g l^{-1} = 3.4 \pm 0.1$ for cloud point grafting and $2 R_g l^{-1} = 2.2 \pm 0.1$ for grafting from ethanol.¹²⁸

In order to deduce rational design guidelines for thermoresponsive coatings, well-defined and thoroughly characterized surface coatings were brought in for a meaningful correlation of surface parameters and biological response. We determined morphology and roughness at 37 and 20 °C by AFM measurements, studied cell adhesion, proliferation and cell sheet detachment of NIH 3T3 mouse fibroblasts and investigated serum protein adsorption from cell culture medium containing 10% fetal bovine serum.¹¹⁰

Intact cell sheets could be harvested from all studied PGE coated surfaces, irrespective of the molecular weight, provided that the morphology of the coating was homogenous and the surface was fully shielded by the hydrated brush, thus under detaching conditions. All coatings prepared from ethanol solution and under cloud point conditions satisfied these requirements, except for the 2 kDa PGE equipped with the disulfide-containing anchor, grafted from ethanol. In this case, the surface was not fully shielded even in the hydrated state of the polymer monolayer. Additionally, morphological inhomogeneities were observed for coatings of the 2 kDa PGE with the alkylthiol anchor as well as for the 24 kDa PGE functionalized with 2-iminothiolane, both prepared by CPG. From these two coatings cells only detached in patches rather than as intact cell sheets.¹¹⁰

Insights of these preceding studies, on the model substrate gold, allowed a sophisticated development of cell-detaching PGE coatings on application-relevant glass substrates. We modified glass substrates with a linear thermoresponsive poly(glycidyl ether) block copolymer with an amine-containing anchor block (PGE-AA). In a simple dip coating procedure, grafting densities were adjusted by grafting from solvent mixtures with different ratios of ethanol and MOPS buffer. A high ethanol content (ethanol: MOPS buffer = 4:1) allowed for grafting under full solubility conditions, whereas a surplus of MOPS buffer (ethanol: MOPS buffer = 1:1.4) facilitated CPG. In contrast to the temperature-induced CPG procedure, the solvent-triggered cloudiness of the coating solution enabled the formation of laterally homogeneous PGE-AA coating with increased grafting densities compared to the full solubility grafted glass surfaces. Degrees of chain overlap of PGE-AA coatings on glass prepared by both methods, full solubility grafting (FSG) and CPG, were observed to be <1 under bad solvent and thus cell adhering conditions, but > 1.4 under theta solvent, hence, cell detaching conditions. The two prerequisites for successful cell sheet detachment, a smooth morphology of the coating and full surface shielding under cell detaching conditions, formulated in the previous study on PGE brushes assembled on gold substrates, were therefore fulfilled by the PGE-AA coatings on glass. Indeed, cloud point grafted PGE-AA coatings on bare glass detached confluent human dermal fibroblast cell sheets, thermally-triggered, with a high reliability of 86% in 20 ± 10 min.¹⁷⁷

These in-depth investigations will contribute to future engineering of PGE coatings on various cell culture relevant substrates such as polystyrene dishes as well as polycarbonate or polyethylene terephthalate membranes optimized for different cell types.

5 OUTLOOK

In order to improve the mechanistic understanding of the herein described thermoresponsive coatings, applied for temperature-triggered cell adhesion and detachment, fundamental studies on the volume phase transition of surface-tethered polymer chains need to be performed. The phase transition temperature of terminally-confined PGE chains might differ from de- and remixing temperatures in solution.

For surface-confined PNIPAM brushes a change in phase transition behavior was observed compared to that of aqueous PNIPAM solutions. For PNIPAM end-tethered polymer chains a relatively broad collapse transition is reported.^{175, 200-202} Furthermore, a dependence of the sharpness of the phase transition on the grafting density was observed. Polymer brushes of low grafting density exhibited sharper transitions than brushes with high grafting density.¹⁰² Okano *et al.* observed a 3-step dehydration of a dense PNIPAM brush on silicon dioxide coated QCM-D sensors while heating and a 2-step rehydration via cooling.²⁰¹ Grafting density and molecular weight of PNIPAM chains as well as the preparation method to produce PNIPAM films influence the final responsive properties, such as the magnitude of the phase transition and the morphology.²⁰²

For a better understanding and to allow for sophisticated engineering of PGE surfaces for certain applications, such as cell culture and cell sheet fabrication, the knowledge of the exact phase transition temperature and regime as well as the phase transitions' impact on bulk and surface properties of the brush are sensible. QCM-D measurements can reveal details of the bulk phase transition within the brush, while equilibrium contact angle measurements can provide details on the transition of the brush surface and its hydrophilicity.²⁰³

In preliminary studies we detected the phase transition of PGEs assembled on planar gold substrates directly by QCM-D measurements and correlated the results with the comonomer composition, the molecular weight, grafting density and degree of chain overlap of the tethered polymer. In addition, a systematic study of PGE coatings on different substrate materials with the same polymer, regarding composition and molecular weight, at comparable grafting density

would be highly interesting, as polymer-substrate interactions might alter the phase transition behavior significantly. Furthermore, polymer brushes in the mushroom-like and brush-like regime should be compared with respect to their phase transition behavior.

To our knowledge, there is only few systematic correlations of phase transition behavior of surface-confined thermoresponsive polymers with cell response.

In solution and on surfaces more combinations of the comonomer ratio of GME to EGE balanced with the molecular weight should be investigated in order to adjust phase transition temperatures suitable for cell sheet fabrication. PGEs with a molecular weight of 25 kDa and a comonomer ratio of GME:EGE of 1:1 exhibit an appropriate phase transition temperature for cell culture applications in solution of approximately 32 °C and might perhaps accelerate cell sheet detachment when applied as a coating. The variation of molecular weight and comonomer ratio to adjust the phase transition temperature might also prove beneficial for the cell harvest of different cell types.

Furthermore, coatings with a higher cell adhesiveness which required an additional mechanical trigger besides the thermal one in order to release cell sheets, might be favorable for the adhesion, proliferation and detachment of intrinsically weakly adhering cells, such as smooth muscle cells. Suitable for such purposes might be the poly(glycidyl ether) block copolymer PGE-AA coating grafted under full solubility conditions on PDA-precoated glass substrates. In general, surface properties should be matched with the respective characteristics of the applied cell type.

6 KURZZUSAMMENFASSUNG/ SHORT SUMMARY

6.1 Kurzzusammenfassung

Im Rahmen dieser Arbeit haben wir Oberflächenparameter temperatursensibler Poly(glycidylether)beschichtungen mit dem Verhalten von Proteinen und Zellen auf diesen Oberflächen korreliert. Daraus haben wir Struktur-Design Parameter für funktionale Beschichtungen mit Einsatz in der Herstellung von Zellmonolagen abgeleitet. Statistische Copolymere und Gradientcopolymere, bestehend aus GME und EGE, wurden mit verschiedenen Molekulargewichten und Comonomerverhältnissen mittels monomeraktivierter und nicht aktivierter anionischer ringöffnender Polymerisation hergestellt. Die Comonomerverteilung innerhalb des Polymers, das Comonomerverhältnis und das Molekulargewicht von Poly(GME-*ran*-EGE) sowie Konzentration und Salzgehalt der Lösung wurden auf ihren Einfluss auf das thermische Verhalten der Polymere in wässrigen Lösungen untersucht. Die Temperatur am Phasenübergang sank mit steigendem EGE Anteil, steigendem Molekulargewicht, steigender Konzentration und steigendem Salzgehalt. Der Phasenübergang gewann mit gleichmäßigerer Verteilung der Comonomer im Copolymer, mit steigendem Molekulargewicht und steigender Konzentration an Schärfe.

Temperatursensible Poly(glycidylether) wurden mit verschiedenen schwefelhaltigen Ankergruppen ausgestattet und auf Goldoberflächen angeordnet um den Einfluss von Oberflächenparametern der Beschichtungen auf Proteinadsorption, das Anhaften von Zellen und das Ablösen von Zellmonolagen zu untersuchen. Durch die Auswahl von Molekulargewicht, schwefelhaltiger Ankergruppe und Beschichtungsmethode konnten Schichtdicke und Kettendichte gezielt beeinflusst werden. Beschichtet wurde entweder aus Ethanollösungen unter Bedingungen vollständiger Löslichkeit des Polymers oder unter Trübungspunktbedingungen aus Polymerlösungen mit PBS Puffer als Lösungsmittel bei 32 °C. Morphologie, "Nass-" und "Trockenschichtdicke" der jeweiligen Beschichtungen wurden mittels AFM, QCM-D und Ellipsometrie Messungen untersucht. Aus den Schichtdicken der Beschichtung kombinierte mit Molekulargewicht, Dichte, Hydratisierungsgrad und Kettenradius ($R = R_g, R_{f,bad}, R_{f,\theta}$) der Polymere wurden oberflächenspezifische Parameter wie Kettendichte, Ankerabstand (l) und

Überlappungsgrad ($2 R l^{-1}$) der Polymerketten berechnet. Der Grad der Oberflächenabdeckung durch das Polymer sowie die Konformation des Polymers in den Beschichtung wurden durch den Wert des Überlappungsgrads der Polymerketten abgeschätzt. Ist der Wert von $2 R l^{-1}$ größer 1.4 wird die Beschichtung dem Bürstenregime zugeordnet, für Werte von $2 R l^{-1}$ kleiner 1 wird eine pilzartige Struktur der Polymerketten auf der Oberfläche angenommen. Es wurden Poly(glycidylether)beschichtungen mit Polymerketten in pilzartiger und bürstenartiger Struktur sowie Beschichtungen mit homogener und inhomogener Morphologie erhalten.

Die Korrelation von Oberflächenparametern mit dem Zellverhalten zeigte ein erfolgreiches Anhaften von Zellen und Ablösen intakter Zellmonolagen lediglich für Poly(glycidylether)beschichtungen mit homogener Morphologie und vollständiger Oberflächenabschirmung unter Bedingungen des Zellablösens, also für Werte von $2 R_{f,0} l^{-1}$ größer 1. Diese beiden Voraussetzungen für die Funktionalität der glycidylether-basierten Beschichtungen, in Bezug auf das Ernten von Zellschichten, wurden für einen gezielten Transfer des Systems von dem Modells substrat Gold auf das anwendungsrelevante Substrat Glass berücksichtigt. Ein Blockcopolymer bestehend aus einem temperatursensiblen Poly(GME-*ran*-EGE)block und einem aminhaltigen Ankerblock wurde zu Beschichtung der Glassubstrate verwendet und seine Eignung für das Anhaften von Zellen und das verlässliche und schnelle Ablösen von Zellmonolagen konnte bestätigt werden.

6.2 Short Summary

Within this thesis we correlated surface parameters of thermoresponsive poly(glycidyl ether) (PGE) coatings with the respective biological response and derived structural design guidelines for functional coatings suitable for cell sheet fabrication. Copolymers of GME and EGE with different molecular weights and comonomer ratios were synthesized by monomer-activated and non-activated anionic ring-opening polymerization, resulting in random and gradient copolymers, respectively. The comonomer distribution within the polymer, comonomer ratios and molecular weight of poly(GME-*ran*-EGE) as well as concentration and salt content in solution were investigated for their impact on the thermal behavior of the polymer in aqueous solution. The copolymers' phase transition temperature decreased with increasing EGE comonomer content, molecular weight, and polymer as well as salt concentration. The sharpness of the phase transition increased with increasingly equal distribution of the two comonomer within the copolymer, increasing molecular weight and concentration.

To investigate the impact of surface parameters of thermoresponsive PGE coatings on the protein adsorption, cell adhesion and cell sheet detachment, we equipped polymers with different sulfur-containing anchor groups and assembled these polymers on gold surfaces. Layer thickness and grafting density were adjusted by the molecular weight of the polymer, the particular sulfur-containing anchor moiety as well as by the coating procedure, grafting under full solubility conditions from an ethanol solution or grafting under cloud point condition from PBS buffer at 32 °C. The respective coatings were investigated for their surface morphology by AFM measurements as well as their "wet" and "dry" layer thickness by QCM-D and ellipsometry measurements, respectively. Surface characterizing parameters such as grafting density, interchain anchor distance (l) and degrees of chain overlap ($2 R l^{-1}$) were calculated from the layer thicknesses, the polymers' molecular weights, density, degree of hydration and the polymer coils' radii ($R = R_g, R_{f,bad}, R_{f,0}$). The surface coverage and the polymers' conformation within the monolayer coating were assessed by the degrees of chain overlap (brush regime: $2 R l^{-1} > 1.4$; mushroom-like regime: $2 R l^{-1} < 1$). We obtained PGE coatings in the mushroom-like and the brush regime with both laterally homogeneous and inhomogeneous morphologies depending on the coating procedure and molecular weight.

Correlations of surface parameters with cell response revealed successful cell adhesion and cell sheet detachment only for PGE coatings on gold with homogeneous morphology and full surface coverage under cell detaching conditions, thus for $2 R_{f0} l^{-1} > 1$. These two prerequisites for functional glycidyl ether-based coatings were considered for a sophisticated transfer of these coatings from the model substrate gold to the more application-relevant substrates glass. A block copolymer consisting of a thermoresponsive poly(GME-*ran*-EGE) block and an amine-containing anchor block was assembled on glass substrates and proved suitable for cell adhesion as well as for reliable and fast cell sheet detachment.

7 REFERENCES

1. Khalili, A.; Ahmad, M., A Review of Cell Adhesion Studies for Biomedical and Biological Applications. *Int. J. Mol. Sci.* **2015**, *16* (8), 18149.
2. Hong, S.; Ergezen, E.; Lec, R.; Barbee, K. A., Real-time Analysis of Cell–Surface Adhesive Interactions Using Thickness Shear Mode Resonator. *Biomaterials* **2006**, *27* (34), 5813-5820.
3. Honarmandi, P.; Lee, H.; Lang, M. J.; Kamm, R. D., A Microfluidic System with Optical Laser Tweezers to Study Mechanotransduction and Focal Adhesion Recruitment. *Lab Chip* **2011**, *11* (4), 684-694.
4. Bačáková, L.; Filová, E.; Rypáček, F.; Švorčík, V.; Starý, V., Cell Adhesion on Artificial Materials for Tissue Engineering. *Physiol. Res.* **2004**, *53* (Suppl. 1), 35-45.
5. Canavan, H. E.; Cheng, X.; Graham, D. J.; Ratner, B. D.; Castner, D. G., Cell Sheet Detachment Affects the Extracellular Matrix: A Surface Science Study Comparing Thermal Liftoff, Enzymatic, and Mechanical Methods. *J. Biomed. Mater. Res. A* **2005**, *75* (1), 1-13.
6. Nandkumar, M. A.; Yamato, M.; Kushida, A.; Konno, C.; Hirose, M.; Kikuchi, A.; Okano, T., Two-dimensional Cell Sheet Manipulation of Heterotypically Co-cultured Lung Cells Utilizing Temperature-responsive Culture Dishes Results in Long-term Maintenance of Differentiated Epithelial Cell Functions. *Biomaterials* **2002**, *23* (4), 1121-1130.
7. Canavan, H. E.; Cheng, X.; Graham, D. J.; Ratner, B. D.; Castner, D. G., Surface Characterization of the Extracellular Matrix Remaining after Cell Detachment from a Thermoresponsive Polymer. *Langmuir* **2005**, *21* (5), 1949-1955.
8. Jung, K.; Hampel, G.; Scholz, M.; Henke, W., Culture of Human Kidney Proximal Tubular Cells - The Effect of Various Detachment Procedures on Viability and Degree of Cell Detachment. *Cell. Physiol. Biochem.* **1995**, *5* (5), 353-360.
9. Cole, M. A.; Voelcker, N. H.; Thissen, H.; Griesser, H. J., Stimuli-responsive Interfaces and Systems for the Control of Protein–Surface and Cell–Surface Interactions. *Biomaterials* **2009**, *30* (9), 1827-1850.
10. Dimitrov, I.; Trzebicka, B.; Müller, A. H. E.; Dworak, A.; Tsvetanov, C. B., Thermosensitive Water-soluble Copolymers with Doubly Responsive Reversibly Interacting Entities. *Prog. Polym. Sci.* **2007**, *32* (11), 1275-1343.
11. Gil, E. S.; Hudson, S. M., Stimuli-responsive Polymers and their Bioconjugates. *Prog. Polym. Sci.* **2004**, *29* (12), 1173-1222.
12. Nash, M. E.; Healy, D.; Carroll, W. M.; Elvira, C.; Rochev, Y. A., Cell and Cell Sheet Recovery from pNIPAm Coatings; Motivation and History to Present Day Approaches. *J. Mater. Chem.* **2012**, *22* (37), 19376-19389.
13. Yamato, M.; Okano, T., Cell Sheet Engineering. *Mater. Today* **2004**, *7* (5), 42-47.
14. Tang, Z.; Okano, T., Recent Development of Temperature-responsive Surfaces and their Application for Cell Sheet Engineering. *Regen. Biomater.* **2014**, 91-102.
15. Haraguchi, Y.; Shimizu, T.; Sasagawa, T.; Sekine, H.; Sakaguchi, K.; Kikuchi, T.; Sekine, W.; Sekiya, S.; Yamato, M.; Umezu, M.; Okano, T., Fabrication of Functional

- Three-dimensional Tissues by Stacking Cell Sheets In Vitro. *Nat. Protoc.* **2012**, 7 (5), 850-858.
16. Shimizu, T.; Yamato, M.; Kikuchi, A.; Okano, T., Cell Sheet Engineering for Myocardial Tissue Reconstruction. *Biomaterials* **2003**, 24 (13), 2309-2316.
 17. Seuring, J.; Agarwal, S., Polymers with Upper Critical Solution Temperature in Aqueous Solution: Unexpected Properties from Known Building Blocks. *ACS Macro Lett.* **2013**, 2 (7), 597-600.
 18. Schild, H. G., Poly(N-isopropylacrylamide): Experiment, Theory and Application. *Prog. Polym. Sci.* **1992**, 17 (2), 163-249.
 19. Halperin, A.; Kröger, M.; Winnik, F. M., Poly(N-isopropylacrylamide) Phase Diagrams: Fifty Years of Research. *Angew. Chem. Int. Edit.* **2015**, 54, 15342-15367.
 20. Somcynsky, T., The Lower Critical Solution Temperature (LCST) of Non-polar Polymer Solutions: An Introduction. *Polym. Eng. Sci.* **1982**, 22 (2), 58-63.
 21. Cowie, J. M. G.; McEwen, I. J., Lower Critical Solution Temperatures of Polypropylene Solutions. *J. Poly. Sci. Polym. Phys. Ed.* **1974**, 12 (2), 441-443.
 22. Cowie, J. M. G.; McEwen, I. J., Influence of Microstructure on the Upper and Lower Critical Solution Temperatures of Poly(methylmethacrylate) Solutions. *J. Chem. Soc., Faraday Trans.* **1976**, 72 (0), 526-533.
 23. Pfohl, O.; Hino, T.; Prausnitz, J. M., Solubilities of Styrene-based Polymers and Copolymers in Common Solvents. *Polymer* **1995**, 36 (10), 2065-2073.
 24. Liu, Z.; Guo, Y.; Inomata, K., Lower Critical Solution Temperature Behavior of Poly(2-chloroethyl vinyl ether-alt-maleic anhydride) in Organic Media. *Polym. J.* **2010**, 42 (11), 901-904.
 25. Seno, K.-I.; Kanaoka, S.; Aoshima, S., Synthesis and LCST-type Phase Separation Behavior in Organic Solvents of Poly(vinyl ethers) with Pendant Imidazolium or Pyridinium Salts. *J. Polym. Sci. Part A* **2008**, 46 (17), 5724-5733.
 26. Mugisawa, M.; Ohnishi, K.; Sawada, H., Preparation of Novel Fluoroalkyl-End-Capped 2-Acrylamido-2-methylpropanesulfonic Acid Cooligomeric Nanoparticles Containing Adamantane Units Possessing a Lower Critical Solution Temperature Characteristic in Organic Media. *Langmuir* **2007**, 23 (11), 5848-5851.
 27. Kim, Y.-J.; Matsunaga, Y. T., Thermo-responsive Polymers and their Application as Smart Biomaterials. *J. Mater. Chem. B* **2017**, 5 (23), 4307-4321.
 28. Tager, A. A.; Safronov, A. P.; Berezyuk, E. A.; Galaev, I. Y., Lower Critical Solution Temperature and Hydrophobic Hydration in Aqueous Polymer Solutions. *Colloid Polym. Sci.* **1994**, 272 (10), 1234-1239.
 29. Aseyev, V. O.; Tenhu, H.; Winnik, F. M., Temperature Dependence of the Colloidal Stability of Neutral Amphiphilic Polymers in Water. In *Conformation-Dependent Design of Sequences in Copolymers II*, Khokhlov, A. R., Ed. Springer Berlin Heidelberg: Berlin, Heidelberg, **2006**, pp 1-85.
 30. Okada, Y.; Tanaka, F., Cooperative Hydration, Chain Collapse, and Flat LCST Behavior in Aqueous Poly(N-isopropylacrylamide) Solutions. *Macromolecules* **2005**, 38 (10), 4465-4471.
 31. Tiktopulo, E. I.; Uversky, V. N.; Lushchik, V. B.; Klenin, S. I.; Bychkova, V. E.; Ptitsyn, O. B., "Domain" Coil-Globule Transition in Homopolymers. *Macromolecules* **1995**, 28 (22), 7519-7524.

32. Tiktopulo, E. I.; Bychkova, V. E.; Ricka, J.; Ptitsyn, O. B., Cooperativity of the Coil-Globule Transition in a Homopolymer: Microcalorimetric Study of Poly(N-isopropylacrylamide). *Macromolecules* **1994**, *27* (10), 2879-2882.
33. Aseyev, V.; Tenhu, H.; Winnik, F. M., Non-ionic Thermoresponsive Polymers in Water. In *Adv. Polym. Sci.*, Müller, A. H. E.; Borisov, O., Eds. Springer Berlin Heidelberg: Berlin, Heidelberg, **2011**, pp 29-89.
34. Osváth, Z.; Iván, B., The Dependence of the Cloud Point, Clearing Point, and Hysteresis of Poly(N-isopropylacrylamide) on Experimental Conditions: The Need for Standardization of Thermoresponsive Transition Determinations. *Macromol. Chem. Phys.* **2017**, *218* (4), 1600470.
35. Philipp, M.; Aleksandrova, R.; Muller, U.; Ostermeyer, M.; Sanctuary, R.; Muller-Buschbaum, P.; Kruger, J. K., Molecular versus Macroscopic Perspective on the Demixing Transition of Aqueous PNIPAM Solutions by Studying the Dual Character of the Refractive Index. *Soft Matter* **2014**, *10* (37), 7297-7305.
36. Kokufuta, M. K.; Sato, S.; Kokufuta, E., LCST Behavior of Copolymers of N-isopropylacrylamide and N-isopropylmethacrylamide in Water. *Colloid Polym. Sci.* **2012**, *290* (16), 1671-1681.
37. Spěvák, J., NMR Investigations of Temperature-Induced Phase Transition in Aqueous Polymer Solutions. *Macromol. Symp.* **2011**, *305* (1), 18-25.
38. Kurzbach, D.; Junk, M. J. N.; Hinderberger, D., Nanoscale Inhomogeneities in Thermoresponsive Polymers. *Macromol. Rapid Commun.* **2013**, *34* (2), 119-134.
39. Healy, D.; Nash, M.; Gorelov, A.; Thompson, K.; Dockery, P.; Belochapkin, S.; Madden, J.; Rochev, Y., Nanometer-scale Physically Adsorbed Thermoresponsive Films for Cell Culture. *Int. J. Polym. Mater.* **2017**, *66* (5), 221-234.
40. Rochev, Y.; O'Halloran, D.; Gorelova, T.; Gilcreest, V.; Selezneva, I.; Gavriluk, B.; Gorelov, A., Rationalising the Design of Polymeric Thermoresponsive Biomaterials. *J. Mater.Sci.- Mater. Med.* **2004**, *15* (4), 513-517.
41. Moran, M. T.; Carroll, W. M.; Gorelov, A.; Rochev, Y., Intact Endothelial Cell Sheet Harvesting from Thermoresponsive Surfaces Coated with Cell Adhesion Promoters. *J. R. Soc. Interface* **2007**, *4* (17), 1151-7.
42. Nagase, K.; Hatakeyama, Y.; Shimizu, T.; Matsuura, K.; Yamato, M.; Takeda, N.; Okano, T., Thermoresponsive Cationic Copolymer Brushes for Mesenchymal Stem Cell Separation. *Biomacromolecules* **2015**, *16* (2), 532-540.
43. Nagase, K.; Hatakeyama, Y.; Shimizu, T.; Matsuura, K.; Yamato, M.; Takeda, N.; Okano, T., Hydrophobized Thermoresponsive Copolymer Brushes for Cell Separation by Multistep Temperature Change. *Biomacromolecules* **2013**, *14* (10), 3423-3433.
44. Cordeiro, A. L.; Zimmermann, R.; Gramm, S.; Nitschke, M.; Janke, A.; Schafer, N.; Grundke, K.; Werner, C., Temperature Dependent Physicochemical Properties of Poly(N-isopropylacrylamide-co-N-(1-phenylethyl) acrylamide) Thin Films. *Soft Matter* **2009**, *5* (7), 1367-1377.
45. Nitschke, M.; Gramm, S.; Götze, T.; Valtink, M.; Drichel, J.; Voit, B.; Engelmann, K.; Werner, C., Thermo-responsive Poly(NiPAAm-co-DEGMA) Substrates for Gentle Harvest of Human Corneal Endothelial Cell Sheets. *J. Biomed. Mater. Res., Part A* **2007**, 1003-1010.

46. Yang, L.; Pan, F.; Zhao, X.; Yaseen, M.; Padia, F.; Coffey, P.; Freund, A.; Yang, L.; Liu, T.; Ma, X.; Lu, J. R., Thermoresponsive Copolymer Nanofilms for Controlling Cell Adhesion, Growth, and Detachment. *Langmuir* **2010**, *26* (22), 17304-17314.
47. Nash, M. E.; Carroll, W. M.; Velasco, D.; Gomez, J.; Gorelov, A. V.; Elezov, D.; Gallardo, A.; Rochev, Y. A.; Elvira, C., Synthesis and Characterization of a Novel Thermoresponsive Copolymer Series and their Application in Cell and Cell Sheet Regeneration. *J. Biomater. Sci., Polym. Ed.* **2013**, *24* (3), 253-268.
48. Malonne, H.; Eeckman, F.; Fontaine, D.; Otto, A.; Vos, L. D.; Moës, A.; Fontaine, J.; Amighi, K., Preparation of Poly(N-isopropylacrylamide) Copolymers and Preliminary Assessment of their Acute and Subacute Toxicity in Mice. *Eur. J. Pharm. Biopharm.* **2005**, *61* (3), 188-194.
49. Oleszko, N.; Walach, W.; Utrata-Wesolek, A.; Kowalczyk, A.; Trzebicka, B.; Dworak, A.; Klama-Baryla, A.; Hoff-Lenczewska, D.; Kawecki, M.; Lesiak, M.; Sieron, A. L., Controlling the Crystallinity of Thermoresponsive Poly(2-oxazoline)-Based Nanolayers to Cell Adhesion and Detachment. *Biomacromolecules* **2015**, *16* (9), 2805-13.
50. Dworak, A.; Utrata-Wesolek, A.; Oleszko, N.; Walach, W.; Trzebicka, B.; Aniol, J.; Sieron, A. L.; Klama-Baryla, A.; Kawecki, M., Poly(2-substituted-2-oxazoline) Surfaces for Dermal Fibroblasts Adhesion and Detachment. *J. Mater. Sci.: Mater. Med.* **2014**, *25* (4), 1149-1163.
51. Wischerhoff, E.; Glatzel, S.; Uhlig, K.; Lankenau, A.; Lutz, J.-F.; Laschewsky, A., Tuning the Thickness of Polymer Brushes Grafted from Nonlinearly Growing Multilayer Assemblies. *Langmuir* **2009**, *25* (10), 5949-5956.
52. Sefcik, L. S.; Kaminski, A.; Ling, K.; Laschewsky, A.; Lutz, J.-F.; Wischerhoff, E., Effects of PEG-Based Thermoresponsive Polymer Brushes on Fibroblast Spreading and Gene Expression. *Cell. Mol. Bioeng.* **2013**, *6* (3), 287-298.
53. Uhlig, K.; Boerner, H. G.; Wischerhoff, E.; Lutz, J.-F.; Jaeger, M. S.; Laschewsky, A.; Duschl, C., On the Interaction of Adherent Cells with Thermoresponsive Polymer Coatings. *Polymers* **2014**, *6* (4), 1164-1177, 14 pp.
54. Anderson, C. R.; Abecunas, C.; Warren, M.; Laschewsky, A.; Wischerhoff, E., Effects of Methacrylate-Based Thermoresponsive Polymer Brush Composition on Fibroblast Adhesion and Morphology. *Cell. Mol. Bioeng.* **2017**, *10* (1), 75-88.
55. Dworak, A.; Utrata-Wesołek, A.; Szveda, D.; Kowalczyk, A.; Trzebicka, B.; Anioł, J.; Sieroń, A. L.; Klama-Baryła, A.; Kawecki, M., Poly[tri(ethylene glycol) ethyl ether methacrylate]-Coated Surfaces for Controlled Fibroblasts Culturing. *ACS Appl. Mater. Interfaces* **2013**, *5* (6), 2197-2207.
56. Lee, B.; Jiao, A.; Yu, S.; You, J. B.; Kim, D.-H.; Im, S. G., Initiated Chemical Vapor Deposition of Thermoresponsive Poly(N-vinylcaprolactam) Thin Films for Cell Sheet Engineering. *Acta Biomater.* **2013**, *9* (8), 7691-7698.
57. Becherer, T.; Heinen, S.; Wei, Q.; Haag, R.; Weinhart, M., In-depth Analysis of Switchable Glycerol Based Polymeric Coatings for Cell Sheet Engineering. *Acta Biomater.* **2015**, *25*, 43-55.
58. Weinhart, M.; Becherer, T.; Haag, R., Switchable, Biocompatible Surfaces Based on Glycerol Copolymers. *Chem. Commun.* **2011**, *47* (5), 1553-1555.
59. Teichmann, J.; Valtink, M.; Gramm, S.; Nitschke, M.; Werner, C.; Funk, R. H. W.; Engemann, K., Human Corneal Endothelial Cell Sheets for Transplantation: Thermo-

- responsive Cell Culture Carriers to Meet Cell-specific Requirements. *Acta Biomater.* **2013**, 9 (2), 5031-5039.
60. Koga, T.; Nakamoto, K.; Odawara, K.; Matsuoka, T.; Higashi, N., Fabrication of Thermo-Responsive Molecular Layers from Self-Assembling Elastin-Like Oligopeptides Containing Cell-Binding Domain for Tissue Engineering. *Polymers* **2015**, 7, 134-146.
 61. Pierna, M.; Santos, M.; Arias, F. J.; Alonso, M.; Rodríguez-Cabello, J. C., Efficient Cell and Cell-Sheet Harvesting Based on Smart Surfaces Coated with a Multifunctional and Self-Organizing Elastin-Like Recombinamer. *Biomacromolecules* **2013**, 14, 1893-1903.
 62. Mie, M.; Mizushima, Y.; Kobatake, E., Novel Extracellular Matrix for Cell Sheet Recovery Using Genetically Engineered Elastin-Like Protein. *J. Biomed. Mater. Res. Part B: Appl. Biomater.* **2008**, 86B, 283-290.
 63. Altomare, L.; Cochis, A.; Carletta, A.; Rimondini, L.; Farè, S., Thermo-responsive Methylcellulose Hydrogels as Temporary Substrate for Cell Sheet Biofabrication. *J. Mater. Sci.: Mater. Med.* **2016**, 27 (95), 1-13.
 64. Thirumala, S.; Gimble, J. M.; Devireddy, R. V., Methylcellulose Based Thermally Reversible Hydrogel System for Tissue Engineering Applications. *Cells* **2013**, 2 (3), 460-75.
 65. Chen, C.-H.; Tsai, C.-C.; Chen, W.; Mi, F.-L.; Liang, H.-F.; Chen, S.-C.; Sung, H.-W., Novel Living Cell Sheet Harvest System Composed of Thermoreversible Methylcellulose Hydrogels. *Biomacromolecules* **2006**, 7, 736-743.
 66. Labbé, A.; Carlotti, S.; Deffieux, A.; Hirao, A., Controlled Polymerization of Glycidyl Methyl Ether Initiated by Onium Salt/Triisobutylaluminum and Investigation of the Polymer LCST. *Macromol. Symp.* **2007**, 249-250, 392-397.
 67. Aoki, S.; Koide, A.; Imabayashi, S.-i.; Watanabe, M., Novel Thermosensitive Polyethers Prepared by Anionic Ring-Opening Polymerization of Glycidyl Ether Derivatives. *Chem. Lett.* **2002**, 31 (11), 1128-1129.
 68. Reinicke, S.; Schmelz, J.; Lapp, A.; Karg, M.; Hellweg, T.; Schmalz, H., Smart Hydrogels Based on Double Responsive Triblock Terpolymers. *Soft Matter* **2009**, 5 (13), 2648-2657.
 69. Oleszko-Torbus, N.; Utrata-Wesołek, A.; Wałach, W.; Dworak, A., Solution Behavior of Thermoresponsive Random and Gradient Copolymers of 2-n-propyl-2-oxazoline. *Eur. Polym. J.* **2017**, 88 (Suppl. C), 613-622.
 70. Salzinger, S.; Huber, S.; Jaksch, S.; Busch, P.; Jordan, R.; Papadakis, C. M., Aggregation Behavior of Thermo-responsive Poly(2-oxazoline)s at the Cloud Point Investigated by FCS and SANS. *Colloid Polym. Sci.* **2012**, 290 (5), 385-400.
 71. Virtanen, J.; Holappa, S.; Lemmetyinen, H.; Tenhu, H., Aggregation in Aqueous Poly(N-isopropylacrylamide)-block-poly(ethylene oxide) Solutions Studied by Fluorescence Spectroscopy and Light Scattering. *Macromolecules* **2002**, 35 (12), 4763-4769.
 72. Jochum, F. D.; Roth, P. J.; Kessler, D.; Theato, P., Double Thermoresponsive Block Copolymers Featuring a Biotin End Group. *Biomacromolecules* **2010**, 11 (9), 2432-2439.
 73. Meeussen, F.; Nies, E.; Berghmans, H.; Verbrugghe, S.; Goethals, E.; Du Prez, F., Phase Behaviour of Poly(N-vinyl caprolactam) in Water. *Polymer* **2000**, 41 (24), 8597-8602.
 74. Makhaeva, E. E.; Thanh, L. T. M.; Starodoubtsev, S. G.; Khokhlov, A. R., Thermoshinking Behavior of Poly(vinylcaprolactam) Gels in Aqueous Solution. *Macromol. Chem. Phys.* **1996**, 197 (6), 1973-1982.

75. Lin, P.; Clash, C.; Pearce, E. M.; Kwei, T. K.; Aponte, M. A., Solubility and Miscibility of Poly(ethyl oxazoline). *J. Polym. Sci. Part B* **1988**, *26* (3), 603-619.
76. Christova, D.; Velichkova, R.; Loos, W.; J. Goethals, E.; Du Prez, F., New Thermo-responsive Polymer Materials Based on Poly(2-ethyl-2-oxazoline) Segments. *Polymer* **2003**, *44*, 2255-2261.
77. Park, J.-S.; Kataoka, K., Comprehensive and Accurate Control of Thermosensitivity of Poly(2-alkyl-2-oxazoline)s via Well-Defined Gradient or Random Copolymerization. *Macromolecules* **2007**, *40* (10), 3599-3609.
78. Hoogenboom, R.; Thijs, H. M. L.; Jochems, M. J. H. C.; van Lankvelt, B. M.; Fijten, M. W. M.; Schubert, U. S., Tuning the LCST of Poly(2-oxazoline)s by Varying Composition and Molecular Weight: Alternatives to Poly(N-isopropylacrylamide)? *Chem. Commun.* **2008**, *44*, 5758-5760.
79. Schäfer-Soenen, H.; Moerkerke, R.; Berghmans, H.; Koningsveld, R.; Dušek, K.; Šolc, K., Zero and Off-Zero Critical Concentrations in Systems Containing Polydisperse Polymers with Very High Molar Masses. 2. The System Water–Poly(vinyl methyl ether). *Macromolecules* **1997**, *30* (3), 410-416.
80. Lutz, J.-F.; Akdemir, Ö.; Hoth, A., Point by Point Comparison of Two Thermosensitive Polymers Exhibiting a Similar LCST: Is the Age of Poly(NIPAM) Over? *J. Am. Chem. Soc.* **2006**, *128* (40), 13046-13047.
81. Lutz, J.-F.; Hoth, A., Preparation of Ideal PEG Analogues with a Tunable Thermosensitivity by Controlled Radical Copolymerization of 2-(2-Methoxyethoxy)ethyl Methacrylate and Oligo(ethylene glycol) Methacrylate. *Macromolecules* **2006**, *39*, 893-896.
82. Heinen, S.; Rackow, S.; Schäfer, A.; Weinhart, M., A Perfect Match: Fast and Truly Random Copolymerization of Glycidyl Ether Monomers to Thermoresponsive Copolymers. *Macromolecules* **2017**, *50* (1), 44-53.
83. Eeckman, F.; Amighi, K.; Moës, A. J., Effect of Some Physiological and Non-physiological Compounds on the Phase Transition Temperature of Thermoresponsive Polymers Intended for Oral Controlled-drug Delivery. *Int. J. Pharmaceut.* **2001**, *222* (2), 259-270.
84. Lee, S. B.; Song, S.-C.; Jin, J.-I.; Sohn, Y. S., A New Class of Biodegradable Thermosensitive Polymers. 2. Hydrolytic Properties and Salt Effect on the Lower Critical Solution Temperature of Poly(organophosphazenes) with Methoxypoly(ethylene glycol) and Amino Acid Esters as Side Groups. *Macromolecules* **1999**, *32* (23), 7820-7827.
85. Zhang, Y.; Cremer, P. S., Interactions Between Macromolecules and Ions: The Hofmeister Series. *Curr. Opin. Chem. Biol.* **2006**, *10* (6), 658-663.
86. Zhang, Y.; Furyk, S.; Bergbreiter, D. E.; Cremer, P. S., Specific Ion Effects on the Water Solubility of Macromolecules: PNIPAM and the Hofmeister Series. *J. Am. Chem. Soc.* **2005**, *127* (41), 14505-14510.
87. Cho, Y.; Zhang, Y.; Christensen, T.; Sagle, L. B.; Chilkoti, A.; Cremer, P. S., Effects of Hofmeister Anions on the Phase Transition Temperature of Elastin-like Polypeptides. *J. Phys. Chem. B* **2008**, *112* (44), 13765-13771.
88. Bloksma, M. M.; Bakker, D. J.; Weber, C.; Hoogenboom, R.; Schubert, U. S., The Effect of Hofmeister Salts on the LCST Transition of Poly(2-oxazoline)s with Varying Hydrophilicity. *Macromol. Rapid Commun.* **2010**, *31* (8), 724-728.

89. Pamies, R.; Zhu, K.; Kjøniksen, A.-L.; Nyström, B., Thermal Response of Low Molecular Weight Poly-(N-isopropylacrylamide) Polymers in Aqueous Solution. *Polym. Bull.* **2009**, *62* (4), 487-502.
90. Afroze, F.; Nies, E.; Berghmans, H., Phase Transitions in the System Poly(N-isopropylacrylamide)/Water and Swelling Behaviour of the Corresponding Networks. *J. Mol. Struct.* **2000**, *554* (1), 55-68.
91. Dworak, A.; Trzebicka, B.; Kowalczyk, A.; Tsvetanov, C.; Rangelov, S., Polyoxazolines - Mechanism of Synthesis and Solution Properties. *Polimery* **2014**, *1*, 88.
92. Müller, S. S.; Moers, C.; Frey, H., A Challenging Comonomer Pair: Copolymerization of Ethylene Oxide and Glycidyl Methyl Ether to Thermoresponsive Polyethers. *Macromolecules* **2014**, *47*, 5492-5000.
93. Kawaguchi, T.; Kojima, Y.; Osa, M.; Yoshizaki, T., Cloud Points in Aqueous Poly(N-isopropylacrylamide) Solutions. *Polym. J.* **2008**, *40* (5), 455-459.
94. Nagase, K.; Kobayashi, J.; Kikuchi, A.; Akiyama, Y.; Annaka, M.; Kanazawa, H.; Okano, T., Influence of Graft Interface Polarity on Hydration/Dehydration of Grafted Thermoresponsive Polymer Brushes and Steroid Separation Using All-Aqueous Chromatography. *Langmuir* **2008**, *24* (19), 10981-10987.
95. Matsuzaka, N.; Takahashi, H.; Nakayama, M.; Kikuchi, A.; Okano, T., Effect of the Hydrophobic Basal Layer of Thermoresponsive Block Co-Polymer Brushes on Thermally-Induced Cell Sheet Harvest. *J. Biomater. Sci. Polym. Ed.* **2012**, *23* (10), 1301-1314.
96. Matsuzaka, N.; Nakayama, M.; Takahashi, H.; Yamato, M.; Kikuchi, A.; Okano, T., Terminal-Functionality Effect of Poly(N-isopropylacrylamide) Brush Surfaces on Temperature-Controlled Cell Adhesion/Detachment. *Biomacromolecules* **2013**, *14* (9), 3164-3171.
97. Richter, R.; Rodenhausen, K.; B. Eisele, N.; Schubert, M., *Springer Ser. Surf. Sci.* **2014**; p223-248.
98. Sestak, M. N., Spectroscopic Ellipsometry Characterization of Thin Films Used in the Food Packaging Industry. *Am. Lab.* **2013**.
99. Daniel, J. B.; William, A. B.; Neal, C.; Jennifer, K.; Neil, H. T., Single-molecule Studies of DNA Transcription Using Atomic Force Microscopy. *Phys. Biol.* **2012**, *9* (2), 021001.
100. Zhang, G., Study on Conformation Change of Thermally Sensitive Linear Grafted Poly(N-isopropylacrylamide) Chains by Quartz Crystal Microbalance. *Macromolecules* **2004**, *37*, 6553-6557.
101. Adam, S.; Koenig, M.; Rodenhausen, K. B.; Eichhorn, K.-J.; Oertel, U.; Schubert, M.; Stamm, M.; Uhlmann, P., Quartz Crystal Microbalance with Coupled Spectroscopic Ellipsometry-study of Temperature-responsive Polymer Brush Systems. *Appl. Surf. Sci.* **2017**, *421* (Part B), 843-851.
102. Ishida, N.; Biggs, S., Direct Observation of the Phase Transition for a Poly(N-isopropylacrylamide) Layer Grafted onto a Solid Surface by AFM and QCM-D. *Langmuir* **2007**, *23* (22), 11083-11088.
103. Zhuang, P.; Dirani, A.; Glinel, K.; Jonas, A. M., Temperature Dependence of the Surface and Volume Hydrophilicity of Hydrophilic Polymer Brushes. *Langmuir* **2016**, *32* (14), 3433-3444.

104. Yamada, N.; Okano, T.; Sakai, H.; Karikusa, F.; Sawasaki, Y.; Sakurai, Y., Thermo-responsive Polymeric Surfaces; Control of Attachment and Detachment of Cultured Cells. *Makromol. Chem. Rapid Comm.* **1990**, *11* (11), 571-576.
105. Fukumori, K.; Akiyama, Y.; Yamato, M.; Okano, T., A Facile Method for Preparing Temperature-Responsive Cell Culture Surfaces by Using a Thioxanthone Photoinitiator Immobilized on a Polystyrene Surface. *ChemNanoMat* **2016**, *2* (5), 454-460.
106. Nash, M. E.; Carroll, W. M.; Foley, P. J.; Maguire, G.; O'Connell, C.; Gorelov, A. V.; Beloshapkin, S.; Rochev, Y. A., Ultra-thin Spin Coated Crosslinkable Hydrogels for Use in Cell Sheet Recovery-synthesis, Characterisation to Application. *Soft Matter* **2012**, *8* (14), 3889-3899.
107. Stöbener, D. D.; Uckert, M.; Cuellar-Camacho, J. L.; Hoppensack, A.; Weinhart, M., Ultrathin Poly(glycidyl ether) Coatings on Polystyrene for Temperature-Triggered Human Dermal Fibroblast Sheet Fabrication. *ACS Biomater. Sci. Eng.* **2017**, *3* (9), 2155-2165.
108. Fukumori, K.; Akiyama, Y.; Yamato, M.; Kobayashi, J.; Sakai, K.; Okano, T., Temperature-responsive Glass Coverslips with an Ultrathin Poly(N-isopropylacrylamide) Layer. *Acta Biomater.* **2009**, *5* (1), 470-476.
109. Nagase, K.; Watanabe, M.; Kikuchi, A.; Yamato, M.; Okano, T., Thermo-Responsive Polymer Brushes as Intelligent Biointerfaces: Preparation via ATRP and Characterization. *Macromol. Biosci.* **2011**, *11* (3), 400-409.
110. Heinen, S.; Cuéllar-Camacho, J. L.; Weinhart, M., Thermoresponsive Poly(glycidyl ether) Brushes on Gold: Surface Engineering Parameters and their Implication for Cell Sheet Fabrication. *Acta Biomater.* **2017**, *59*, 117-128.
111. Uhlig, K.; Boysen, B.; Lankenau, A.; Jaeger, M.; Wischerhoff, E.; Lutz, J.-F.; Laschewsky, A.; Duschl, C., On the Influence of the Architecture of Poly(ethylene glycol)-based Thermoresponsive Polymers on Cell Adhesion. *Biomicrofluidics* **2012**, *6*, 024129-1-11.
112. Kong, B.; Choi, J. S.; Jeon, S.; Choi, I. S., The Control of Cell Adhesion and Detachment on Thin Films of Thermoresponsive Poly[(N-isopropylacrylamide)-*r*-((3-(methacryloylamino)propyl)-dimethyl(3-sulfopropyl)ammonium hydroxide)]. *Biomaterials* **2009**, *30* (29), 5514-5522.
113. Mizutani, A.; Kikuchi, A.; Yamato, M.; Kanazawa, H.; Okano, T., Preparation of Thermoresponsive Polymer Brush Surfaces and Their Interaction with Cells. *Biomaterials* **2008**, *29* (13), 2073-2081.
114. Fukumori, K.; Akiyama, Y.; Kumashiro, Y.; Kobayashi, J.; Yamato, M.; Sakai, K.; Okano, T., Characterization of Ultra-Thin Temperature-Responsive Polymer Layer and Its Polymer Thickness Dependency on Cell Attachment/Detachment Properties. *Macromol. Biosci.* **2010**, *10* (10), 1117-1129.
115. Akiyama, Y.; Kikuchi, A.; Yamato, M.; Okano, T., Ultrathin Poly(N-isopropylacrylamide) Grafted Layer on Polystyrene Surfaces for Cell Adhesion/Detachment Control. *Langmuir* **2004**, *20* (13), 5506-5511.
116. Okano, T.; Yamada, N.; Okuhara, M.; Sakai, H.; Sakurai, Y., Mechanism of Cell Detachment from Temperature-modulated, Hydrophilic-Hydrophobic Polymer Surfaces. *Biomaterials* **1995**, *16* (4), 297-303.

117. Okano, T.; Yamada, N.; Sakai, H.; Sakurai, Y., A Novel Recovery System for Cultured Cells Using Plasma-treated Polystyrene Dishes Grafted with Poly(N-isopropylacrylamide). *J. Biomed. Mater. Res.* **1993**, *27*, 1243-1251.
118. Kwon, O. H.; Kikuchi, A.; Yamato, M.; Sakurai, Y.; Okano, T., Rapid Cell Sheet Detachment from Poly(N-isopropylacrylamide)-grafted Porous Cell Culture Membranes. *J. Biomed. Mater. Res., Part A* **2000**, *50*, 82–89.
119. Karakeçili, A. G.; Satriano, C.; Gümüşderelioğlu, M.; Marletta, G., Thermoresponsive and Bioactive Poly(vinyl ether)-based Hydrogels Synthesized by Radiation Copolymerization and Photochemical Immobilization. *Radiat. Phys. Chem.* **2008**, *77* (2), 154-161.
120. Pan, Y. V.; Wesley, R. A.; Luginbuhl, R.; Denton, D. D.; Ratner, B. D., Plasma Polymerized N-Isopropylacrylamide: Synthesis and Characterization of a Smart Thermally Responsive Coating. *Biomacromolecules* **2001**, *2* (1), 32-36.
121. Healy, D.; Nash, M. E.; Gorelov, A.; Thompson, K.; Dockery, P.; Beloshapkin, S.; Rochev, Y., Fabrication and Application of Photocrosslinked, Nanometer-Scale, Physically Adsorbed Films for Tissue Culture Regeneration. *Macromol. Biosci.* **2017**, *17* (2), 1600175-n/a.
122. Takahashi, H.; Nakayama, M.; Yamato, M.; Okano, T., Controlled Chain Length and Graft Density of Thermoresponsive Polymer Brushes for Optimizing Cell Sheet Harvest. *Biomacromolecules* **2010**, *11* (8), 1991-1999.
123. Li, L.; Zhu, Y.; Li, B.; Gao, C., Fabrication of Thermoresponsive Polymer Gradients for Study of Cell Adhesion and Detachment. *Langmuir* **2008**, *24* (23), 13632-13639.
124. Zhao, B.; Brittain, W. J., Polymer brushes: surface-immobilized macromolecules. *Prog. Polym. Sci.* **2000**, *25* (5), 677-710.
125. Kim, M.; Schmitt, S. K.; Choi, J. W.; Krutty, J. D.; Gopalan, P., From Self-Assembled Monolayers to Coatings: Advances in the Synthesis and Nanobio Applications of Polymer Brushes. *Polymers* **2015**, *7*, 1346-378.
126. Inoue, S.; Kakikawa, H.; Nakadan, N.; Imabayashi, S.-i.; Watanabe, M., Thermal Response of Poly(ethoxyethyl glycidyl ether) Grafted on Gold Surfaces Probed on the Basis of Temperature-Dependent Water Wettability. *Langmuir* **2009**, *25* (5), 2837-2841.
127. Jia, P.; He, M.; Gong, Y.; Chu, X.; Yang, J.; Zhao, J., Probing the Adjustments of Macromolecules during Their Surface Adsorption. *ACS Appl. Mater. Interfaces* **2015**, *7*, 6422-6429.
128. Heinen, S.; Weinhart, M., Poly(glycidyl ether)-Based Monolayers on Gold Surfaces: Control of Grafting Density and Chain Conformation by Grafting Procedure, Surface Anchor, and Molecular Weight. *Langmuir* **2017**, *33* (9), 2076-2086.
129. Rollason, G.; Davies, J. E.; Sefton, M. V., Preliminary Report on Cell Culture on a Thermally Reversible Copolymer. *Biomaterials* **1993**, *14* (2), 153-155.
130. Reed, J. A.; Lucero, A. E.; Hu, S.; Ista, L. K.; Bore, M. T.; López, G. P.; Canavan, H. E., A Low-Cost, Rapid Deposition Method for “Smart” Films: Applications in Mammalian Cell Release. *ACS Appl. Mater. Interfaces* **2010**, *2* (4), 1048-1051.
131. Dzhoyashvili, N. A.; Thompson, K.; Gorelov, A. V.; Rochev, Y. A., Film Thickness Determines Cell Growth and Cell Sheet Detachment from Spin-Coated Poly(N-Isopropylacrylamide) Substrates. *ACS Appl. Mater. Interfaces* **2016**, *8* (41), 27564-27572.

132. Nakayama, M.; Yamada, N.; Kumashiro, Y.; Kanazawa, H.; Yamato, M.; Okano, T., Thermoresponsive Poly(N-isopropylacrylamide)-Based Block Copolymer Coating for Optimizing Cell Sheet Fabrication. *Macromol. Biosci.* **2012**, *12* (6), 751-760.
133. Sakuma, M.; Kumashiro, Y.; Nakayama, M.; Tanaka, N.; Umemura, K.; Yamato, M.; Okano, T., Thermoresponsive Nanostructured Surfaces Generated by the Langmuir-Schaefer Method Are Suitable for Cell Sheet Fabrication. *Biomacromolecules* **2014**, *15* (11), 4160-4167.
134. Sakuma, M.; Kumashiro, Y.; Nakayama, M.; Tanaka, N.; Umemura, K.; Yamato, M.; Okano, T., Control of Cell Adhesion and Detachment on Langmuir-Schaefer Surface Composed of Dodecyl-terminated Thermo-responsive Polymers. *J. Biomater. Sci., Polym. Ed.* **2014**, *25* (5), 431-443.
135. Zdyrko, B.; Luzinov, I., Polymer Brushes by the “Grafting to” Method. *Macromol. Rapid Commun.* **2011**, *32*, 859-869.
136. Piehler, J.; Brecht, A.; Valiokas, R.; Liedberg, B.; Gauglitz, G., A High-density Poly(ethylene glycol) Polymer Brush for Immobilization on Glass-type Surfaces. *Biosens. Bioelectron.* **2000**, *15* (9), 473-481.
137. Cunliffe, D.; Alarcon, C. D.; Peters, V.; Smith, J. R.; Alexander, C., Thermoresponsive Surface-grafted Poly(N-isopropylacrylamide) Copolymers: Effect of Phase Transitions on Protein and Bacterial Attachment. *Langmuir* **2003**, *19* (7), 2888-2899.
138. Piehler, J.; Brecht, A.; Geckeler, K. E.; Gauglitz, G., Surface Modification for Direct Immunoprobes. *Biosens. Bioelectron.* **1996**, *11* (6), 579-590.
139. Lee, H.; Dellatore, S. M.; Miller, W. M.; Messersmith, P. B., Mussel-inspired Surface Chemistry for Multifunctional Coatings. *Science* **2007**, *318* (5849), 426-430.
140. Love, J. C.; Estroff, L. A.; Kriebel, J. K.; Nuzzo, R. G.; Whitesides, G. M., Self-Assembled Monolayers of Thiolates on Metals as a Form of Nanotechnology. *Chem. Rev.* **2005**, *105* (4), 1103-1170.
141. Schwartz, D. K., Mechanisms and Kinetics of Self-assembled Monolayer Formation. *Annu. Rev. Phys. Chem.* **2001**, *52* (1), 107-137.
142. Debono, R. F.; Loucks, G. D.; Manna, D. D.; Krull, U. J., Self-assembly of Short and Long-chain n-alkyl Thiols onto Gold Surfaces: A Real-time Study Using Surface Plasmon Resonance Techniques. *Can. J. Chem.* **1996**, *74* (5), 677-688.
143. Lavrich, D. J.; Wetterer, S. M.; Bernasek, S. L.; Scoles, G., Physisorption and Chemisorption of Alkanethiols and Alkyl Sulfides on Au(111). *J. Phys. Chem. B* **1998**, *102* (18), 3456-3465.
144. Fonticelli, M.; Azzaroni, O.; Benitez, G.; Martins, M. E.; Carro, P.; Salvarezza, R., Molecular Self-Assembly on Ultrathin Metallic Surfaces: Alkanethiolate Monolayers on Ag(1 × 1)-Au(111). *J. Phys. Chem. B* **2004**, *108*, 1898-1905.
145. Unsworth, L. D.; Tun, Z.; Sheardown, H.; Brash, J. L., Chemisorption of Thiolated Poly(ethylene oxide) to Gold: Surface Chain Densities Measured by Ellipsometry and Neutron Reflectometry. *J. Colloid Interf. Sci.* **2005**, *281*, 112-121.
146. Emilsson, G.; Schoch, R. L.; Feuz, L.; Höök, F.; Lim, R. Y. H.; Dahlin, A. B., Strongly Stretched Protein Resistant Poly(ethylene glycol) Brushes Prepared by Grafting-To. *ACS Appl. Mater. Interfaces* **2015**, *7*, 7505-7515.
147. Haensch, C.; Hoeppener, S.; Schubert, U. S., Chemical Modification of Self-assembled Silane Based Monolayers by Surface Reactions. *Chem. Soc. Rev.* **2010**, *39* (6), 2323-2334.

148. Schaeferling, M.; Kambhampati, D., *Protein Microarray Technology*. Wiley-VCH: Weinheim, **2004**.
149. Hoyer, K.; Becherer, T.; Qiang, W.; Haag, R.; Friess, W.; Kuchler, S., Polyglycerol Coatings of Glass Vials for Protein Resistance. *Eur. J. Pharm. Biopharm.* **2013**, *85* (3), 756-764.
150. Weinhart, M.; Becherer, T.; Schnurbusch, N.; Schwibbert, K.; Kunte, H.-J.; Haag, R., Linear and Hyperbranched Polyglycerol Derivatives as Excellent Bioinert Glass Coating Materials. *Adv. Eng. Mater.* **2011**, *13* (12), B501-B510.
151. Yang, Z.; Galloway, J. A.; Yu, H., Protein Interactions with Poly(ethylene glycol) Self-Assembled Monolayers on Glass Substrates: Diffusion and Adsorption. *Langmuir* **1999**, *15* (24), 8405-8411.
152. Lee, S.-W.; Laibinis, P. E., Protein-resistant Coatings for Glass and Metal Oxide Surfaces Derived from Oligo(ethylene glycol)-terminated Alkyltrichlorosilanes. *Biomaterials* **1998**, *19* (18), 1669-1675.
153. Rutland, M. W.; Parker, J. L., Surface Forces between Silica Surfaces in Cationic Surfactant Solutions: Adsorption and Bilayer Formation at Normal and High pH. *Langmuir* **1994**, *10* (4), 1110-1121.
154. Hayes, W. A.; Schwartz, D. K., Two-Stage Growth of Octadecyltrimethylammonium Bromide Monolayers at Mica from Aqueous Solution below the Krafft Point. *Langmuir* **1998**, *14* (20), 5913-5917.
155. Dubas, S. T.; Schlenoff, J. B., Factors Controlling the Growth of Polyelectrolyte Multilayers. *Macromolecules* **1999**, *32* (24), 8153-8160.
156. Kirwan, L. J.; Maroni, P.; Behrens, S. H.; Papastavrou, G.; Borkovec, M., Interaction and Structure of Surfaces Coated by Poly(vinyl amines) of Different Line Charge Densities. *J. Phys. Chem. B* **2008**, *112* (46), 14609-14619.
157. Mészáros, R.; Varga, I.; Gilányi, T., Adsorption of Poly(ethyleneimine) on Silica Surfaces: Effect of pH on the Reversibility of Adsorption. *Langmuir* **2004**, *20* (12), 5026-5029.
158. Angelescu, D. G.; Nylander, T.; Piculell, L.; Linse, P.; Lindman, B.; Tropsch, J.; Detering, J., Adsorption of Branched-Linear Polyethyleneimine-Ethylene Oxide Conjugate on Hydrophilic Silica Investigated by Ellipsometry and Monte Carlo Simulations. *Langmuir* **2011**, *27* (16), 9961-9971.
159. Dejeu, J.; Diziain, S.; Dange, C.; Membrey, F.; Charraut, D.; Foissy, A., Stability of Self-Assembled Polymer Films Investigated by Optical Laser Reflectometry. *Langmuir* **2008**, *24* (7), 3090-3098.
160. Heydari, G.; Tyrode, E.; Visnevskij, C.; Makuska, R.; Claesson, P. M., Temperature-Dependent Deicing Properties of Electrostatically Anchored Branched Brush Layers of Poly(ethylene oxide). *Langmuir* **2016**, *32* (17), 4194-4202.
161. Heuberger, M.; Drobek, T.; Spencer, N. D., Interaction Forces and Morphology of a Protein-Resistant Poly(ethylene glycol) Layer. *Biophys. J.* **2005**, *88* (1), 495-504.
162. Lee, J.; McGrath, A. J.; Hawker, C. J.; Kim, B.-S., pH-Tunable Thermoresponsive PEO-Based Functional Polymers with Pendant Amine Groups. *ACS Macro Lett.* **2016**, *5* (12), 1391-1396.
163. Silverstein, T. P., The Real Reason Why Oil and Water Don't Mix. *J. Chem. Educ.* **1998**, *75* (1), 116.

164. Sudo, Y.; Sakai, H.; Nabae, Y.; Hayakawa, T.; Kakimoto, M.-a., Preparation of Hyperbranched Polystyrene-g-poly(N-isopropylacrylamide) Copolymers and its Application to Novel Thermo-responsive Cell Culture Dishes. *Polymer* **2015**, *70*, 307-314.
165. Loh, X. J.; Cheong, W. C. D.; Li, J.; Ito, Y., Novel Poly(N-isopropylacrylamide)-poly[(R)-3-hydroxybutyrate]-poly(N-isopropylacrylamide) Triblock Copolymer Surface as a Culture Substrate for Human Mesenchymal Stem Cells. *Soft Matter* **2009**, *5* (15), 2937-2946.
166. Loh, X. J.; Gong, J.; Sakuragi, M.; Kitajima, T.; Liu, M.; Li, J.; Ito, Y., Surface Coating with a Thermoresponsive Copolymer for the Culture and Non-Enzymatic Recovery of Mouse Embryonic Stem Cells. *Macromol. Biosci.* **2009**, *9* (11), 1069-1079.
167. Wei, Q.; Becherer, T.; Noeske, P.-L. M.; Grunwald, I.; Haag, R., A Universal Approach to Crosslinked Hierarchical Polymer Multilayers as Stable and Highly Effective Antifouling Coatings. *Adv. Mater.* **2014**, *26* (17), 2688-2693.
168. Anderson, T. H.; Yu, J.; Estrada, A.; Hammer, M. U.; Waite, J. H.; Israelachvili, J. N., The Contribution of DOPA to Substrate-Peptide Adhesion and Internal Cohesion of Mussel-Inspired Synthetic Peptide Films. *Adv. Funct. Mater.* **2010**, *20* (23), 4196-4205.
169. Rodríguez, R.; Blesa, M. A.; Regazzoni, A. E., Surface Complexation at the TiO₂(anatase)/Aqueous Solution Interface: Chemisorption of Catechol. *J. Colloid Interf. Sci.* **1996**, *177* (1), 122-131.
170. Lee, H.; Scherer, N. F.; Messersmith, P. B., Single-molecule Mechanics of Mussel Adhesion. *Proc. Natl. Acad. Sci.* **2006**, *103* (35), 12999-13003.
171. Ku, S. H.; Lee, J. S.; Park, C. B., Spatial Control of Cell Adhesion and Patterning Through Mussel-Inspired Surface Modification by Polydopamine. *Langmuir* **2010**, *26* (19), 15104-15108.
172. Wei, Q.; Zhang, F. L.; Li, J.; Li, B. J.; Zhao, C. S., Oxidant-induced Dopamine Polymerization for Multifunctional Coatings. *Polym. Chem.* **2010**, *1* (9), 1430-1433.
173. Lee, H.; Messersmith, P. B., Surface-independent, Surface-modifying, Multifunctional Coatings and Applications Thereof. Google Patents: **2009**.
174. Furusawa, H.; Sekine, T.; Ozeki, T., Hydration and Viscoelastic Properties of High- and Low-Density Polymer Brushes Using a Quartz-Crystal Microbalance Based on Admittance Analysis (QCM-A). *Macromolecules* **2016**, *49*, 3463-3470.
175. Liu, G.; Zhang, G., Collapse and Swelling of Thermally Sensitive Poly(N-isopropylacrylamide) Brushes Monitored with a Quartz Crystal Microbalance. *J. Phys. Chem. B* **2005**, *109* (2), 743-747.
176. Xu, F. J.; Zhong, S. P.; Yung, L. Y. L.; Kang, E. T.; Neoh, K. G., Surface-Active and Stimuli-Resonsive Polymer-SI(100) Hybrids from Surface-Initiated Atom Transfer Radical Polymerization for Control of Cell Adhesion. *Biomacromolecules* **2004**, *5*, 2392-2403.
177. Heinen, S.; Rackow, S.; Cuéllar-Camacho, J. L.; Donskyi, I.; Weinhart, M., Transfer of Functional Thermoresponsive Poly(glycidyl ether) Coatings for Cell Sheet Fabrication from Gold to Glass Surfaces. *submitted* **2017**.
178. Nash, M. E.; Carroll, W. M.; Nikoloskya, N.; Yang, R.; Connell, C. O.; Gorelov, A. V.; Dockery, P.; Liptrot, C.; Lyng, F. M.; Garcia, A.; Rochev, Y. A., Straightforward, One-Step Fabrication of Ultrathin Thermoresponsive Films from Commercially Available

- pNIPAm for Cell Culture and Recovery. *ACS Appl. Mater. Interfaces* **2011**, 3 (6), 1980-1990.
179. Kingshott, P.; Thissen, H.; Griesser, H. J., Effects of Cloud-point Grafting, Chain Length, and Density of PEG Layers on Competitive Adsorption of Ocular Proteins. *Biomaterials* **2002**, 23, 2043-2056.
 180. Ghezzi, M.; Thickett, S. C.; Telford, A. M.; Easton, C. D.; Meagher, L.; Neto, C., Protein Micropatterns by PEG Grafting on Dewetted PLGA Films. *Langmuir* **2014**, 30, 11714-11722.
 181. Nishida, K.; Yamato, M.; Hayashida, Y.; Watanabe, K.; Yamamoto, K.; Adachi, E.; Nagai, S.; Kikuchi, A.; Maeda, N.; Watanabe, H.; Okano, T.; Tano, Y., Corneal Reconstruction with Tissue-Engineered Cell Sheets Composed of Autologous Oral Mucosal Epithelium. *N. Engl. J. Med.* **2004**, 351 (12), 1187-1196.
 182. Ohki, T.; Yamato, M.; Ota, M.; Takagi, R.; Murakami, D.; Kondo, M.; Sasaki, R.; Namiki, H.; Okano, T.; Yamamoto, M., Prevention of Esophageal Stricture After Endoscopic Submucosal Dissection Using Tissue-Engineered Cell Sheets. *Gastroenterol.* **2012**, 143 (3), 582-588.e2.
 183. Kuramoto, G.; Takagi, S.; Ishitani, K.; Shimizu, T.; Okano, T.; Matsui, H., Preventive Effect of Oral Mucosal Epithelial Cell Sheets on Intrauterine Adhesions. *Hum. Reprod.* **2015**, 30 (2), 406-416.
 184. Sawa, Y.; Miyagawa, S.; Sakaguchi, T.; Fujita, T.; Matsuyama, A.; Saito, A.; Shimizu, T.; Okano, T., Tissue Engineered Myoblast Sheets Improved Cardiac Function Sufficiently to Discontinue LVAS in a Patient with DCM: Report of a Case. *Surg. Today* **2012**, 42 (2), 181-184.
 185. Iwata, T.; Yamato, M.; Tsuchioka, H.; Takagi, R.; Mukobata, S.; Washio, K.; Okano, T.; Ishikawa, I., Periodontal Regeneration with Multi-layered Periodontal Ligament-derived Cell Sheets in a Canine Model. *Biomaterials* **2009**, 30 (14), 2716-2723.
 186. Sato, M.; Yamato, M.; Hamahashi, K.; Okano, T.; Mochida, J., Articular Cartilage Regeneration Using Cell Sheet Technology. *Anat. Rec.* **2014**, 297 (1), 36-43.
 187. Ebihara, G.; Sato, M.; Yamato, M.; Mitani, G.; Kutsuna, T.; Nagai, T.; Ito, S.; Ukai, T.; Kobayashi, M.; Kokubo, M.; Okano, T.; Mochida, J., Cartilage Repair in Transplanted Scaffold-free Chondrocyte Sheets Using a Minipig Model. *Biomaterials* **2012**, 33 (15), 3846-3851.
 188. Kanzaki, M.; Yamato, M.; Yang, J.; Sekine, H.; Kohno, C.; Takagi, R.; Hatakeyama, H.; Isaka, T.; Okano, T.; Onuki, T., Dynamic Sealing of Lung Air Leaks by the Transplantation of Tissue Engineered Cell Sheets. *Biomaterials* **2007**, 28 (29), 4294-4302.
 189. Yamamoto, K.; Yamato, M.; Morino, T.; Sugiyama, H.; Takagi, R.; Yaguchi, Y.; Okano, T.; Kojima, H., Middle Ear Mucosal Regeneration by Tissue-engineered Cell Sheet Transplantation. *npj Regen. Med.* **2017**, 2 (1), 6.
 190. Ohashi, K.; Yokoyama, T.; Yamato, M.; Kuge, H.; Kanehiro, H.; Tsutsumi, M.; Amanuma, T.; Iwata, H.; Yang, J.; Okano, T.; Nakajima, Y., Engineering Functional Two- and Three-dimensional Liver Systems In Vivo Using Hepatic Tissue Sheets. *Nat. Med.* **2007**, 13 (7), 880-885.
 191. Yokoyama, T.; Ohashi, K.; Kuge, H.; Kanehiro, H.; Iwata, H.; Yamato, M.; Nakajima, Y., In Vivo Engineering of Metabolically Active Hepatic Tissues in a Neovascularized Subcutaneous Cavity. *Am. J. Transplant.* **2006**, 6 (1), 50-59.

192. Shimizu, H.; Ohashi, K.; Utoh, R.; Ise, K.; Gotoh, M.; Yamato, M.; Okano, T., Bioengineering of a Functional Sheet of Islet Cells for the Treatment of Diabetes Mellitus. *Biomaterials* **2009**, *30* (30), 5943-5949.
193. Neo, P. Y.; Teh, T. K. H.; Tay, A. S. R.; Asuncion, M. C. T.; Png, S. N.; Toh, S. L.; Goh, J. C.-H., Stem Cell-derived Cell-sheets for Connective Tissue Engineering. *Connect. Tissue Res.* **2016**, *57* (6), 428-442.
194. Tsumanuma, Y.; Iwata, T.; Washio, K.; Yoshida, T.; Yamada, A.; Takagi, R.; Ohno, T.; Lin, K.; Yamato, M.; Ishikawa, I.; Okano, T.; Izumi, Y., Comparison of Different Tissue-derived Stem Cell Sheets for Periodontal Regeneration in a Canine 1-wall Defect Model. *Biomaterials* **2011**, *32* (25), 5819-5825.
195. Tsumanuma, Y.; Iwata, T.; Kinoshita, A.; Washio, K.; Yoshida, T.; Yamada, A.; Takagi, R.; Yamato, M.; Okano, T.; Izumi, Y., Allogeneic Transplantation of Periodontal Ligament-Derived Multipotent Mesenchymal Stromal Cell Sheets in Canine Critical-Size Supra-Alveolar Periodontal Defect Model. *BioRes. Open Access* **2016**, *5* (1), 22-36.
196. Kato, Y.; Iwata, T.; Morikawa, S.; Yamato, M.; Okano, T.; Uchigata, Y., Allogeneic Transplantation of an Adipose-Derived Stem Cell Sheet Combined With Artificial Skin Accelerates Wound Healing in a Rat Wound Model of Type 2 Diabetes and Obesity. *Diabetes* **2015**, *64* (8), 2723-2734.
197. Kaibuchi, N.; Iwata, T.; Yamato, M.; Okano, T.; Ando, T., Multipotent Mesenchymal Stromal Cell Sheet Therapy for Bisphosphonate-related Osteonecrosis of the Jaw in a Rat Model. *Acta Biomater.* **2016**, *42* (Supplement C), 400-410.
198. Takahashi, H.; Matsuzaka, N.; Nakayama, M.; Kikuchi, A.; Yamato, M.; Okano, T., Terminally Functionalized Thermoresponsive Polymer Brushes for Simultaneously Promoting Cell Adhesion and Cell Sheet Harvest. *Biomacromolecules* **2012**, *13* (1), 253-260.
199. Nagase, K.; Kimura, A.; Shimizu, T.; Matsuura, K.; Yamato, M.; Takeda, N.; Okano, T., Dynamically Cell Separating Thermo-functional Biointerfaces with Densely Packed Polymer Brushes. *J. Mater. Chem.* **2012**, *22* (37), 19514-19522.
200. Balamurugan, S.; Mendez, S.; Balamurugan, S. S.; O'Brien, M. J.; López, G. P., Thermal Response of Poly(N-isopropylacrylamide) Brushes Probed by Surface Plasmon Resonance. *Langmuir* **2003**, *19* (7), 2545-2549.
201. Annaka, M.; Yahiro, C.; Nagase, K.; Kikuchi, A.; Okano, T., Real-time Observation of Coil-to-globule Transition in Thermosensitive Poly(N-isopropylacrylamide) Brushes by Quartz Crystal Microbalance. *Polymer* **2007**, *48* (19), 5713-5720.
202. Montagne, F.; Polesel-Maris, J.; Pugin, R.; Heinzelmänn, H., Poly(N-isopropylacrylamide) Thin Films Densely Grafted onto Gold Surface: Preparation, Characterization, and Dynamic AFM Study of Temperature-Induced Chain Conformational Changes. *Langmuir* **2009**, *25* (2), 983-991.
203. Laloyaux, X.; Mathy, B.; Nysten, B.; Jonas, A. M., Surface and Bulk Collapse Transitions of Thermoresponsive Polymer Brushes. *Langmuir* **2010**, *26* (2), 838-847.

LIST OF PUBLICATIONS AND CONFERENCE CONTRIBUTIONS

Peer Reviewed Publications

1. Heinen, S.; Rackow, S.; Cuellar-Camacho, J. L.; Donskyi, I.; Weinhart, M., Transfer of Functional Thermoresponsive Poly(glycidyl ether) Coatings for Cell Sheet Fabrication from Gold to Glass Surfaces. *submitted 2017*.
2. Heinen, S., Cuéllar-Camacho, J. L., Weinhart, M., Thermoresponsive Poly(glycidyl ether) Brushes on Gold: Surface Engineering Parameters and their Implication for Cell Sheet Fabrication, *Acta Biomaterialia*, **2017**, 59, 117-128.
3. Heinen, S., Weinhart, M., Poly(glycidyl ether)-based Monolayers on Gold Surfaces: Control of Grafting Density and Chain Conformation by Grafting Procedure, Surface Anchor, and Molecular Weight, *Langmuir*, **2017**, 33 (9), 2076-2086.
4. Heinen, S., Rackow, S., Schäfer, A., Weinhart, M., A Perfect Match: Fast and Truly Random Copolymerization of Glycidyl Ether Monomers to Thermoresponsive Copolymers, *Macromolecules*, **2017**, 50, 44-53.
5. Becherer, T., Heinen, S., Wei, Q., Haag, R., Weinhart, M., In-Depth Analysis of Switchable Glycerol Based Polymeric Coatings for Cell Sheet Engineering, *Acta Biomaterialia*, **2015**, 25, 43-55.

Poster Presentations

6. Heinen, S., Cuéllar-Camacho, J. L., Rackow, S., Weinhart, M., Thermoresponsive Poly(glycidyl ether)s and Coatings Thereof: Polymerization, Surface Engineering, and Application in Cell Sheet Engineering, Poster Price, LANXEES-Summer-School, Aachen, Germany, **2017**.
7. Heinen, S., Cuéllar-Camacho, J. L., Weinhart, M., Thermoresponsive Polymer Coatings for Cell Sheet Fabrication: A Structure-Property Relationship, Leibniz Young Polymer Scientist Forum des DWI – Leibniz-Institut für Interaktive Materialien e.V. and Evonik Industries AG, Aachen, Germany, **2016**.

8. Heinen, S., Becherer, T., Weinhart, M., Understanding and Engineering Parameters for Biocompatible, Thermoresponsive Polymer Coatings and Temperature Triggered Cell Adhesion and Detachment, Gordon Research Conference on Biomaterials and Tissue Engineering, Girona, Spain, **2015**.

9. Lemper, S., Becherer, T., Wei, Q., Weinhart, M., Relation Between Microstructure of Biocompatible, Thermo-Responsive Polymer Coatings and Cell Adhesion and Detachment, Jahrestagung der Deutschen Gesellschaft für Biomaterialien, Dresden, Germany, *BioNanoMat.* **2014**; 15, P125.

Oral Presentations

10. Heinen, S., Cuéllar-Camacho, J. L., Weinhart, M., Thermoresponsive Polymer Coatings for Cell Sheet Fabrication: A Structure-Property Relationship, Presentation at the 10th World Biomaterial Congress in Montreal, Canada, **2016**.

11. Schirner, M., Heinen, S., Haag, R., Weinhart, M., Synthetische Heparinoide zur Beschichtung von Medizinprodukten, Project presentation for the GO-Bio Jury, BMBF, Berlin, Germany, **2016**.

12. Lemper, S., Sindram, J., Antifouling Spray Coatings for Biomedical Glass Surfaces, Pitch-Presentation at the Research to Market Challenge Presentation of Awards in the course of the Charité Entrepreneurship Summit, Berlin, Germany, **2014**.